Politecnico di Torino

Department of Control and Computer Engineering

Master's degree in Computer Engineering

Data Mining in the Automotive Industry for Predictive Maintenance

Analysis of the Oxygen Sensor Clogging Phenomenon

Supervisor

Elena Baralis

Co-supervisor

Tania Cerquitelli

Flavio Giobergia

Academic Year 2016-2017

Summary

The work presented in this thesis is focused on the topic of predictive maintenance, or prognostics, approached with a data-driven perspective. Models that use a data-driven approach to prognostics learn models directly from the data, rather than using a hand-build model based on human expertise [1]. The topic of prognostics has become particularly interesting in recent years: the arrival of Internet-enabled everyday devices (the so-called Internet of Things) allows for the automatic collection of data large amounts of data which can in turn be processed and used for inferring the health conditions of the object being monitored.

This monitoring process suits particularly well the automotive industry: nowadays, vehicles are being loaded with sensors monitored with smarter, connected Engine Control Units and, in a not-so-distant future, these vehicles will become smarter still, with self-driving capabilities and even greater data-collection functionalities. All this data being collected represents a precious resource that can be used to extract insightful information and, as such, it should not go unused. Predicting a vehicle's malfunctionings is of vital importance for both the health of the vehicle itself and for the safety of the passengers.

Given these premises, it follows naturally that all this data being collected should be put to use in order to improve the maintenance operations on the vehicle, in order to minimize possible risks. This is precisely the ambitious goal that has been set for this work of thesis. The goal gets even more ambitious when considering that the problem is being approached with no expertise in the automotive domain. This proved to be an advantage in that it did not introduce any kind of bias in the elaboration of the results: these, though, have been evaluated by the domain experts that collaborated on this project, helping consolidate or discard conclusions.

The study started from some previously collected test bench data provided by an automobile manufacturer, and with a problem the company was interested in tackling using a data-driven approach. This problem concerns the oxygen (or lambda) sensor which, if malfunctioning, degrades the performance of the vehicle, with the excessive pollution and fuel consumption problems that come with it.

The data available has been studied using different data mining techniques in

order to gain insightful information from it and, from this, different predictive models have been built. Their performance have been evaluated in different situations using different criteria to better understand the limitations and the potential available.

A process comprised of three essential parts has been identified: these parts are the labelling, the data preprocessing and the training of the classification models. Each of these high-level parts contains different steps, based on the operations required by the dataset. The data available is in the form of cycles, with each one of them lasting approximately 1 hour and containing a collection of variables measured on-board. Of particular interest is the fact that the labelling and the data preprocessing operations are done on different datasets, given the structure of the data available.

The training and the classification operations make use of different machine learning models with complementary advantages and disadvantages. The results have been measured in terms of accuracy, precision, recall and, in particular, of F_1 score, allowing for an estimation of the potential performance of the models trained. The results are satisfactory, with high values in terms of the different metrics used.

On top of this experiment, many others have been built. Many consist in the redefinition of some components of the presented process in order to better understand which parts could be improved and which are the most robust. Other experiments change the definition of the labels used for the dataset: the initial definition provided has been discussed and changed: this helped better understanding the rationale behind the decisions taken by the classifiers.

Finally, additional explorations of the dataset have been carried out: although not strictly relevant to the goals of the project, these analyses uncovered interesting information regarding the dataset and some problems contained within. These problems consisted in the apparently unjustified existence of clusters of values within the dataset. This exploration first highlighted the existence of these clusters, then tried to provide a description of them and, finally, it attempted to provide a domain-agnostic explanation for their existence.

This work tackled a prognostics problem that has not been found to be covered elsewhere in the literature, using a novel process tailored to the kind of data available, but easily adaptable to different scenarios. Some of the limitations of the datasets (e.g. the homogeneity of the tracks used) only allowed for limited testing of the proposed solution: additional experimentations would be required using real-world data instead of data collected from a test bench. This is scheduled be done in the upcoming future.

This pilot project helped getting a better understanding of the potentials and

the limitations of data mining applied in an automotive context. It should be mentioned that, for this work of thesis, only a "small" amount of data has been used. As such, this work cannot be classified as a "big data" one. Despite that, the scaling up of this work to handle the real-time data collected from millions of vehicles undoubtedly requires a big data approach, with the benefits and problems that come with it.

Acknowledgements

Almost exactly a year ago I started working on this thesis. Much has happened since then, many doors opened and many others closed. Now the time has come for me to close the "thesis" door as well, and what a door it is: to say that this thesis has taught me a lot would be an understatement and, for that, I certainly have to thank a lot of people. So, here comes.

First and foremost, my biggest thanks goes to professor Elena Baralis. She has proven to be an excellent supervisor (not that I had doubts about it), extremely pleasurable to work with, particularly insightful and always ready to help out when I found myself in a tight spot (which occurred more times than I'm proud to admit). An equally important acknowledgement goes to professor Tania Cerquitelli, who first introduced me to the beauties of the DataBase and Data Mining Group and saw to this project all the way to the end when others would have probably opted for a more relaxing alternative in her stead (congratulations on the arrival of Lorenzo, by the way!). Additional acknowledgements should go to professor Marco Mellia for his involvement in the project (and I'd like to wish him the best of luck for the ambitious endeavors he is currently working on) and to professor Letizia Tanca for her kind availability as external supervisor for this thesis. I should also immensely thank the people from the automotive company who took part in this project: I could not have asked for a better group with whom to collaborate.

While this work of thesis took a good chunk of my time during this last year, I would be remiss if I did not thank the people who surrounded me in my day-to-day life. A huge, huge thanks goes to my parents, who had to put up with me not only this past year, but the previous twenty-something ones as well, as did my sister, who probably is the one person who got more stressed out than I did for this thesis: an enormous thanks to her is definitely well deserved.

And last, I would like to thank all my friends and those who have been close to me during this past year and the years before this. Many and more names come to mind; writing them all here would significantly increase the length of these Acknowledgements, which is already considerable. Despite that, I cannot help but thank the one person who I felt closer than anybody else this past year, who inspired me and helped me stay motivated, whose presence was enough to

motivate me to always strive for excellence.

The list of people could go on, but I guess this is a good moment to cut it short. All the people I mentioned have changed my life for the better and I hope that they are and will be, even slightly, proud of me. I know I am.

Contents

List of Figures

List of Tables

Chapter 1

Introduction

1.1 Clogging of the oxygen sensor

In an automotive setting, the oxygen (or lambda) sensor is a device used to measure the proportion of oxygen in the exhaust gas of an internal combustion engine. This information is used to regulate the fuel injection so as to achieve optimal efficiency and to determine whether the catalytic converter is performing properly.

This oxygen sensor is subject to clogging due to the accumulation of soot contained in the exhaust gas the sensor is constantly exposed to. The clogging of this sensor results in a slower measurement of the oxygen level.

In turn, this slower response implies a suboptimal behavior in terms of efficiency: the engine control unit (ECU) cannot determine the right combustion mixture, resulting in an increase in the vehicle's fuel consumption. Additionally, given the sensor's relevance for the catalytic converter, more harmful emissions are released in the environment.

The situation is exacerbated by the fact that slower readings for the oxygen sensor cannot be easily detected by the ECU: this implies that the clogging of the lambda sensor is usually only detected when it is already too late, i.e. when (and if, in many cases) the driver notices a significant increase in fuel consumption. This happens because the slower response time cannot be noticed in a straightforward manner by the ECU.

1.2 Prognostics

The typical way problems are detected is through diagnostics, whereby failures and malfunctions are detected after they occur, possibly through the support of the ECU itself (on-board diagnostics). Given the hard-to-notice nature of the lambda sensor clogging, a different approach to the problem is in order.

The activity of prognostics consists in using the available information on a system to make predictions on the problems that might occur in the near future. This discipline is usually declined in either of two approaches:

- **Model-based**: this type of prognostics uses the available domain knowledge to produce a physical model of the system of interest. The model can be developed on different levels of detail, depending on the desired trade-off between accuracy and simplicity
- **Data-driven**: this type of prognostics uses pattern recognition and machine learning techniques to build agnostic predictive models

It is unlikely for a purely data-driven model to exist since, expertise in the domain is required to some extent for both preparation of the data and interpretation of the results. Even for model-based approaches, a data-driven component may exist. The right term for these approaches would be "hybrid" but, since either of the two is typically predominant, a distinction can be made between the two.

1.3 Objectives

This thesis will approach the oxygen sensor clogging problem with a data-driven approach to prognostics, exploring the decisions made throughout the process definition and implementation, as well as highlighting strengths and weaknesses of this methodology. Finally, the results of the predictive model will be discussed and conclusions about the overall work will be drawn.

The identified process will be presented in its final form after multiple revisions and improvements. Alternative process choices, along with additional data explorations will be presented in Chapters 8 through 10. Some of these explorations are preparatory for a future extension of the project to a real-life scenario: while this study focused on test bench datasets, the final goal of the project is that of deploying the solution to millions of vehicles. This scaling up requires further research that has only partly been covered by this study: despite that, this study provides the foundations for further, more relevant experiments.

The decision of using a data-driven approach, rather than the traditional model-based one, comes from the ever-increasing quantity of data available nowadays. ECUs collect data from hundreds of sensors dislocated all around the vehicle, with extremely high sampling frequencies. If this amount of data is collected for all the hundreds of millions of vehicles around the world, a big data opportunity ensues. On top of that, there is an ever-increasing interest in autonomous vehicles: this new technology would come with an even larger amount of data from all the additional sensors that these vehicles require.

Getting ready for all of this is a cumbersome and daunting task, but the sooner the first step in this direction is taken, the better. Working on a prognostics project centered around the oxygen sensor is one of the ways a company can get exposure to this new, data-driven world.

1.4 Contents overview

Chapter 1 provided an overview of the problem that will be faced in this work of thesis, explaining the topic at hand and stating the objectives set. Chapter 2 offers a review of the literature found that is relevant to the topic of predictive maintenance: this defines the state of the art and, by the end, an attempt to highlight the main novel points of this work is made. Chapter 4 presents the domain knowledge available and the standard data mining process: based on these and on the initial objectives, an overview of the high-level process identified is provided. Chapter 3 introduces the dataset available, highlighting the way this was collected and the way it is structured: these considerations will be used throughout the rest of the thesis to make considerations.

Chapter 5 offers an in-depth analysis of the first part of the identified process: in particular, it covers the labelling process and the components it is comprised of (response time measurement, smoothing, class definition and assignment). Chapter 6 covers the data preprocessing operations, dividing them into feature selection and data transformation. Chapter 7 presents the machine learning models used for the classification of the dataset based on the clogginess and the evaluation metrics and techniques used.

Chapter 8 shows how many of the assumptions made *a priori* based on some rationale can and have been modified to support alternative approaches: when available, the *a posteriori* results will be presented so as to compare the presented solution with possible alternatives. Chapter 9 offers additional experiments, this time based on the change in decisions made when defining the classes of values: this highlights how changing these classes influences the performance of the models, with the interesting conclusions that come with it. Chapter 10 covers an initially unscheduled further data exploration, aimed at uncovering an unexpected behavior that led to the formation of well-defined clusters of data: these clusters are analyzed, described and a possible cause for their existence is then proposed.

Chapter 11 provides a quick overview of the implementation details, specifying the hardware and software tools and libraries used for this project. Chapter 12 shows the findings of this work of thesis, with comments concerning the most interesting of the results achieved. Finally, Chapter 13 contains the conclusions of this work, highlighting the most interesting takeaways, explaining the main points

of novelty and the major limitations, with final considerations on the possible future outcomes for the project.

Chapter 2

Literature review

As everyday objects get smarter, the potential for early fault detection increases: rather than waiting for a component to break down, an early detection might allow for immediate intervention. This results in lower costs, less time wasted and more satisfied customers. It is not surprising, then, that the interest in prognostics (at times referred to as predictive maintenance) has grown significantly in the last few years. The most common types of prognostics are the *model-based* and the *data-driven* ones, along with hybrid approaches that leverage the advantages of both. Figure 2.1 shows both how the topic of predictive maintenance has been trending in recent years and how model-based prognostics is more recurring, when compared to the more recently introduced data-driven one. The presented graph is not intended to be exhaustive (additional keywords should have been used), but it provides a clear idea of the increasing interest in the subject.

The topic of prognostics is often paired with that of health management, so much so that the Prognostics and Health Management (PHM) is a recurring theme in articles and conferences. The IEEE organizes every year the International Conference on Prognostics and Health Management, while the PHM Society is an organization solely dedicated to the promotion of the topic. Many of the publications that have been analyzed are from these two sources. Additionally, given the current trend that has been observed in the prognostics-related publications, these two sources are expected to provide insightful material for the years to come and, as such, are worth keeping an eye on.

The topic of prognostics is too widespread and heterogeneous to be thoroughly explored for understanding what the current state of the art in the automotive industry is: many of the applications of PHM are found in fields that are only weakly – if at all – related to the automotive field and can be safely left out in order to narrow the research down to a more manageable number. The literature review has been based on Scopus, a database of peer-reviewed research literature.

The initial research was based on the title, the abstract and the keywords,

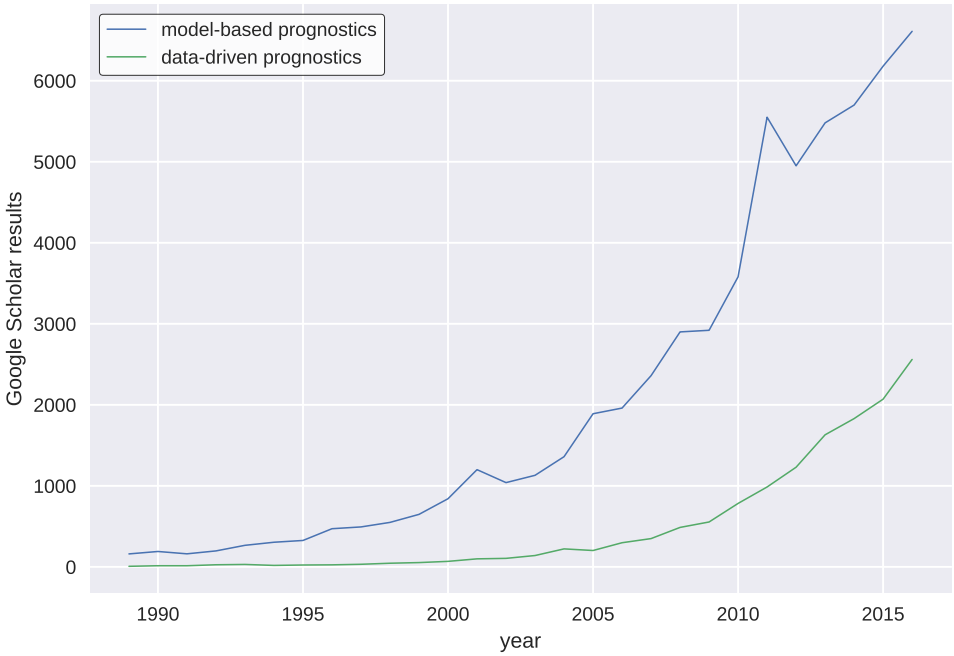

Figure 2.1: Trend for data-driven vs model-based prognostics in Google Scholar[1]

using the words "prognostics" and "automotive": this yielded 135 results. Of these results, 16 have been excluded because of conflicting keywords that implied scarce relevance to the topic of interest. The remaining 119 have been further filtered, iteratively removing irrelevant material based on the contents of the title, the abstract and finally the document itself. Most of the discarded contents where either too general in nature (with the automotive setting being only briefly mentioned), or too detailed (many of the prognostics documents discarded where focusing on particularly narrow applications that were not significantly relevant, such as the study of solder joints longevity). The final number of articles and conference papers kept is of 30.

Of these documents, 5 are overviews covering different possible approaches to prognostics: some of these approaches are model-based, while others are data-driven. In some cases, these overviews briefly cover the "prognostics" topic as a whole, providing possible algorithms for tackling the problems: this is the case with "A review of recent trends in machine diagnosis and prognosis algorithms", where different approaches (among the others, Artificial Neural Networks and Genetic Algorithms) are proposed, along with references to successful case studies for each candidate. Other documents provide overviews of more specific systems and analyze possible faults that might occur: this occurs, for example, in "Diagnostics

[1]Data from Google Scholar trends collected from `https://csullender.com/scholar/`

and prognostics needs and requirements for electrified vehicles powertrains", where Electric Vehicle (EV) powertrains are introduced, along with a series of possible faults that might occur in it (in rotors, bearings, inverters and so on). This type of documents provides interesting high-level insights of the prognostics field, either concerning possible approaches, or presenting possible problems to tackle.

The rest of the articles are PHM case studies, similar in nature to the one that is approached in this thesis. The parts (or subsystems) that have been studied in these publications are many, although two intertwined targets appear to be of major interest: batteries (6 documents) and electric vehicles (7 documents) are the most recurring themes. These papers are mostly concerned with estimating the State of Health (SoH) and the State of Charge (SoC) of batteries: for example, the conference paper "A machine learning approach to predict future power demand in real-time for a battery operated car" proposes a data-driven approach to the estimation of the SoC in EVs that overcomes some of the problems that are part of the limitations of the model-based solution.

Other problems that are tackled in literature concern the engine oil quality [5], injector cylinders misfiring [6] and many others. Of these documents, only 4 expressly state that the predictive maintenance aspect can be carried out on-board, that is without requiring the dismounting of the component or running specific tests. Of the others, it is not trivial – given the lack of specific domain knowledge – to understand whether an on-board implementation would be feasible, since many of the publications either use simulators (such as "Estimation of damage behaviour for model-based prognostic", which simulates the suspensions of a vehicle) or, as is the case with the already mentioned "A machine learning approach to predict future power demand in real-time for a battery operated car", miniaturized cars are used instead of real ones. Despite the uncertainty due to the lack of domain expertise, the clear takeaway from these considerations is that there is only a limited number of works that are backed by real data and that can be easily run on-board, thus providing a major strength for this work of thesis.

As far as algorithms are concerned, the most recurring one used (with 4 of the 30 papers analyzed using it) is the Kalman filter [8]. This filter is used to make estimates of variables that cannot be measured directly, or variables that can be measured using multiple, inaccurate (e.g. due to noise) sensors. In the study proposed in "Remaining useful life prediction based on noisy condition monitoring signals using constrained Kalman filter", the authors use Kalman filtering to estimate the remaining useful life (RUL) of lead-acid batteries: the problem that the Kalman filter helped solving was the presence of noise affecting the signals examined.

This chapter presented a portion of the literature available regarding prog-

nostics applied to the automotive industry. Some of the trends and approaches have been shown, with some of the limitations identified. The research project presented in this thesis will attempt to contribute to the existing literature by applying a data-driven approach to the oxygen sensor clogging problem: the dataset used has been collected from a real engine (with all the advantages and drawbacks of the case) and the model will be developed, if possible, so as to be online-ready for actual vehicles (and not limited to simulators or mock-ups). The goal for the model construction is that of making it as interpretable as possible, in order to allow the domain experts to understand the reasoning behind the choices made. The oxygen sensor has not been found to be in the available literature. Despite the decision of approaching a single problem, but the study will attempt to identify a methodology that can be adapted to different situations.

Chapter 3

Dataset overview

The study has been carried out in collaboration with an automobile manufacturer. This company provided a large collection of previously collected test bench data, along with the domain expertise required to validate intermediate and final results, and the provision of feedback and support as needed.

3.1 Dataset overview

The dataset provided was collected in 2016 for other unrelated activities and was repurposed for this study. The decision of using an already available dataset resulted in a series of advantages: the collection of new data would have resulted in significant additional costs and a delay in the start of the activity. On the other hand, the collection activity was designed with a different purpose in mind and by different engineers from the ones involved in this project: this complicated parts of the study and affected some of the results. Considering that this was a pilot project, these nuisances have been deemed more than acceptable.

3.1.1 Test bench cycles

The data available has been recorded in a controlled environment within the company. This controlled environment, called test bench, consists in a dedicated room containing an engine continuously running: the ECU reads data from the sensors and dedicated software collects it and stores it for later use. Other external sensors (only available in this ad-hoc environment, but not "on the road") are also measured and stored.

The engines are controlled using a predefined track for the gas pedal (or accelerator): this track simulates different driving conditions, depending on the purposes of the test in place. The track used for this dataset was approximately 1 hour (3750 seconds) long. Each of these 1-hour runs is called a cycle. Cycles are executed one

after the other throughout the day.

Different contiguous groups of cycles for the same engine (which will be referred to as "experiments") were provided as part of the initial dataset. Of these experiments, only a subset was deemed useful by the domain experts for this study: the others, either because of underlying technicalities in the measurements, or because of the scarce evidence of the clogging problem, have been set aside.

The remaining datasets contained the recordings for the engines of two different vehicles, which will be referred to as Model1 and Model2. Other technical names used for the data collection activities are not relevant to this study and have been ignored: as such they will not be reported in this work.

For each cycle, different signals have been recorded: each of these signal (also referred to, throughout the document, as *variables*) are either the output of sensors dislocated throughout the engine, or are computed from other existing variables using internal models.

3.1.2 Dual recording approach

The Model1 and Model2 datasets have been recorded using two different software, ProgramA and ProgramB. These two tools have different characteristics and have been used for similar – yet complementary – purposes. The main differences between ProgramA and ProgramB are reported in Table 3.1. The two tools worked in parallel, collecting data on the same exact cycles, but while ProgramA covered its entirety, ProgramB only focused on the final part. This final part, as it will be explained in more detail in Section 5.1, will be used to understand whether a cycle should be considered as clogged or not.

	ProgramA	**ProgramB**
Duration (s)	3750	300
Sampling frequency (Hz)	1	320
Number of variables[1]	50	440
Number of Model1 cycles	400	390
Number of Model2 cycles	186	184

Table 3.1: Differences between ProgramA and ProgramB

Although ProgramA and ProgramB theoretically recorded the same exact cycles, the actual number of available cycles differs between the two: possible malfunctionings of the tools might have resulted in some of the recordings being lost or not stored at all (although this is little more than speculation, having the datasets been recorded by people not involved in this project).

[1]This is the most common number of variables recorded by each tool. Some cycles contained a different number variables, depending on decisions and events that occurred at recording time

The following are in depth explanation of the two tools based on the information reported in Table 3.1.

ProgramA

ProgramA records the entire 3750 seconds cycle, using a 1 Hz sampling frequency. This results in approximately[2] 3750 samples for each of the 50 variables recorded. Figure 3.1 shows the accelerator signal used as the track for each cycle. The figure shows how the engine is stressed with an high frequency accelerator signal, which is not usually found in normal driving conditions. Given that all datasets available followed the same predefined track, the results obtained from this study are not directly scalable to an "on-the-road" scenario, but it would require some adjustments.

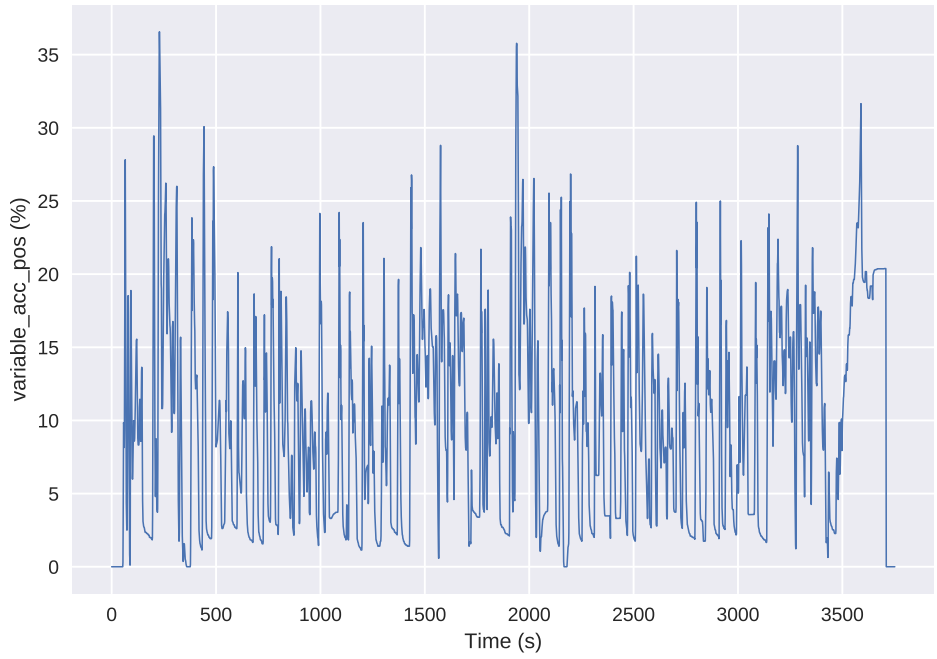

Figure 3.1: Acceleration pedal signal, recorded with ProgramA (entire cycle)

The theoretical track used is supposedly (see Chapter 10) the same for all cycles, but slight variations between cycles exist due to the fallibility of measurements. While this statement may be obvious, this fact should be kept into account when working with some of the signals.

[2]The actual duration of the cycle varies slightly between cycles

ProgramB

ProgramB is the second software tool used to collect engine data. It samples 440 signals[3] with a sampling frequency of 320 Hz. Of the entire cycle, ProgramB only records the final 300 seconds: this is the part where the *cut-off* occurs. The cut-off is the moment when the gas pedal is released after a particularly intense and steady acceleration. This part of the cycle is of particular interest as the cut-off will be used to understand whether the cycles are clogged (i.e. the sensor is clogged) or not.

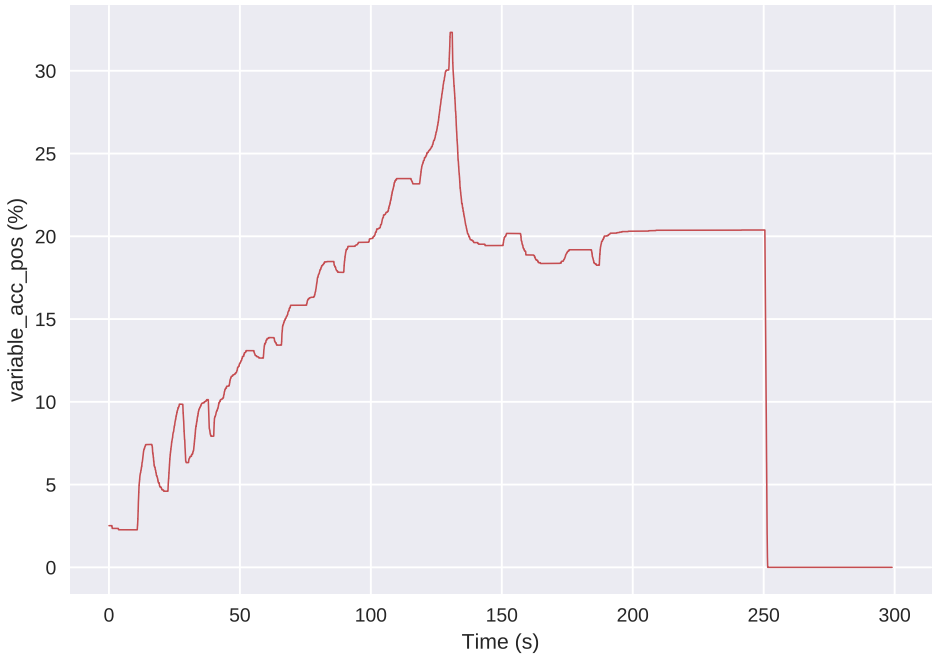

Figure 3.2: Acceleration pedal signal, recorded with ProgramB (final 300 seconds)

Figure 3.2 shows the accelerator behavior for the final 300 seconds of a given cycle. The cut-off is clearly highlighted by the step that occurs around the 250^{th} second. To get a better sense of what portion of the cycle ProgramB records, Figure 3.3 displays both the ProgramA and ProgramB recordings for the same cycle.

As already mention (and as it will be explained in further detail in Subsection 5.1), the cut-off phase is used understand to what degree the clogging problem is occurring: as such, having a more frequently sampled signal is necessary. On the other hand, sampling the entire cycle with a 320 Hz sampling frequency would have resulted in significantly larger datasets, without particularly benefiting the

[3] As mentioned, some of the signals may actually be derived from others using existing models: 440 is the total number of signals returned by ProgramB

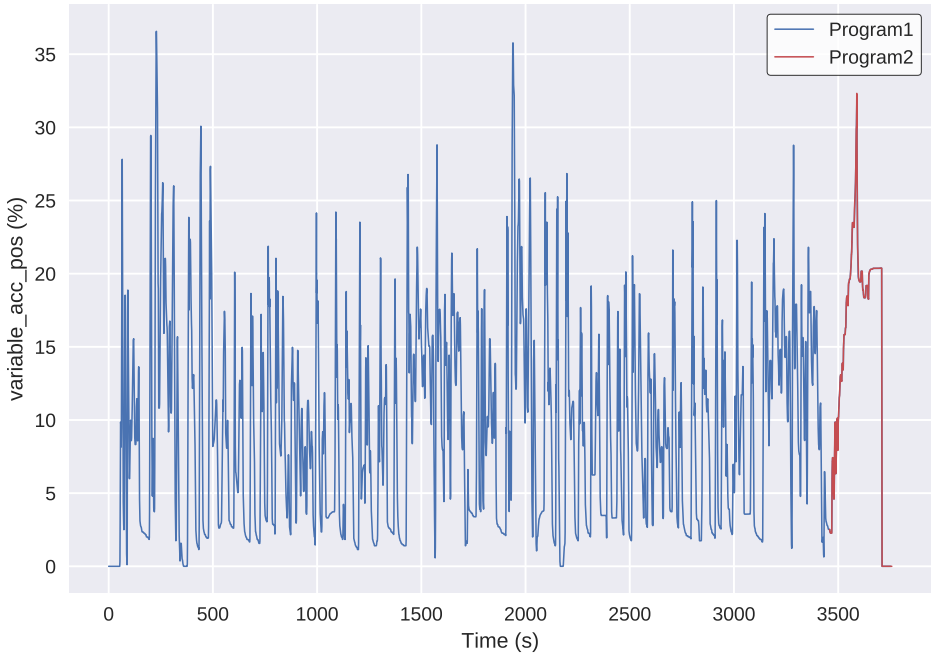

Figure 3.3: Acceleration pedal signal, recorded with both ProgramA (in blue) and ProgramB (in green)

overall study (it would have actually gone the opposite direction, since the future steps require lowering the sampling frequency, as explained in Section 8.4).

3.1.3 Variables overview

ProgramA and ProgramB collect a significant amount of signals, with some of these signals being exclusive to either tool. These signals (also referred to as variables) can be divided in two main categories:

- **ECU variables**: these variables are measured by the Engine Control Unit and are therefore available on any vehicle with that ECU
- **Test bench variables**: these variables are measured using external sensors only available during the test bench and are not available outside of it (e.g. during on-road tests, or in real-life scenarios)

The final purpose of this study is that of applying the prognostics system to off-the-shelf vehicles: as such, using signals originating from additional sensors added in the test bench is not particularly useful and, on the contrary, it might result in hard-to-scale results (given the lack of those sensors in the subsequent steps).

The ECU variables, on the other hand, are readily available on all vehicles. These variables are grouped in different categories based on the type of value

monitored. Each of these categories is identified by a 3-letters string.

Given the lack of automotive expertise, these variables and categories have been treated with an unbiased approach. The support provided by the company's domain experts helped understanding the results obtained and whether these were meaningful and relevant.

3.1.4 Other considerations

Table 3.1 highlighted how the number of cycles available for Model1 is significantly larger (more than twice in size) than that of Model2. Given the data-driven approach of the study, a larger amount of data is preferred: for this reason, the entirety of the study has been carried out using Model1. Model2 has been later introduced to test the process on a brand new dataset (see Section 8.6).

Finally, to get a sense of the overall size of the dataset (for further considerations on the tools used for the study), the average size for a single ProgramA cycle was roughly of 1.6 MB, while the average ProgramB file was 43.7 MB large. Given the cardinalities for the two Model1 datasets, the overall size was roughly $1.6\,MB \cdot 400 + 43.7\,MB \cdot 390 \approx 17.3\,GB$. This kind of data can be handled using a large enough main memory and certainly on a single machine: as such, big data techniques will not be used. Despite that, the final goal requires processing data from millions of vehicles: when scaling up to that size, the big data paradigm will be necessary.

Chapter 4

Process identification

Given the dataset and given the company's requirements, a process going from raw data to clogging identification needs to be established. This process needs to consider the domain knowledge already available as a starting point and integrate it into the data mining process.

4.1 Domain knowledge available

The domain knowledge available for the clogging problem allows for the correct identification of clogged situations in the available cycles. As already mentioned in the introduction, a clogged lambda sensor results in a slower response. The cut-off operation that occurs at the end of each cycle is a good moment for measuring the response time: given that roughly all cycles go through the same cut-off, the response times measured are comparable between one another. This should give an idea of how clogged each cycle is when compared to the others. The other important notion learned was that the soot was expected to cumulate in the lambda sensor: as a consequence, the clogging was expected to increase as the cycles went on.

Given the importance of what happens during the cut-off, it makes sense that a higher sampling frequency (on ProgramB) was used during this phase, while the entirety of the cycle is recorded, with ProgramA, at a lower rate. Since ProgramB only contains a few minutes' worth of data out of each hour, the ProgramA information should be used as input to model in order to provide it with recordings that span the entire period of time available.

4.2 Data mining process

The problem at hand can be identified as a "classification" one: given a cycle, the goal is that of classifying it as either clogged or not (and possibly "almost clogged", since the clogging of the sensor happens gradually). For the cycles available, the information on the clogging status can be extracted from the ProgramB dataset, while the data required to make the classification is provided by ProgramA. The typical mining process shown in Figure 4.1, often referred to as Knowledge Discovery in Databases [10], goes through the phases of data selection, preprocessing, transformation, mining and evaluation/interpretation: these are the phases will be applied to the case at hand.

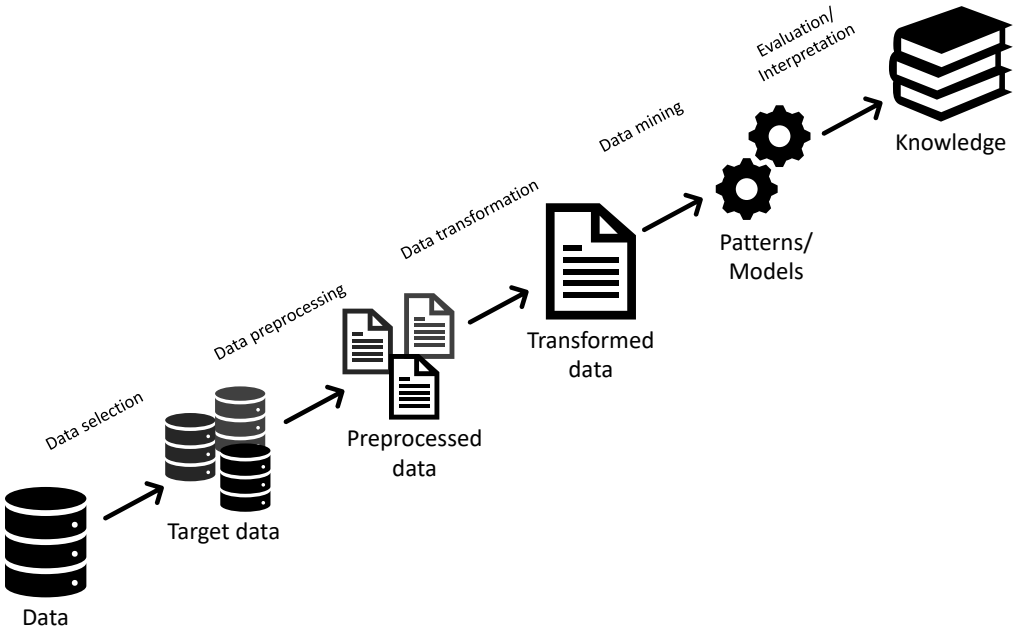

Figure 4.1: A visual representation of the typical data mining process

- **Data selection**: in this phase, only the necessary data is kept. For this study, only the data about Model1 has been kept. Some additional cycles have been discarded during the mapping phase
- **Data preprocessing**: in this phase, operations such as feature selection and labeling are carried out. In particular, only a subset of the available signals will be kept and the ProgramB cycles will be analyzed so as to measure the response time
- **Data transformation**: in this phase, the variables available are transformed so as to become more suitable inputs for the classifier
- **Data mining**: this is the phase where different machine learning algorithms are used to extract information from the available datasets. More precisely,

this kind of problem requires the classification of the cycles (as either clogged or not clogged)

- **Evaluation/interpretation**: this is the phase where the results of the classifiers are analyzed (when meaningful) and the models are evaluated based on their performance

While the above list describes how the different phases identified during the study fit the typical data mining process, the peculiarities of the scenario available cannot be highlighted properly. Since these peculiar aspects required a tailored process to be developed, the next part will provide a high-level description of it.

4.3 High-level process

Figure 4.2 contains a block diagram of the high-level model identified for the process. For each block, a brief description is provided in the following list and will be described in more detail in the following chapters. The diagram clearly highlights how the dual dataset is approached by first working on the separate files to extract the required information, with the results only being merged afterwards.

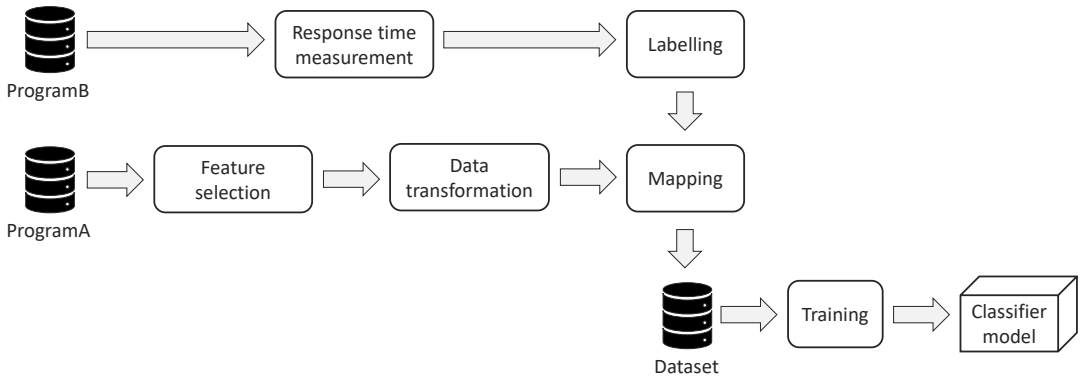

Figure 4.2: Block diagram for the identified process

- **Response time measurement**: in order to understand whether a cycle is clogged or not, the response time after the cut-off needs to be measured, using the definition provided by the domain experts on the ProgramB dataset
- **Labelling**: based on the response time, cycles are labelled as either clogged or not (or, to predict future clogging situations, as "almost clogged")
- **Feature selection**: in order to reduce the number of ProgramA variables used, any existing redundancies have been removed through a feature selection process

- **Data transformation**: given the large number of possible inputs (i.e. $n_{variables} \cdot n_{samples}$, with $n_{samples} = 3750$) compared to the low number of cycles (≈ 390), some kind of transformation is required for the classifier to properly handle the problem
- **Mapping**: the unlabelled dataset resulting from the data transformation step receives the labels computed at the labelling step, producing the final dataset
- **Training**: the final dataset is used to train a model for later use on unseen data

A trained classifier is the output of this process. This classifier can then be used on previously unseen data, as shown in Figure 4.3. In this case only the simil-ProgramA data is available (since transmitting the more frequently sampled ProgramB data to a central server would pose problems in terms of bandwidth required): after the extraction of the relevant variables and their transformation, the existing model is applied to make a prediction on the state of the lambda sensor.

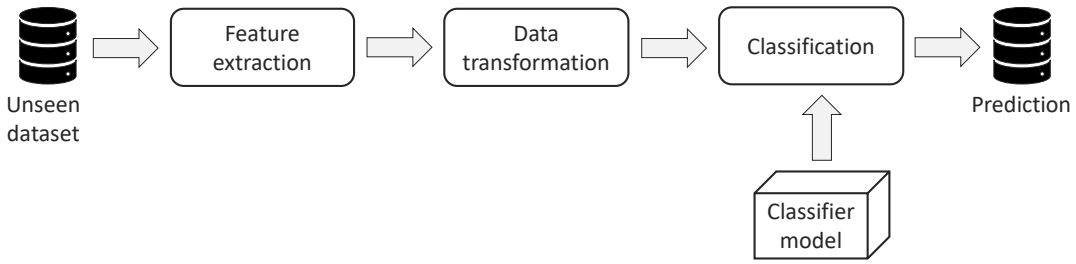

Figure 4.3: Block diagram for the classification of unseen data

Chapter 5

Label assignment

This section provides a detailed description for the steps of the process that comprise the labelling operation. These are the steps performed on the ProgramB dataset, and consist in response time measurement, smoothing and assignment of the class label. As shown in Figure 4.2, the initial steps taken for the ProgramA and ProgramB datasets can be executed in parallel: the order proposed for the presentation, therefore, does not reflect an order in the execution of the two sub-processes.

5.1 Response time measurement

During the final part of each cycle, the gas pedal is first kept at a steady level for a set period of time, then it is released: this releasing of the accelerator is referred to as cut-off. The oxygen level measured in the exhaust gas is directly influenced by the acceleration pedal state (i.e. the oxygen level depends on the engine load). After the pedal is released, the oxygen level will start rising until it reaches the final 21% value. The time it takes for the oxygen level to reach this value (as measured by the lambda sensor) is referred to as response time.

Figure 5.1a shows the oxygen level as reported throughout the final 300 seconds by ProgramB. It has been observed that the ramp following the cut-off is always contained between the seconds 245 and 260 of the ProgramB recording: thus, in order to simplify the process, only this range will be considered while discussing the measurement operation. The zoomed version of the ramp is represented in Figure 5.1b

Defining when the ramp reaches the 21% value is not trivial, as the value might be overshot, or never actually reached. For this reason, the domain experts' definition of response time is slightly different from the previously provided one and is defined as the time it takes for the oxygen level to reach 63% of the transitory

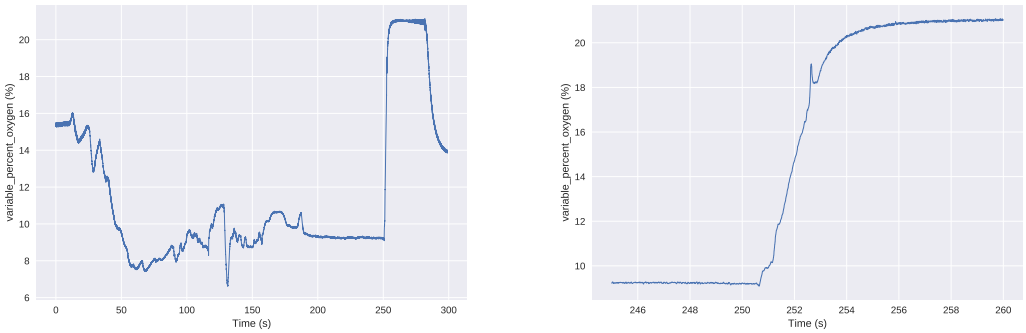

(a) $0s \div 300s$ (b) $245s \div 260s$

Figure 5.1: Oxygen level, as measured in ProgramB

from the initial value to 21%, as explained in Equation 5.1

$$t_r = t(O_2 = 0.63 \cdot (O_{2end} - O_{2start})) - t(O_2 = O_{2start}) \tag{5.1}$$

With $O_{2end} = 21\%$ being the expected O_2 concentration found in the atmosphere. Figure 5.2 provides a visual interpretation of what the response time represents. Since O_{2end} is already known, O_{2start} is needed to compute the response time for a given cycle. The start time (i.e. $t(O_2 = O_{2start})$) can be intuitively identified in

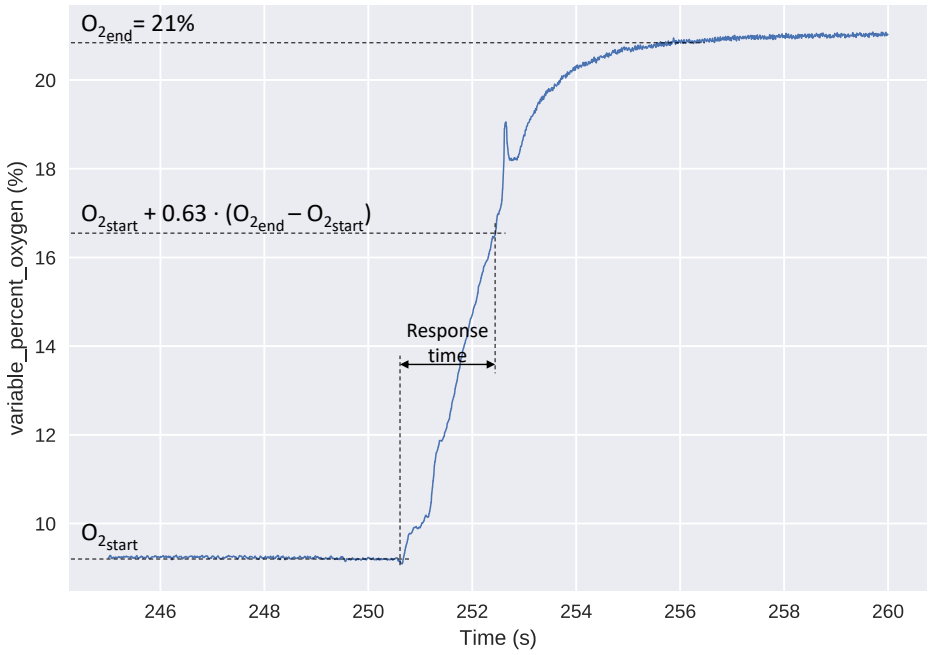

Figure 5.2: Response time measurement process

Figure 5.1a as the moment when the ramp starts rising after the "flat" part. When

using an algorithm, though, the identification of this moment is not trivial due to the noise present. In order to solve this problem, a sliding window starting in the flat part on the left-hand side of the signal and spanning 20 samples is used and the standard deviation of the values in the window is computed. When this standard deviation exceeds a threshold value, it means that the ramp has started, as the rightmost values in the window significantly differ from the leftmost ones. Figure 5.3 shows both the oxygen level, and the sliding standard deviation computed using a sliding window of 20 samples. The threshold value has been defined so as to match the start of the ramp and not previous noise. Both oxygen level and sliding standard deviation have been normalized to the $0 \div 1$ range for graphical reasons.

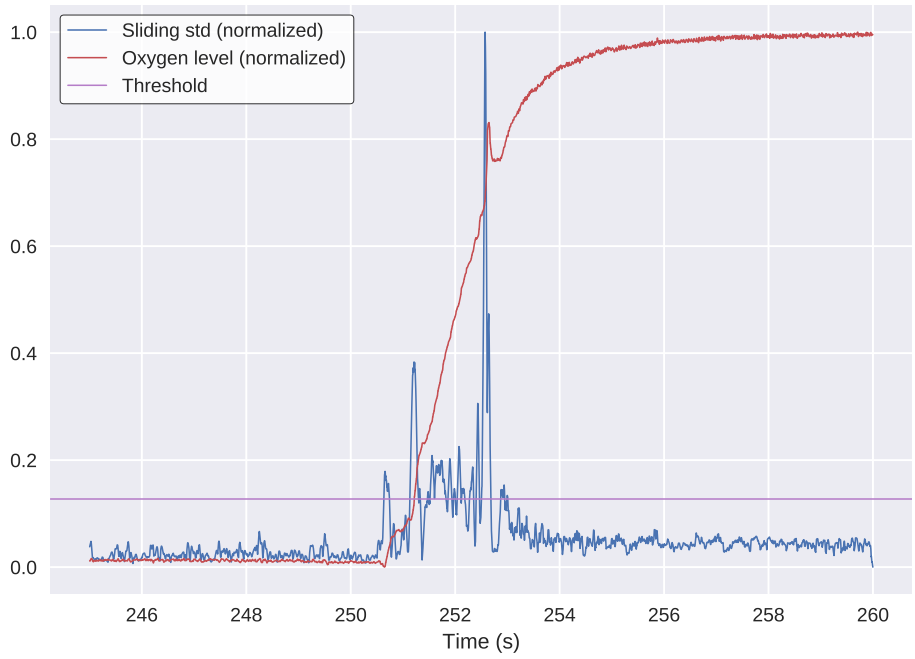

Figure 5.3: Cut-off oxygen ramp, with sliding standard deviation

A similar approach is that of computing the moving average of the oxygen level values and select as starting point the first one exceeding a different threshold: both approaches avoid false triggering due to noisy points by "smoothing" the curve (i.e. by introducing operations on a window of values, rather than basing the considerations on a single one). Of these two approaches, the standard-deviation-based one has been selected as the threshold defined did not depend on the average oxygen level, which might differ between cycles.

After applying the aforementioned process to all ProgramB cycles, a measurement of the response time is available for each cycle. Since the timestamp of each

cycle was known, a graph representing the response time trend from the beginning to the end of the experiments could be plotted and is shown in Figure 5.4a. This plot highlights different interesting aspects, that will be illustrated below.

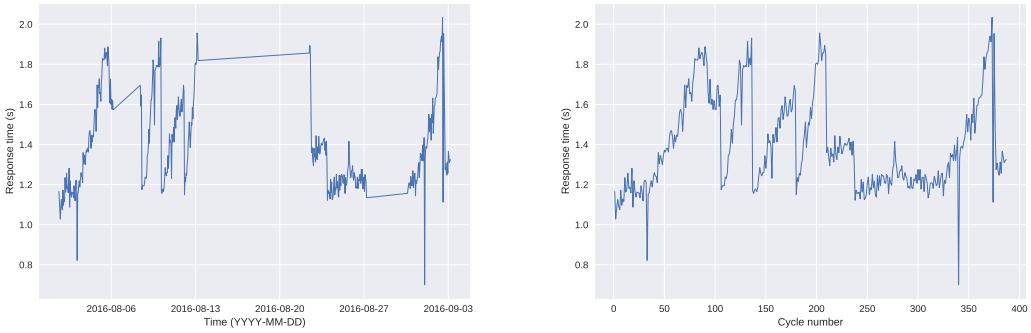

(a) Dates on x axis

(b) Cycle number on x axis

Figure 5.4: Response time trend throughout the experiment

First, some small plateaus, and a larger one, can be immediately noticed. These represent the moments where the experiment was not being carried out and, because of that, no cycles were available: the plotting tool interpolates that part by connecting the leftmost and rightmost points available by the gap. Since the engine is not altered during these pauses, its state should remain unchanged between the last cycle preceding a pause and the first one following it. Given this assumption, the pauses can be removed (this is easily achieved by changing the time dimension to represent the cycle number instead of a date and time), resulting in the graph shown in Figure 5.4b.

Second, and most importantly, the response time trend is not monotonic, as one would expect given the nature of the clogging (i.e. due to the accumulation of soot within the sensor). Instead, the general trend is that of an increasing response time, followed by a rather abrupt "reset" where the response time plummets, only to start raising up once again. This behavior has been interpreted by the domain experts as the soot "crystallizing" only to be shaken off the sensor upon turning the engine on. Based on the data and the domain knowledge available, this explanation could neither be corroborated nor contradicted but, since it did not affect the rest of the study, this notion was not considered any further.

Additionally, some spikes are easily noticeable in the plot. These spikes may either be due to problems with the measuring technique, or be the result of cycles with particularly different cut-offs. These cycles could be removed, but instead they have been kept, since no rationale has been provided as to what makes a measurement "out of range". Subsection 12.1.1 explains how these spikes affect the results of the classifiers: in light of these considerations, a different approach

that discards these cycles could be introduced.

A final consideration concerns the values of the response times, which range anywhere between 1 and 2 seconds. Measuring these responses using the 1 Hz sampling frequency provided by ProgramA would have yielded useless results: this justifies the utilization of the ProgramB dataset for this operation.

An independent method of measuring the response time has been tested to validate the results derived from the domain experts' measurement process. The method and the results are discussed in Section 8.2.

5.2 Labelling

Given the response time for each cycle, the next step is that of inferring whether the given cycle is clogged or not. The clogging condition results in the response time being slower, but no formal thresholds defining the meaning of "clogged" were available. Thus, this section will explore the process used for the definition of these values and the problems and solutions found during this process.

5.2.1 Definition of the number of classes

A seemingly trivial decision is that of the number of different classes to be used to divide the dataset. This decision, though, will heavily influence the performance of the classifiers, as these models need the dataset to be partitioned so that classes are internally cohese and well separated from one another.

The understanding of the clogging problem available, though, did not allow for a definite separation in classes. The first decision that has been pursued (and that will be adopted throughout the definition of the process) is that of defining three classes of "clogginess" referred to as 'green' (for unclogged cycles), 'yellow' (for cycles that are starting to clog) and 'red' (for clogged cycles).

This number of classes has been agreed upon with the domain experts and allows for a tangible understanding of the results of the classifier (by contrast, defining a large number of classes would have introduced confusion as to what each class is representative of). This decision of adopting three classes will be changed in some of the further explorations presented in Chapter 9.

5.2.2 Definition of the threshold values

The following step is that of defining the threshold values for each of the defined classes. Given the physical constraints of the response time, it is reasonable to assume the lower bound of the green class to be 0 and the upper bound of the red class to be $+\infty$. This leaves the definition of two additional thresholds (i.e. the

ones defining the yellow class bounds, thereby defining the missing bounds for the red and green ones).

As it happened with the definition of the number of classes, this decision was not significantly aided by the domain knowledge available, resulting in the necessity of making a decision based only on the information available. The piece of information that drove the definition of the thresholds was the fact that the red class (i.e. clogged situations) was expected to be a minority when compared to the other situations.

For the green and yellow classes, on the other hand, there is not much that can be said, particularly in light of the reset events that sometimes occur and that do not strongly correlate the cardinalities of the yellow and red classes. Without any additional information, these two classes may be divided so as to have similar cardinalities.

A final driver for this decision could be qualitative analysis of the distribution of response time values. The distribution is presented in Figure 5.5, which already represents the final decisions made for the response time values.

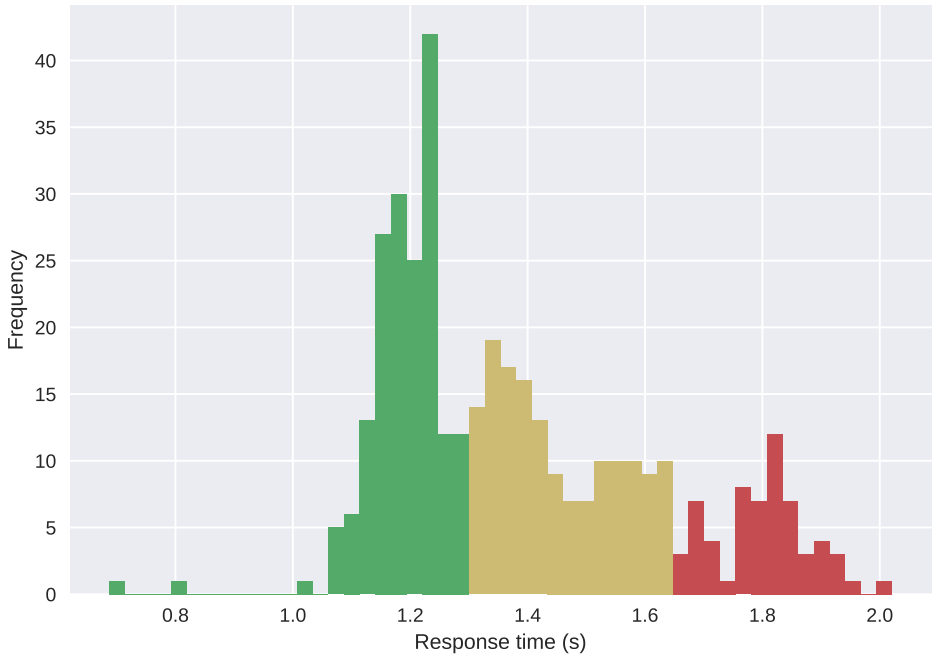

Figure 5.5: Distribution of response times: the colors represent the assigned classes based on the defined thresholds

The response time ranges chosen for the three classes are reported in Table 5.1. As already explained, the labels assigned to the cycles have a significant influence on the performance of the classifiers. Since both the number of classes and the thresholds defined have been assigned based on heuristics that might change as the

Label	Range (s)
Green	[0, 1.3)
Yellow	[1.3, 1.66)
Red	[1.66, $+\infty$)

Table 5.1: Ranges defined for the three classes

domain knowledge on the matter increases, these decisions have been introduced in the process as parameters to be tuned at a later time and, indeed, Chapter 9 explores possible alternatives in the definition of the classes.

5.2.3 Smoothing of the response times

The logical step following the definition of the classes would be that of labeling each cycle based on the class the response time belongs to: there is a problem, though, with this straightforward reasoning. Figure 5.6 illustrates the (already presented) response time evolution throughout the cycles of the experiment. The horizontal lines represent the upper and lower bounds for the yellow class. The problem is with the jagged profile of the curve: if labels were to be assigned based on the simple comparison against the defined thresholds, sequences of subsequent cycles that are crossing the thresholds would be alternatively assigned different labels. This behavior is counterintuitive and undesired, as the accumulation of soot is expected to occur gradually.

The approach used to lessen the entity of this problem is based on the assumption that subsequent cycles should have similar response times, based on the earlier considerations. Thus, in order to smooth the curve, values have been replaced using a moving average. For the i^{th} value, a moving window is centered in that value and encompasses the surrounding k right and k left elements, resulting in a window of $2k + 1$ total elements. k is a parameter that needs to be configured based on the desired result. Intuitively, low values of k result in a limited smoothing effect (at its extreme, $k = 0$ leaves the curve unaltered); instead large values of k lead to an exceedingly smoothed curve, with a loss in local significance ($k = n_{cycles}$ transforms the curve into a constant function).

An acceptable trade-off has been found using both quantitative and qualitative approaches. Since the problem that is being solved is that too many changes in label occur, a plot of the number of total changes of label as k increases (Figure 5.7) has been analyzed. The knee of the curve is located around $k = 2$ (i.e. a window size of 5 elements).

Although the identified value for k is intuitively small, a visual inspection of the profile of the smoothed curve with this value helps understand whether the resulting alteration in values is acceptable or not. Figure 5.8 shows the results for

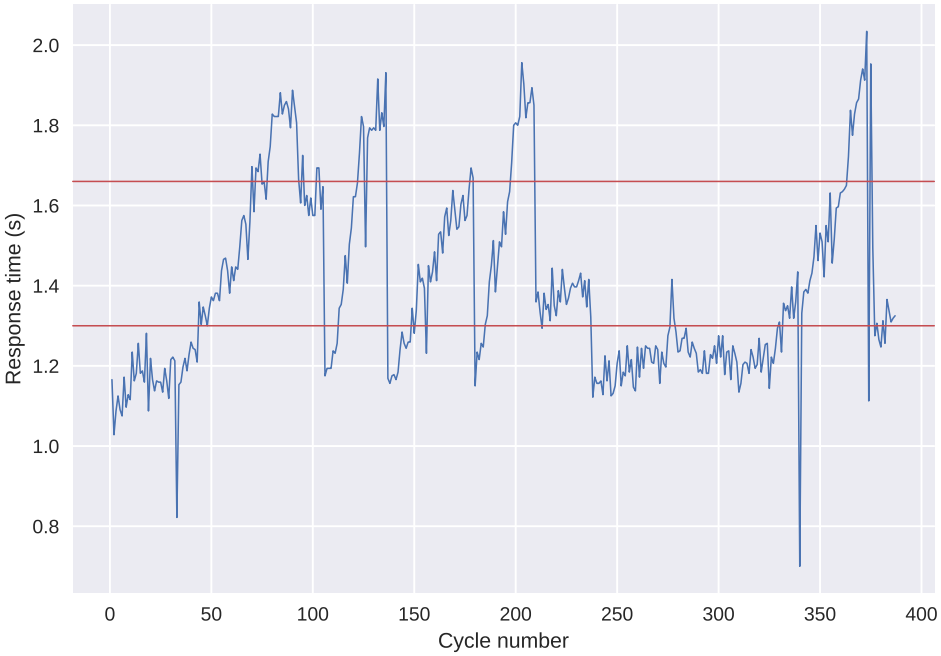

Figure 5.6: Response time trend throughout the experiment. The horizontal lines show the positions of the thresholds

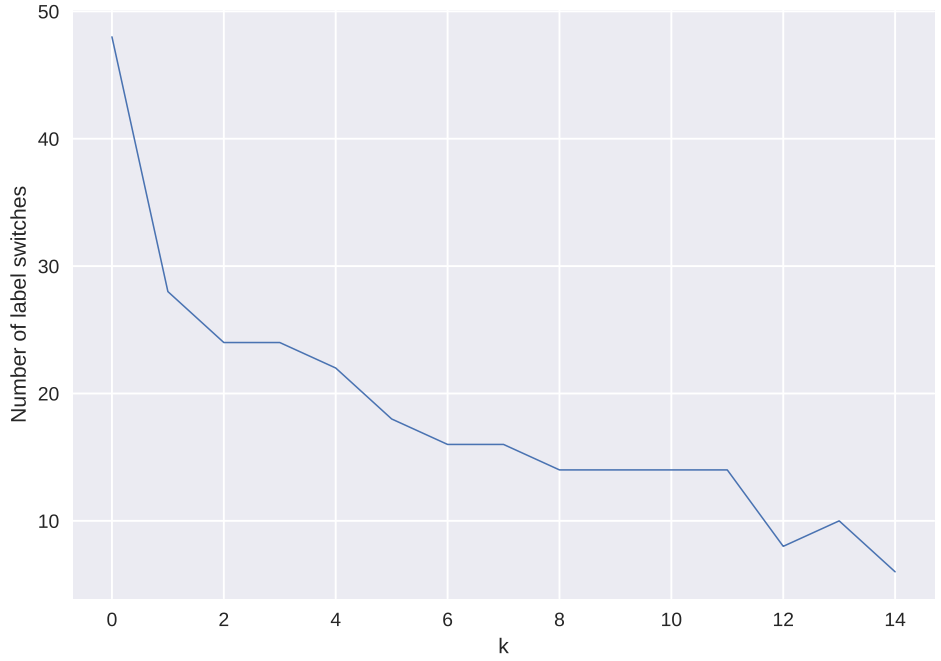

Figure 5.7: Number of label switches occurring as k increases

4 different values of k (0 through 3): the vertical bands are colored based on the assigned label for each cycle. In general, the profile of the curve for $k = 2$ has been deemed acceptable from this perspective as well.

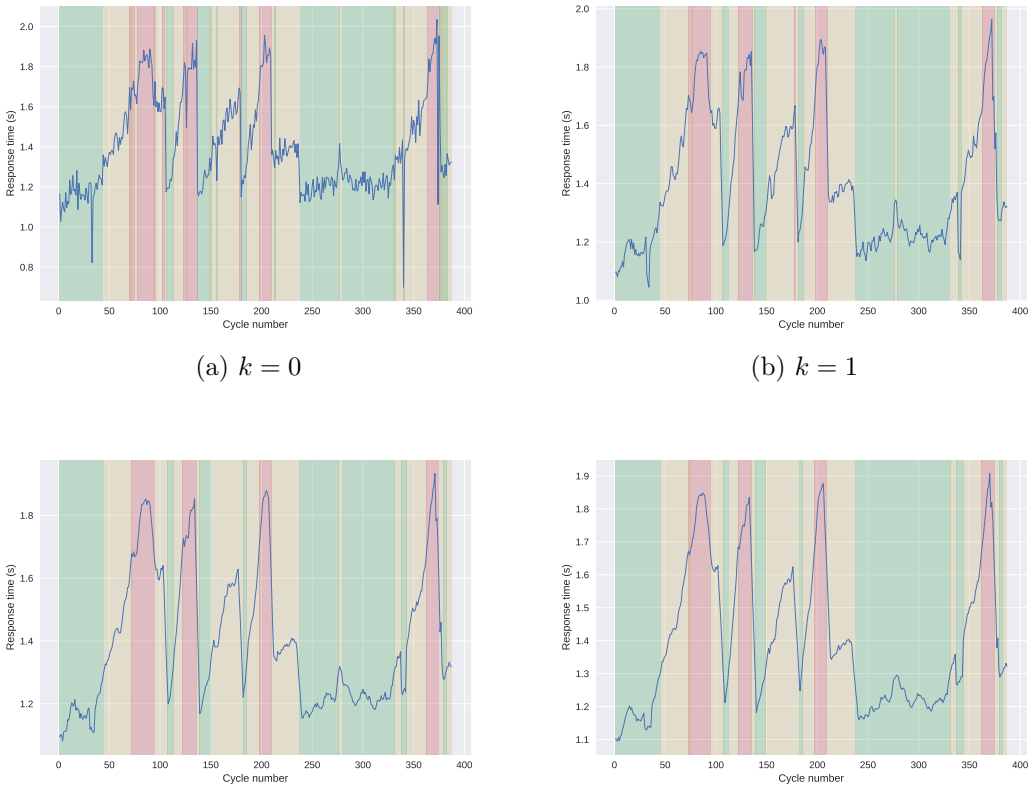

(a) $k = 0$

(b) $k = 1$

(c) $k = 2$

(d) $k = 3$

Figure 5.8: Response time trend smoothed with different k values

From the smoothed values, the labels can be assigned to each ProgramB cycle: the cardinalities for the three classes are reported in Table 5.2. The ones proposed are the values derived from those ProgramB values that have a ProgramA counterpart: as explained in Section 6.3, some ProgramB cycles are missing the ProgramA counterpart (or vice versa), thus reducing the total number of data points available.

Class	**Cardinality**
Green	164
Yellow	163
Red	61

Table 5.2: Cardinalities for the three identified classes

Chapter 6

Data preprocessing

The data that will be processed by the classifiers is the one coming from ProgramA. This data, though, is not in a shape that can be easily digested and used by the classifiers. This chapter will explain why, along with the decisions made in order to improve the situation.

6.1 Feature selection

The feature selection process is required in order to remove redundancy from the description of the system (i.e. the cycle) available. Some of the advantages that come with a reduction in the number of variables are:

- More concise representation of each cycle: this makes the entire problem easier for the classifiers to handle, particularly in light of the limited number of cycles available
- Easier understandability of the classifier: some of the classification models tested are interpretable. If a lower number of variables is provided, the generated output will consequently be more concise and understandable
- Better collection of data on the field: considering the long-term applications of this process, collecting a lower number of signals would result in a reduction in terms of both costs required for the sensors used and bandwidth needed for the transmission of the signals to a centralized server

Some of the common approaches used for dimensionality reduction that consist in combining available features to produce new ones (e.g. the Principal Component Analysis [11]) are not suitable for this kind of problem; since the available insights provided by the domain experts would be difficult to translate to the new set of combined variables. As a result, the feature selection applied needs to preserve

the existing features and discard the redundant ones: because of that, the desired output of this operation is a subset of the original variables.

6.1.1 Correlation-based feature selection

The first step in this direction is that of defining a method for determining the similarity between any two signals in a given cycle. The most straightforward approach is that of using the Pearson correlation coefficient, defined (for two datasets $x = \{x_1, ..., x_n\}$ and $y = \{y_1, ..., y_n\}$ by Equation 6.1.

$$r = \frac{\sum_{i=1}^{n}(x_i - \bar{x})(y_i - \bar{y})}{\sqrt{\sum_{i=1}^{n}(x_i - \bar{x})^2}\sqrt{\sum_{i=1}^{n}(y_i - \bar{y})^2}} \tag{6.1}$$

The main advantages of this coefficient is that it represents the similarity using a scalar number and, additionally, this number is bounded between -1 and +1. Values close to -1 indicate strong negative correlations, while positive correlations have coefficient values approaching +1. Values close to 0, instead, represent no linear correlation.

In order to understand whether actual redundancy exists within the variables available, the correlation coefficient between each pair of variables has been computed for a cycle, using a subset of variables: the resulting correlation matrix has then been plotted as a heatmap. Figure 6.1 represents the correlation matrix for one of the cycles available. At a glance, the correlations between variables are evident.

Before the definition of the feature selection process, some variables can be discarded *a priori*. The first significant pruning occurs when removing all the test bench variables: these, as explained, are not available on vehicles and, as such, should not be considered (as requested by the company). The second elimination regards discrete variables: these have been set aside as they are hardly comparable with continuous signals. Dropping these variables also discards constant signals, which contain no information expected to be relevant and complicates the computation of the correlation coefficients (introducing Not a Number – or NaN – values). An entire category of variables (the one containing information on the fault status of the system) has been ignored upon instructions. The number of variables that made it this far varies from 31 to 37. The final pruning occurs because ProgramA cycles contain a variable number of signals: the reasons for this are unknown, but the result is that only a subset of all signals is shared among all cycles. The feature selection process should only be applied to this subset of variables since, if any of these non-ubiquitous features were to be selected, the following steps would have

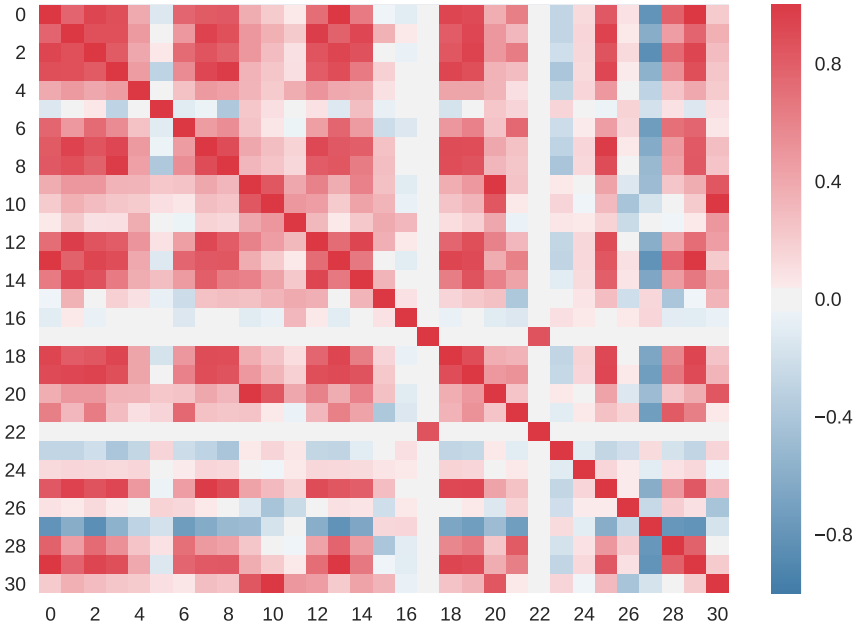

Figure 6.1: Heatmap for the correlation matrix for a given cycle. The variable names have been replaced with numbers for visualization's sake

to deal with missing values, adding complexity instead of reducing it. The total number of features kept, therefore, is of 31.

The selection algorithm has been designed so as to iteratively extract the most representative variables from the initial pool of available signals, so as to finally have a list of independent (where "independent" can be defined in terms of correlation) variables ordered by descending degree of representativeness of the other signals. The following are the steps of the algorithms.

1. For each cycle k, the correlation coefficient between each pair of variables i and j is computed and stored as $r_{k,ij} = r_{k,ji}$.

2. For each pair of variables i and j, the overall correlation coefficient $r_{ij} = r_{ji}$ is computed as the average correlation coefficient for that pair of variables over all the cycles: $r_{ij} = \frac{1}{n} \sum_{k=1}^{n} r_{k,ij}$

3. The list of "remaining variables" L is initialized with all the variables available

4. For each variable i in L, the sum of squared correlation coefficients s_i is computed: $s_i = \sum_{j \in L} r_{ij}^2$

5. The variable

$$b = \underset{i \in L}{\operatorname{argmax}}\, s_i$$

is extracted from L as the most representative of the variables left

6. All variables $v \in L$ such that $r_{vb} \geqslant r_{min}$ are extracted from L in that they are well represented by b

7. If L is empty, the algorithm terminates, otherwise it continues with Step 4

Algorithm 1 contains the pseudocode that implements these steps.

Algorithm 1 Correlation-based feature selection

```
1:  function FeatureSelection(C, V)
2:      R_k ← {}
3:      R ← {}
4:      for k ← C do
5:          R_k[c] ← {}
6:          for i ← V do
7:              for j ← V do
8:                  R_k[k][i][j] ← corr(get(k, i), get(k, j))
9:              end for
10:         end for
11:     end for
12:     for v ← V do
13:         for w ← V do
14:             R[v][w] ← 0
15:             for k ← C do
16:                 R[v][w] ← R[v][w] + R_k[k][v][w]
17:             end for
18:             R[v][w] ← R[v][w]/|C|
19:         end for
20:     end for
21:     L ← V
22:     B ← {}
23:     while |L| > 0 do
24:         b ← null
25:         s_b ← 0
26:         for v ← V do
27:             s ← 0
28:             for w ← V do
```

```
29:                 s ← s + R[v][w]^2
30:             end for
31:             if s > s_b then
32:                 s ← s_b
33:                 b ← v
34:             end if
35:         end for
36:         append(B, b)
37:         for v ← V do
38:             if |R[v][b]| ⩾ r_min then
39:                 drop(L, v)
40:             end if
41:         end for
42:     end while
43:     return B
44: end function
```

6.1.2 Tuning of the r_{min} parameter

The correlation-based feature selection algorithm presented requires a single parameter r_{min} to be selected. This parameter represents the minimum correlation coefficient below which two signals are considered as not strongly correlated: the selected features will all be correlated with a coefficient smaller than r_{min}. Redundant features that are dropped by the algorithm, on the other hand, are correlated with only one of the "representative" features with a coefficient larger than or equal to r_{min}.

The selection of this value requires making a trade-off between the number of selected features and their ability to well represent the discarded variables. The value can be selected either by setting an *a priori* constraint on the desired representativeness of the selected features, or by studying the evolution of the number of selected features as the coefficient changes.

Since the algorithm takes the absolute value of each correlation coefficient (because negative correlations are correlations nonetheless), it makes sense to only analyze values for $r_{min} \in [0, 1]$. Intuitively, $r_{min} = 0$ implies that the lowest number of variables is selected (possibly only 1), given that each selected feature "covers" all others that are not completely independent from it (i.e. correlation coefficient not 0). By contrast, setting $r_{min} = 1$ results in the largest number of features selected, as each selected feature only covers for the completely correlated ones.

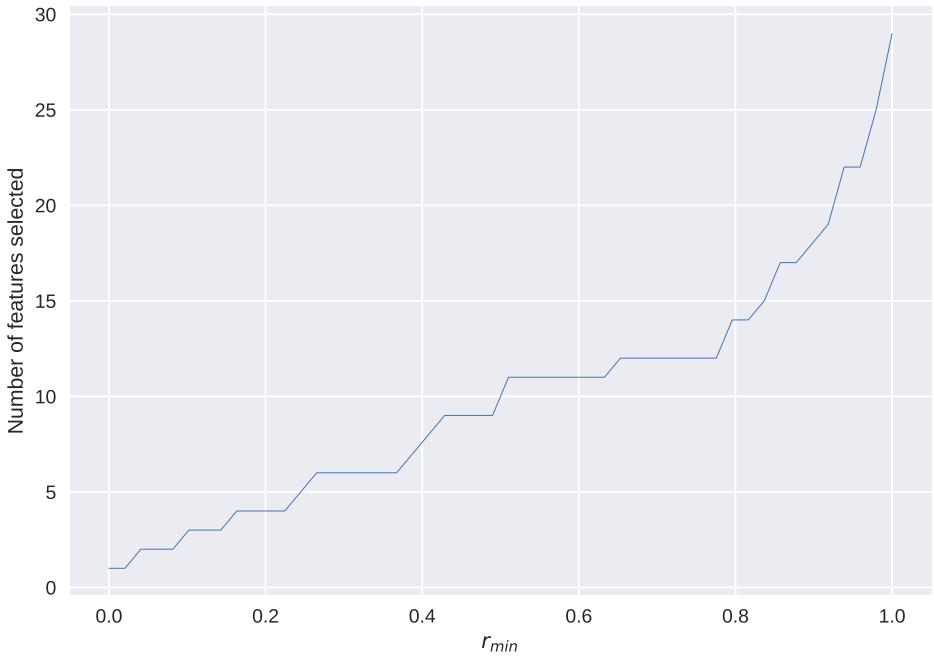

Figure 6.2: Number of features selected as r_{min} increases

Figure 6.2 illustrates how the number of features selected grows as r_{min} increases. The elbow of the curve occurs slightly below the 0.8 value: in order to "play it safe", 0.8 has been chosen for r_{min}. Using this large correlation threshold guarantees that all discarded signals have a very strong correlation with the selected ones, keeping the amount of discarded information to a minimum.

6.1.3 Selection outcomes

The described feature selection algorithm was applied to the available ProgramA cycles, in order to reduce the overall number of features to be further processed. The algorithm selected the 14 features shown in Table 6.1.

The feature selection algorithm presented is the result of an iterative refinement process, with intermediate results that provide interesting insights on the dataset. Furthermore, even though the selection process is only required to lower the number of features used, the results yield useful information (e.g. which features are being monitored redundantly): because of this, and in order to validate the results of the ProgramA feature selection, the algorithm has been tested on the ProgramB cycles as well. Since this chapter is dedicated to the description of the identified process, these additional experiments do not belong here: as such, they will be presented in Subsection 12.1.1.

Variable name
variable_concentration_NOx_B
variable_pressure_rail
variable_angle_fuel_AD
variable_quantity_fuel_C
variable_temp_engine
variable_quantity_reductant
variable_percent_oxygen_A
variable_quantity_fuel_A
variable_quantity_fuel_B
variable_valve_position_A
variable_temperature_exh_gas_1
variable_temperature_exh_gas_3
variable_temperature_manifold
variable_NOxCatalist_Storage

Table 6.1: Features selected from ProgramA

6.2 Data transformation

The feature selection process narrowed the number of ProgramA variables from 50 down to 14. Since ProgramA collects approximately 3750 samples for each variable for each cycle, the number of potential inputs for the classifier is $14 \cdot 3750 = 52500$. While this number of features is not, by itself, unapproachable, it is when backed by a limited number of instances (i.e. cycles). Even the most generous of estimates for the adequate features/instances ratio is far from considering 390 cycles as enough to handle 52500 features.

As a consequence, the number of features needs to be somehow lowered to a more manageable number. The most intuitive approach would be that of sampling the signals with an adequate sampling frequency. After analyzing the spectra of the variables, this option has been discarded, as a sampling frequency lower than the one already adopted would result in a significant loss of data. Furthermore, in order to get the number of features down to a manageable number (approximately 1000, a similar order of magnitude to that of the instances), the sampling frequency required would have had to be that of Equation 6.2, where $n_{features}$ is the number of desired features (1000), n_{vars} is the number of variables available after the feature selection process (14), and T_{cycle} is the duration of the cycle, in seconds (3750).

$$f_s = \frac{n_{features}}{n_{vars} \cdot T_{cycle}} \tag{6.2}$$

The resulting sampling frequency is approximately 0.02 Hz, equivalent to a period of 50 seconds, an unacceptable value. As a consequence, a different approach is needed.

6.2.1 Summarization of the signals

An alternative to sampling is that of summarizing each signal using a limited number of statistics: since this number is independent of the number of samples, the total number of features used can be tuned based on the necessities. Defining the right statistics to use is not trivial, and can be done by iteratively evaluating subsets of statistics in terms of performance of the resulting classifier. As will be shown, the initial choice for the statistics results in a satisfying classifier and is stable in certain situations of interest. Because of that, and because of the significantly time-consuming operations that would be required in re-training and re-tuning the classifiers, the initial decision for the summary statistics has been kept, knowing that possible alternatives can be explored and evaluated quantitatively.

6.2.2 Summary statistics definition

Given the significant consumption of time that comes with testing each group of summary statistics, an attempt at defining meaningful ones was made. The following considerations stem from previous experience and from the understanding of the problem at hand.

Mean and standard deviation

The first two summary statistics introduced are the mean and the standard deviation for each of the sampled signals. These two values allow to identify behaviors where the signal is offset by a positive or negative amount (mean) and the entity of the oscillations around the mean, summarizing the entity of the amplitude of the signals (standard deviation).

Percentiles

The mean and the standard deviation are enough to describe a gaussian distribution, but this assumption of normality does not hold for the distribution of samples for the signals. As such, additional information is required. One such piece of information chosen are the percentiles: a percentile indicates the value below which a given percentage of samples fall.

Given the potentially infinite number of percentiles available (though the limited number of samples is an upper bound), a meaningful subset of these needs to be identified. A first visual approach was that of plotting the cumulative distribution functions for each variable of a subset of green and red cycles[1], and

[1]Note that this requires already having defined the label for each ProgramA cycle. This will

draw conclusions on the most meaningful percentiles based on where the curves differed the most (the CDF maps values in the distribution to their percentile). This approach has been attempted, but a visual inspection only took into account a limited number of cycles and did not yield overall meaningful results.

The second approach has been that of sampling the $0 \div 100$ interval evenly, drawing *a posteriori* conclusions on whether this sampling needs to be changed. The initial percentiles used are from 10 to 90 with increments of 10, for a total of 9 percentiles.

6.2.3 Introduction of the derivatives

For each of the 14 variables, $9 + 2 = 11$ statistics are used, for a total of 154 features. This number is significantly lower than the initial 52500. The price paid for this reduction is that the time component is no longer represented: the statistics summarize the distribution of values, not their evolution over time.

In order to partially reintroduce this lost components, the 11 summary statistics have been computed for the "derivatives" of each signal, thus doubling the overall number of features, but still keeping it down to a manageable number.

The "derivative" of a signal is computed as the difference between subsequent samples: as such, a more accurate definition would be that of difference quotient. For practical reasons, the terms will be used interchangeably throughout the text.

The introduction of the distribution of the derivatives' values partially models the time component: slower signals will have a distribution of derivatives shifted towards lower absolute values and vice versa.

Since the difference quotient can be easily computed from the available data and does not impact too greatly the total number of features, all derivatives have been kept throughout the definition of the process. Adding the derivatives, though, doubles the number of features, from 154 to 308: this might affect the performance of the classifier. Because of this, additional experiments where the derivatives have been discarded are available in Subsection 8.5.1.

6.3 Mapping ProgramA to ProgramB

The pairing of ProgramA and ProgramB cycles is required in order to assign the right labels to the ProgramA cycles available. The two systems have different approaches to recording the date and time. While seemingly trivial, some implementation details are noteworthy.

be explained in Section 6.3, but the information required for the operation makes it feasible at this point in the process

6.3.1 ProgramA timestamping

The naming convention adopted for the recording of the ProgramA files required the final part to be `YYYYMMDD_hhmmss` (Year, Month, Day, hour, minutes, seconds). This represents the date and time the recording was started. The `master` variable represented the time (in seconds) throughout the cycle, starting from 0. With the information available, the Unix timestamp (i.e. the number of seconds elapsed from the midnight of January 1^{st}, 1970) for the beginning and the end of each ProgramA cycle can be computed (the end timestamp is the initial timestamp plus the final value for `master`).

6.3.2 ProgramB timestamping

For ProgramB, the situation is more straightforward: one of the variables available as part of each ProgramB file is called `TASTimeStamp` and, as the name suggests, it contains the Unix timestamp, in microseconds, for each sample. The minimum and the maximum values for this variable provide the initial and final timestamps for the final part of the cycle.

6.3.3 Overlapping ProgramA and ProgramB

Despite the intuition that the ProgramB recording is the final portion of the ProgramA cycle, pairing ProgramA and ProgramB files based on the latter's timestamps being included in the former does not successfully match all cycles. This happens because, in many cases, the ProgramB recording was stopped *after* the ProgramA one. Additionally, the fact that the number of ProgramA and ProgramB cycles available is not the same implies that there may be ProgramA files without an ProgramB counterpart, and possibly vice versa. Because of this second consideration, both initial and final timestamps need to be considered when matching the cycles.

The approach used is that of allowing some "slack" time after the ProgramA cycle ends: in other words, the final ProgramA timestamp is increased of a small number of seconds t_s (10 seconds has been found to be enough) before finding the match. The match between the ProgramA cycle with start and end timestamps $T_{s,c}$, $T_{e,c}$ and the ProgramB cycle with $T_{s,i}$, $T_{e,i}$ occurs if $T_{s,c} < T_{s,i} < T_{e,i} < T_{e,c}+t_s$.

After the introduction of the slack time, 388 out of the 390 ProgramA cycles available were matched with their ProgramB counterpart. The result is significantly better than an earlier attempt that did not factor in this detail: while not significantly important from the theoretical point of view, it is still an detail that should be kept into account when replicating the study.

Chapter 7

Classification

7.1 Classification

The data available is now labelled and partially transformed. Some additional transformation (to normalize the dataset) will be used for the classifiers that are sensible to this kind of operation. This section will be concerned with the exploration of different classification models, selected based on their strengths and weaknesses. Each classifier will be tuned and evaluated based on specific performance metrics. Finally, the best results achieved will be presented.

7.1.1 Classifiers used

In literature, a myriad of classifiers have been presented, each with its strengths and weaknesses: there is no classifier that is overall preferable to others. In order to get the best results, different classifiers with different pros and cons have been tested. The study has been carried out with two purposes in mind: the first one is that of learning what is that actually drives the problem, the second is that of building a performant classifying algorithm. Because of this, the chosen algorithms leverage either of these two aspects. The models used are proposed below.

Decision tree

Decision trees are a classification model based on a tree structure [12]: the training phase builds the tree, while the classification phase requires, for each input, to traverse the tree from the root to one of the leaves. Each leaf contains a label that is assigned to the input being processed upon landing on the given leaf. Each node of the tree contains a test on one of the features of the input: based on the outcome of the test, one of the branches is followed and new tests are performed, until a leaf is reached.

Many advantages of the decision trees have made them a successful classification model. Upon these, their interpretability is one of the most important ones. Unlike most classifiers that act like black boxes, decision trees provide clear explanations for the choices made, since each decision is in the form of a test on the input features. This does not happen with other classifiers such as neural network or Support Vector Machines: precisely for this reason, and because the company was interested in understanding the reasoning behind the classifications made, decision trees have been introduced as part of the proposed classifiers.

Another advantage of decision trees is the rapid training time. This is allowed by the greedy approach used for the construction of the tree structure. At each node, the split introduced is chosen basing the decision only on local optimality, measured in terms of homogeneity (or purity) of the splits (using indicators such as the Gini index [13]). The classification is even faster, since assigning a label is a matter of traversing the tree.

Each root-to-leaf path in the decision tree can be rewritten as a rule to be followed to label new data: in short, the label of the leaf is assigned if the logical AND of the tests of the nodes on the root-to-leaf path is verified.

On the other hand, decision trees have some limitations that render them inadequate for complex problem. Some problems are intrinsic in the nature of the model, while others can be partially overcome.

One such problem is the tendency of decision trees to overfit the dataset: the generation process keeps expanding the tree until all the training points are perfectly labelled: when small groups of points need to be split, the criteria used for the split may not be significant at all, and only be relevant to the points being used. Because of this, the model naturally tends to overfit the training set, yielding unsatisfactory results for new predictions. This problem can be mitigated by introducing an early stop in the expansion of the tree: when a set depth is reached (or the split has reached a set purity), the splitting process is halted and the label assigned to the leaf is that of the majority class present. A classification model that stems from decision trees and overcome this problem is the random forest: a number of decision trees are created using different subsets of the training set and decisions are made based on the predictions of the totality of the trees. This approach has not been pursued for this project because of the low number of data points available.

Another harder-to-overcome problem is that due to the type of separation made by the algorithm. The tests made by decision trees only use one variable at a time: considering the input space, decision trees can only split points using hyperplanes that are orthogonal to the dimensions available. As such, simple problems (such as that of splitting points on a 2D plane using the $y = x$ function) cannot be solved

efficiently.

The interpretability of decision trees has been valued beyond these limitations and, as it will be later discussed, the overall results of this classifier have been satisfying. As part of the proposed results, Figure 7.2 shows one of the decision trees built using the available dataset: in this case, the hyperparameters optimization made it so that trees deeper than a certain value are truncated, thus reducing the effect of overfitting (if this is not the case and the tree is expanded until all leaf nodes are pure, the leaves are very fragmented, with one or two samples each and with test nodes that base their decisions on "noise" contained in the dataset).

Neural networks

Neural networks are one of the most popular machine learning algorithm, with many applications in the most diverse fields. Of the different types of neural networks available (each with different applications, implementations, advantages and limitations), the one used for this classification problem has been the Multi-Layer Perceptrons (MLP) one [14].

An MLP uses a base unit called a perceptron: this perceptron has a list of inputs and a single output. The inputs are taken into account for the decision of the output based on weights learned during the training phase: a weighted sum of the inputs is then passed through a so-called activation function to get the output. This activation function is typically non-linear: the non-linearity is what makes the perceptron interesting when combined in layers (as it is the case with MLP). A single perceptron can handle problems where the input space can be separated using a single hyperplane. For more complex problems, multiple perceptrons organized in multiple layers can be used.

The training phase requires iterating multiple times through the inputs available, so as to tune the weights according to the desired outputs. At each iteration, the weights of each neuron are adjusted based on how well the network behaved (when compared to the expected result) using algorithms such as the backpropagation one. After a fixed number of iterations, or when the weights are no longer updated (because a local optimum has been reached) the training stops, and the network is ready to be used. The fact that the training iterates multiple times over the inputs available makes the model robust against noise, but the process is particularly time consuming (particularly when the number of neurons to be trained is large). Additionally, neural networks are characterized by a large number of hyperparameters that need to be tuned: as explained in Subsection 7.1.2, the tuning of these values require generating and evaluating a large number of classifiers: given the long time required for training each neural network, the overall training time may at times be prohibitive. Trade-offs between the size of the network or the

number of hyperparameters tuned and the time required often need to be made.

Neural networks can tackle complex problems, but they are not free from some limitations that prevent them from being a universal solution (as they are sometimes portrayed to be). One of these limitations is that of the time-consuming training: despite that, the training is done sporadically and pre-trained models can be exported to low-performance devices. Once trained, new predictions require little time and computing power.

Neural networks, differently from decision trees, are a non-interpretable model: matrices of weights are all that can be analyzed. While some inferences can be made based on the weights of some networks, this model is generally referred to as being a black box. While this is not a problem when getting a prediction, some scenarios may require valid reasons to support the decisions taken by an algorithm: neural network do not provide this kind of explanation. Because of this, and because – as already stated – the company requested some insights on the functioning of the models, neural networks could not be selected as the only model proposed.

Support Vector Machine

A third model used is the Support Vector Machine (SVM) [15]. Unlike other models (such as neural networks) that try to find one possible hyperplane (or more complex functions), an SVM finds a plane so as to maximize the distance between the clusters of points for each class and the plane. This is a convex optimization problem and, as such, the solution found is guaranteed to be a global optimum, rather than a local one: this represents one of the best features of SVM. Another advantage is that SVM can separate both linearly separable and non-linearly separable classes, depending on how the classifier if configured.

SVM share the same significant disadvantage neural networks have: they are not interpretable and, additionally, they do not even provide the confidence of the prediction, which may in some cases be considered desirable. This negative aspect has been mitigated, as already mentioned, by introducing decision trees as an additional classifier.

Classification rules

Classification rules (and, in particular, RIPPER [16]) have been tested as an alternative to decision trees. Like decision trees, this classification model is interpretable, with the additional advantage of reducing the complexity of the extracted rules when possible: decision trees, due to their root-to-leaf path, do not have this property (in some cases, some of the tests may be redundant but cannot be omit-

ted, as they are part of the already-build tree).

Despite this advantage, the preliminary results obtained with the classification rules were not promising, often worse than those obtained with the decision trees. For this reason, this classification model has been set aside.

7.1.2 Validation

Each classifier has a series of parameters that need to be set *a priori*: these are called hyperparameters, to separate them from the parameters that are tuned during the training.

Different combinations of hyperparameters need to be tested, in order to find the best configuration. Using the entire dataset to first train and then assess the quality of classifier would result in overfitting, since the hyperparameters would be tuned to best suit the dataset. On the other hand, splitting the dataset in a training set and a test set would result in smaller datasets: given the already small size of the original dataset, this option should not be pursued.

This problem is solved by using the k-fold cross-validation technique. It requires splitting the dataset in k equal parts, or folds. Then, k different classifiers are trained: for each one of them, $k-1$ parts are used for training and 1 for testing. The operation is repeated k times, until all folds have been used once as test set. The results of each classifier (in terms of the metrics defined in Subsection 7.1.3) are combined to obtain an overall performance index. Figure 7.1 explains how this process occurs.

Typically, the k folds are selected randomly from the dataset. Given the low cardinality of the "red" class, forming random folds may result in some folds containing no red cycles at all, thus resulting problematic in terms of efficiency. For this reason, a variation of the k-fold technique, called stratified k-fold, has been used instead: in this case, the samples for each fold are selected so as to preserve the original distribution of labels.

Basing the evaluation of each hyperparameters configuration on cross-validation, a grid search for the best configuration has been carried out: for each hyperparameter a set of possible values has been defined, then each possible combination of values has been tested and evaluated. Eventually, the most promising configuration has been selected.

7.1.3 Performance evaluation

A performance index needs to be defined in order to understand how well a given classifier is behaving. All the indices proposed in this study require the computation of the confusion matrix C, an $n \times n$ matrix, with n being the number of labels.

The cell at the i^{th} row and j^{th} column C_{ij} contains the number of elements that belong to the i^{th} class and have been assigned, by the classifier, to the j^{th} one. As such, the elements on the main diagonal are those that have been correctly assigned, the others are not.

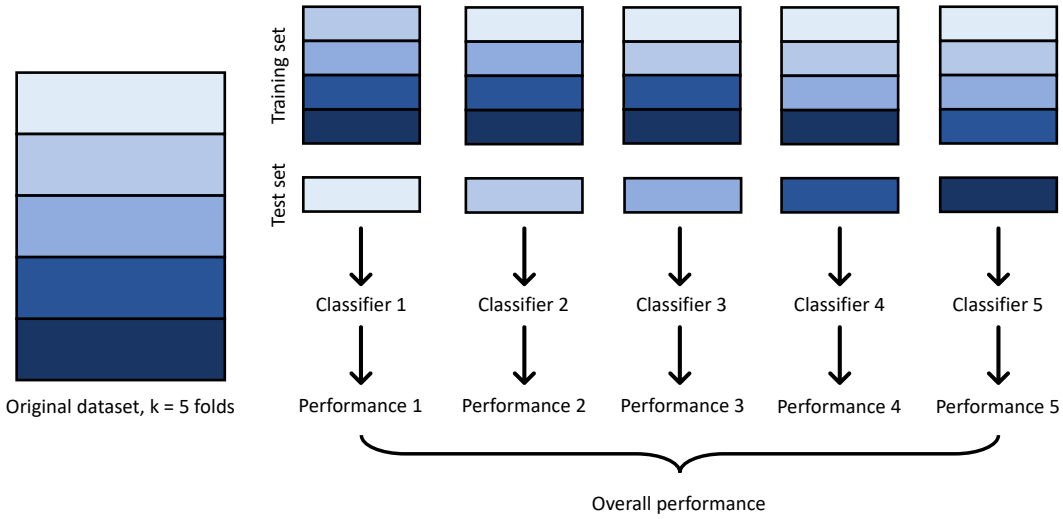

Figure 7.1: Explanation of the k-fold validation procedure

The first metric used is the accuracy: this is defined as the fraction of elements that have been assigned correctly to their class. Equation 7.1 defines the accuracy in terms of confusion matrix values.

$$accuracy = \frac{\sum_{i=1}^{n} C_{ii}}{\sum_{i=1}^{n}\sum_{j=1}^{n} C_{ij}} \tag{7.1}$$

While accuracy is a useful metric in some cases, it presents a significant flaw that makes it unreliable in particular scenarios such as the one at hand. When the classes are unbalanced (i.e. there are minorities and majorities), a classifier that predicts all elements as belonging to the majority classes will get large accuracy scores, given the small impact that the minority classes have on this metric.

Unfortunately, the minority classes are most often the ones that are of most interest, as it happens with the clogging problem: the ultimate goal of the project is that of detecting the presence of soot. Consequently, the classifier needs to be good at recognizing minority elements.

For this reason, other metrics, called precision and recall, have been introduced. These metrics are defined for a class k according to Equations 7.2 and 7.3. For a given class, the precision represents the fraction of correctly assigned samples

among all the samples assigned to that class, while recall represents the fraction of correctly assigned samples among all the samples that are known to belong to that class. Precision and recall, for this classification problem, have been defined for all classes, but the focus was on the red one, being this the one considered as the most interesting.

$$precision = \frac{C_{kk}}{\sum_{i=1}^{n} C_{ik}} \tag{7.2}$$

$$recall = \frac{C_{kk}}{\sum_{i=1}^{n} C_{ki}} \tag{7.3}$$

These two metrics are in "conflict" between one another: maximizing the precision implies only classifying those elements that are certainly part of the red class, thus missing out on the "dubious" ones, resulting in a low recall, and vice versa. Because of this, the harmonic mean of the two metrics, called the F_1 score, has been taken instead. Equation 7.4 defines the F_1 score in terms of precision and recall.

$$F_1\ score = 2 \cdot \frac{precision \cdot recall}{precision + recall} \tag{7.4}$$

The F_1 score for the red class has been used as the main criteria for evaluating the classifiers in order to assess how balanced they are. From the collaboration with the manufacturer, though, it was pointed out that, since having the oxygen sensor checked is a hassle for the car owner, precision should be preferred over recall: in this way, the number of false positives is reduced to a minimum. Section 8.7 will consider this alternative option.

7.1.4 Results

The results are proposed in terms of accuracy, precision, recall and F_1 score for the green, yellow and red classes. Although all these metrics are reported in the presented tables, the ones of most interest are those concerning the red class: as explained, this is the minority – yet most interesting – class.

Table 7.1a contains the results for the decision tree classifier, Table 7.1b the ones for the neural network and Table 7.1c the ones for the SVM.

The overall scores are satisfactory, significant of the fact that the classifiers can actually handle the red class well, despite the low cardinality. The decision tree, as expected, performed slightly worse than the alternatives. This underperformance is compensated by the interpretability of the model. Indeed, the tree is the only

	Green	Yellow	Red
Precision	0.8365	0.7529	0.8475
Recall	0.8110	0.7853	0.8197
F_1 score	0.8235	0.7688	0.8333
Accuracy		0.8015	

(a) Decision tree results

	Green	Yellow	Red
Precision	0.8869	0.8679	0.9016
Recall	0.9085	0.8466	0.9016
F_1 score	0.8976	0.8571	0.9016
Accuracy		0.8814	

(b) Neural network results

	Green	Yellow	Red
Precision	0.9026	0.8303	0.8261
Recall	0.8476	0.8405	0.9344
F_1 score	0.8742	0.8354	0.8769
Accuracy		0.8582	

(c) SVM results

Table 7.1: Results for the classification problem

model for which the internal representation can be meaningful: Figure 7.2 shows the decision tree build using the available cycles.

An already mentioned different way of visualizing the performance for each of the classes is that of the confusion matrices. These matrices are reported in Figure 7.3 for each of the three classifiers. The main diagonals of the matrices contain the large bulk of cycles: this means that most green, yellow and red cycles have been classified correctly by the three models, in accordance with the large values of precision, recall and F_1 score obtained.

On top of the already presented tables, the results have been processed so as to provide a visual representation of which cycles are predicted wrong by each classifier. These prediction bars are presented in Figure 7.4. For any of the bars, each vertical line represents the label for a single cycle. The topmost bar shows the correct labels (referred to as truth), as defined by Figure 5.8c. The lines of the following bars, one for each classifier, are gray when the prediction made is correct, and either green, yellow or red depending on the erroneous prediction made.

Additional considerations regarding the results achieved, and how they compare to those obtained during additional experiments, will be made in Chapter 12.

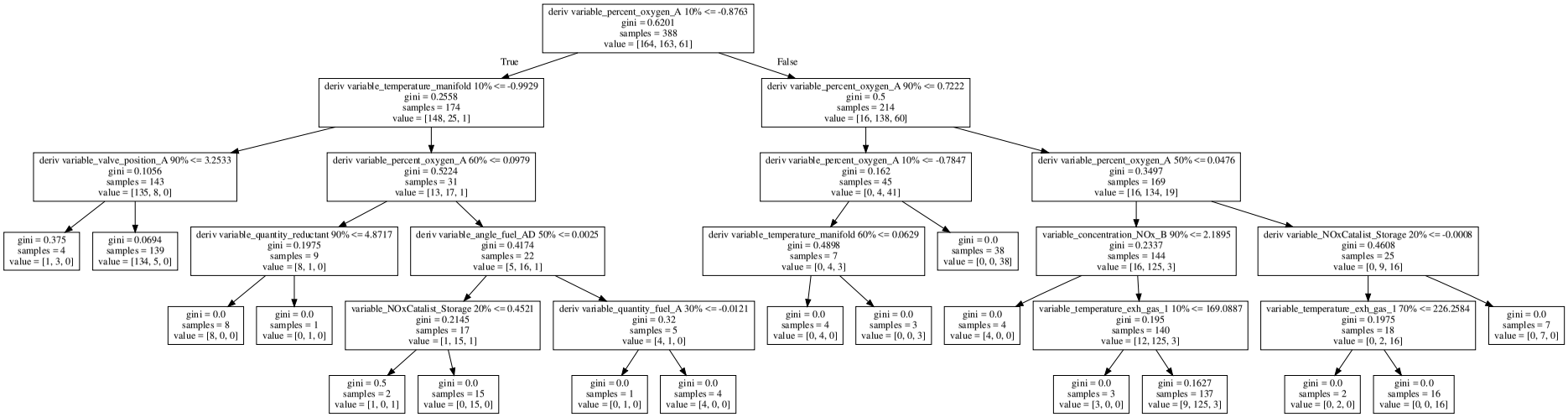

Figure 7.2: Decision tree built using the available dataset

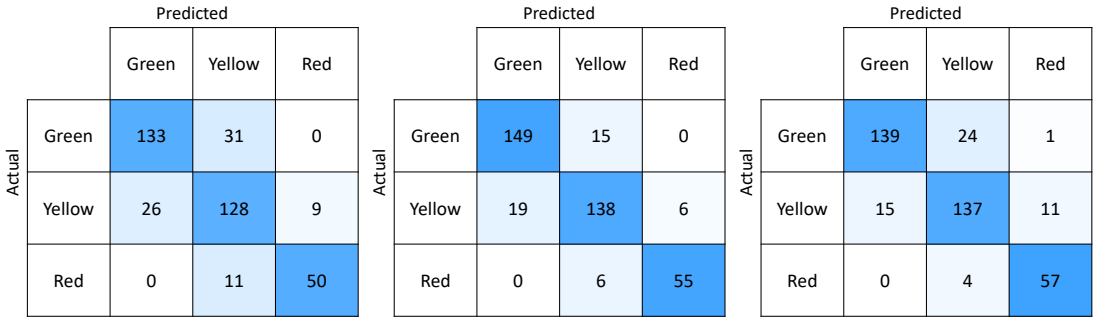

(a) Decision tree (b) Neural network (c) SVM

Figure 7.3: Confusion matrices for the three classifiers

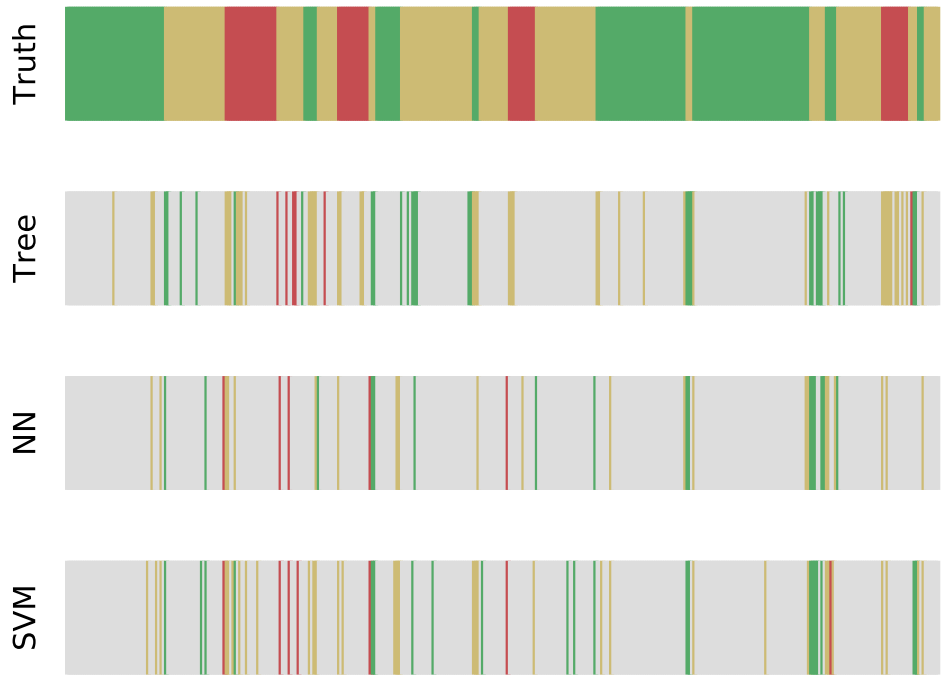

Figure 7.4: Prediction bars for the three available classifiers. The topmost bar represents the correct values, the following bars are gray if the prediction made was correct, or green/yellow/red depending on the (erroneous) prediction the classifier made

Chapter 8

Process explorations

The process presented in Chapters 5 through 7 is the polished result of a more complex exploration of the data available and the possible experiments that can be derived from it. Many of these explorations have yielded interesting results: this chapter is a collection of these, along with the motivations for each one and results achieved.

8.1 Feature selection process

Multiple options have been explored for the feature selection process, both in terms of algorithm used and data processed with it. The result proposed in Subsection 6.1.1 is the one considered to be the most suitable for the process. Some alternative options will be proposed in this section.

8.1.1 Category-ful feature selection

The variables available belong to a number of different categories, depending on their role in the functioning of the engine. While these categories have been considered as opaque, since the domain knowledge available was limited, the variables belonging to each category are expected to be correlated, given the commonalities shared.

As a consequence, an alternative to the feature selection process proposed is the one where, instead of applying it to the entirety of the variables available, the algorithm is applied separately to each set of features belonging to each category. The expected result is that a larger number of features is kept as significant, since inter-classes correlations (expected to exist) are not considered by the selection algorithm, thus introducing some redundancy in the filtered features.

This algorithm was discarded because it does not guarantee the independency (below a set threshold) of the selected features. It has been implemented, and will

be proposed in this section, because it highlights the existing correlations between signals belonging to the same categories, thus providing useful insights on which sensors are actually needed and which are not. This is useful because, as it happens for the original feature selection, it provides insights about which features should be recorded when additional costs occur for each additional recorded variable (as is the case when deploying this solution on a larger scale).

The features selected using this revised version of the algorithm are available in Table 8.1. The overall number of features is at least the same as the number of categories.

Category	**Variable**
press_sensors	variable_press_sens
oxygen_sensors	variable_percent_oxygen_A
temp_sensors_man	variable_temperature_manifold
acc	variable_acc_pos
manifold_sens	variable_engair_flowflowFilt
eng_s	variable_eng_speed
exh_temp_sensors	variable_temperature_exh_gas_2
	variable_temperature_exh_gas_3
eng_temp	variable_temp_engine
DTC	variable_DTC_A
EGR	variable_valve_position_A
NOX	variable_concentration_NOx_B
Fuel_Inj	variable_fuel_quan_1
	variable_quantity_fuel_C
	variable_quantity_fuel_B
	variable_angle_fuel_AD
	variable_quantity_fuel_A
Fuel_rail	variable_pressure_rail
air	variable_pres_boost
Catal	variable_NOxCatalist_Storage
	variable_quantity_reductant

Table 8.1: Features selected using a category-ful feature selection, by category

8.1.2 Feature selection in ProgramB

The entire feature selections done so far has only been applied to the ProgramA cycles available, with no consideration for ProgramB. This makes sense from a process-centric perspective, since the features that need to be processed by the classifiers are those of the ProgramA cycles.

Despite that, the feature selection algorithm can provide useful information about the features available in ProgramB: on the one hand, it provides the same kind of insights it did for ProgramA; on the other, if the features selected are

consistent with the ones selected by ProgramA, it gives validation for the features selected during the process.

Since the number of features in ProgramB is significantly larger than that of ProgramA (440 versus 50) and since the ProgramA features are a subset of the ProgramB ones, a larger number of features is intuitively expected to be extracted from the ProgramB selection with respect to that in ProgramA. These selected features may not be the same as those of ProgramA, since the larger number of features also provides a larger selection pool but, despite that, the features selected by ProgramA should all be represented by those selected in ProgramB.

Table 8.2 shows the list of features extracted in ProgramB, using the feature selection algorithm and the parameters described in Subsection 6.1.1.

Variable
variable_Torque
variable_NOxCatalist_Storage
variable_AirFlow
variable_time_fuel_A
variable_percent_oxygen_B
variable_Temp_coolant
variable_battery
variable_air_intake
variable_angle_fuel_CD
variable_DTC_B
variable_temperature_manifold
variable_Vflow_DPF
variable_temp_Induct
variable_concentration_NOx_A
variable_concentration_NOx_B
variable_percent_oxygen_C
variable_valve_position_B
variable_press_oil
variable_press_amb
variable_time_fuel_corr3
variable_Mflow_DPF
variable_DTC_A
variable_percent_oxygen_D
variable_temperature_exh_gas_2
variable_afr_A
variable_quantity_reductant
variable_ResFlow
variable_model
variable_valve_position_C

Table 8.2: Features selected from ProgramB

Since the ProgramA variables are a subset of those in ProgramB, as mentioned,

it is expected that all the variables selected in ProgramA are well represented by those selected in ProgramB. This, though, is not the case. Table 8.3 shows the matching between the variables from the two datasets. Some of the variables, such as variable_concentration_NOx_B, are selected for both cases as most representative. In other cases, such as with variable_pressure_rail, a different variable is selected in ProgramB (variable_air_intake), but the correlation between the two is still strong: since ProgramB has a larger number of variables available, it makes sense that different variables are selected. In still other cases (the ones highlighted in *italic*), the variables did not even make it through the "correlation matrix generation" phase: this is because these variables were not present in all the ProgramB cycles and have thus been discarded. Since, in these cases, the aggregate correlation coefficients were not available, a different approach has been used to figure out whether the variables were represented by others among the selected ones: a single ProgramB cycle has been selected and the correlation matrix has been computed between the variables of this cycle. Then, the correlation between the ProgramA variable and any of the ones selected in ProgramB is checked. Since this approach only considers single cycles, the results are not as global in nature as the previous one: the result is that, with the threshold of 0.8 for the minimum correlation, none of the three "not found" variables is covered but, by the decreasing this threshold to 0.75, there is a match for all of them. In two of the cases, multiple variables are found to be representative: this can only happen because the feature selection on ProgramB was carried out with a larger minimum threshold (0.8).

8.2 Response time measurement

The initial definition of response time provided was that of the time needed to reach the final 21% oxygen level after the cut-off. This definition is ambiguous since, in many of the available cycles, the 21% level is reached asymptotically, yielding meaningless measurements. On top of this, the high frequency noise on the signals make it hard to detect the exact start of the cut-off.

Because of these reasons, an independent approach to the measurement of the response time has been introduced, as a form of validation of the method proposed by the company's domain experts (reported in Subsection 5.1). This made it possible to verify whether the techniques used yield similar results and, if not, further investigations could be made to figure out what was causing the problem, and which approached behaved the best.

The oxygen level behavior when the cut-off occurs has already been presented in Figure 5.1b. The behavior is approximately that of a ramp. The proposed approach to measuring the response time is that of approximating this ramp with

ProgramA variable	**ProgramB variable(s)**
variable_concentration_NOx_B	variable_concentration_NOx_B
variable_pressure_rail	variable_air_intake
variable_quantity_fuel_A	variable_Torque
variable_quantity_fuel_C	*variable_Torque*
variable_temp_engine	variable_Temp_coolant
variable_quantity_reductant	variable_quantity_reductant
variable_percent_oxygen_A	variable_Torque
variable_temperature_manifold	variable_temperature_manifold
variable_quantity_fuel_B	*variable_press_oil*
	variable_quantity_reductant
variable_valve_position_A	*variable_concentration_NOx_A*
	variable_concentration_NOx_B
variable_temperature_exh_gas_1	variable_air_intake
variable_temperature_exh_gas_3	variable_Vflow_DPF
variable_angle_fuel_AD	variable_angle_fuel_CD
variable_NOxCatalist_Storage	variable_NOxCatalist_Storage

Table 8.3: Matching of features selected in ProgramA with those selected in ProgramB

four segments and measuring the response time on the approximated signal. Two of the segments used are constants, approximating the initial and final oxygen level. The other two segments are used to approximate the rising of the ramp.

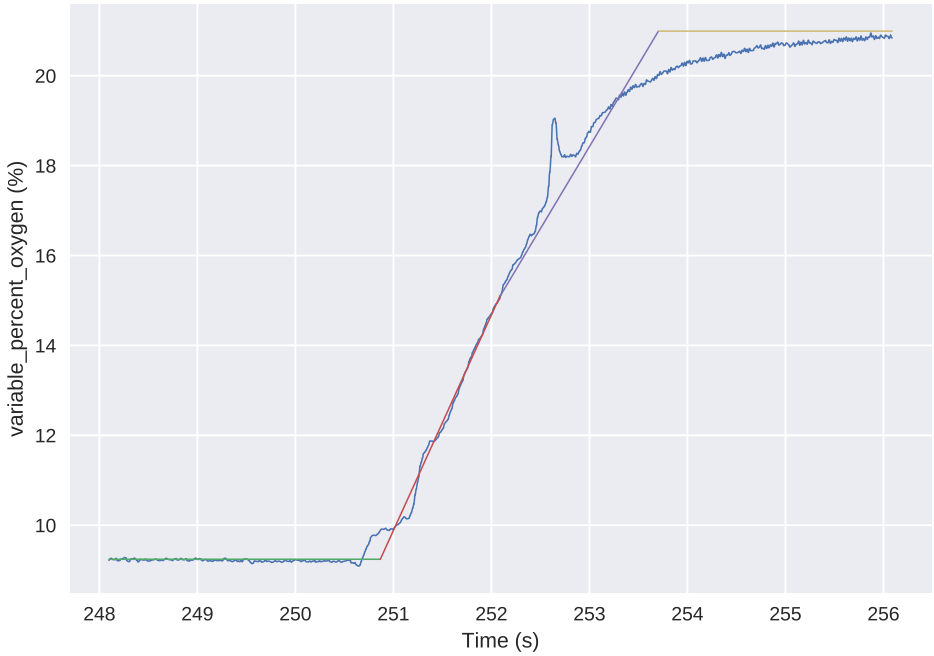

Figure 8.1: Original ramp approximated with 4 segments (represented using different colors)

Figure 8.1 shows the original ramp (in blue) and the four segments using different colors. The identification of these four segments is done following these steps:

1. The bounds where the ramp is contained are identified, as already explained in Subsection 5.1: the ramps for all cycles are required to be in this $245 \div 260$ seconds time slot

2. The initial and final constant values are computed as the average the initial and final N samples (with N selected so as not to be too large and include parts of the ramp, nor too small and only represent a local subset of samples)

3. Given the initial and final constant values, a step signal is built, and it is made slide over the ramp signal. The similarity (measured as the Sum of Squared Errors) between the two signals is computed for each shift. The shift that yields the smallest SSE is selected (Figure 8.2a)

4. The point where the constant value of the step changes is selected as the center of the ramp: this will be referred to as the i^{th} value for the signal

5. The definition of the second (green) segment occurs by iteratively building a line that connects the i^{th} point to the $(i-j)^{th}$ one, with j starting from 1 and increasing until the red (first) segment exists no more. For each different segment, the SSE is computed

6. The first and second segments selected are those that result as having the lowest SSE (Figure 8.2b)

7. Steps 5 and 6 are repeated for the definition of the third and fourth segments, connecting the i^{th} point to the $(i+j)^{th}$ one (Figure 8.2c)

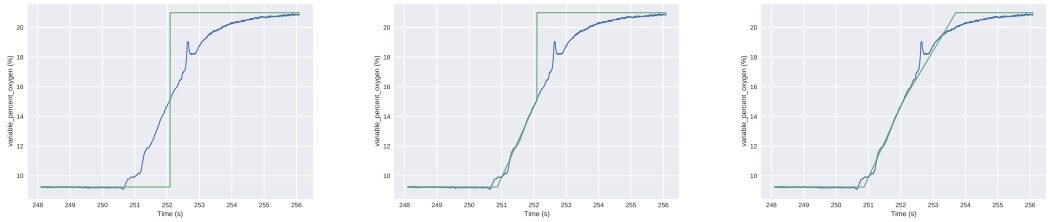

(a) Centering the step function (b) Second segment (c) Third segment

Figure 8.2: Identification of the four segments

Applying this process to all the cycles available then returns a new response time as measured on the approximated signal. This response time, when compared to the original one measured in Subsection 5.1, is expected to be higher: this method measures the entire rise, while the other one stops when 63% of the transition is reached. Figure 8.3 compares the response times measured using the two different approaches. Intuitively, the results are consistent and, by measuring the correlation between the two series of numbers, the resulting coefficient is 0.82: this implies a strong correlation between the two methods.

Only one method is required during the process, and since the company expressed its preference in using the "63%" one, the method described in this subsection has been set aside and only used as a validation of the results obtained. The additional advantage of the original method over this segment-based one is in the reduced entity of the noise introduced: since the original process only focuses on the initial part of the rise (more uniform throughout the cycles), the resulting response times are less subject to uncertain measurements.

8.3 Exclusion of the smoothing process

The smoothing process described in Subsection 5.2.3 transforms the response times measured so as to render them more consistent between adjacent cycles. This

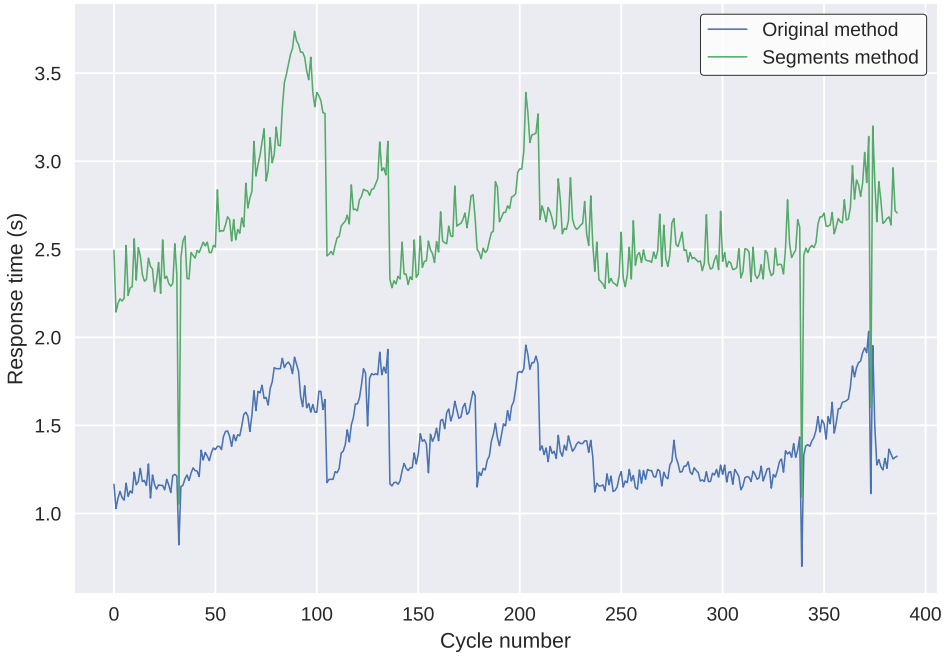

Figure 8.3: Comparison of the response times as measured using the two proposed methods

operation is based on the assumption of continuity between cycles as far as the clogging problem is concerned, but it is true nonetheless that this operation is actually changing the measured values.

In order to assess whether the results of this operation are actually helping towards better classifiers, a separate experiment where the response times have not been smoothed has been carried out (in other words, the k parameter of the smoothing process has been set to 0).

The results of this experiment are proposed in Table 8.4, and the prediction bars are shown in Figure 8.4. The red-related performance of the classifiers are worse when compared to the original problem, while the green-related ones improve. The bars show that the classifier attempts (and fails) to classify as red a large number of cycles: this possibly happens because the cycles labelled as red upon which the classifiers based their trainings were not actually red (notice how some scattered red cycles can now be be found), thus providing unreliable information upon which the classifiers base their knowledge.

The conclusion that can be drawn from this experiment is that the smoothing process is indeed useful in order to improve the classifiers' performance. The effectiveness of the selection of the parameter k could be discussed in terms of influence on the performance of the classifiers. This, as many of the other possible further experiments, would result in a larger number of classifiers being trained,

	Green	Yellow	Red
Precision	0.8855	0.7744	0.7586
Recall	0.8750	0.7987	0.7213
F_1 score	0.8802	0.7864	0.7395
Accuracy		0.8196	

(a) Decision tree results

	Green	Yellow	Red
Precision	0.9226	0.8354	0.7581
Recall	0.9226	0.8302	0.7705
F_1 score	0.9226	0.8328	0.7642
Accuracy		0.8608	

(b) Neural network results

	Green	Yellow	Red
Precision	0.9250	0.8239	0.7681
Recall	0.8810	0.8239	0.8689
F_1 score	0.9024	0.8239	0.8154
Accuracy		0.8557	

(c) SVM results

Table 8.4: Performance results for the classifiers trained with the dataset labelled without applying the smoothing process

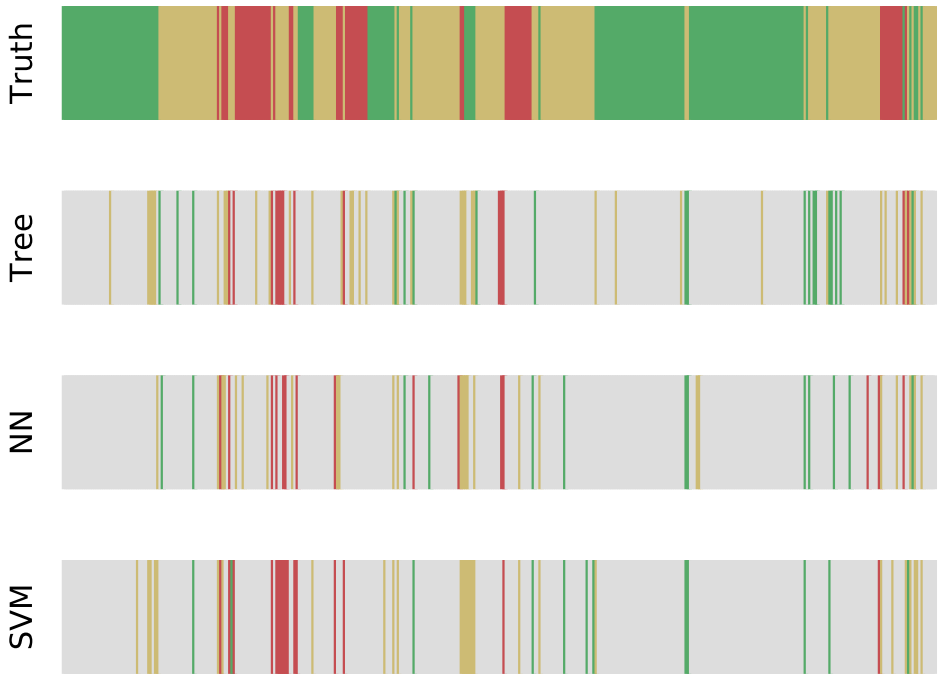

Figure 8.4: Prediction bars for the classifier using labels assigned without the smoothing process

with significant time being consumed for the purpose. Because of this, many of the possible further explorations will not be pursued unless deemed of particular relevance (many additional experiments that did not yield useful results have not been reported).

8.4 Downsampling of the signals

The ProgramA cycles available have been sampled with a frequency of 1 Hz: while this is an acceptable value for a local (and possibly test bench) measurement, it gets unfeasible when this information needs to be sent on the cloud for remote processing: this is the idea behind the scaling up and, in order to even consider having the ECU send the data to a server, the sampling frequency needs to be lowered.

This downsampling is expected to degrade the quality of the signals acquired and, as a natural consequence, this should degrade the performance of the classifier. Starting from this assumption, the F_1 score for each classifier has been computed as the sampling frequency decreases. The result is shown in Figure 8.5, and it is evident that the results are not compatible with the expected degradation.

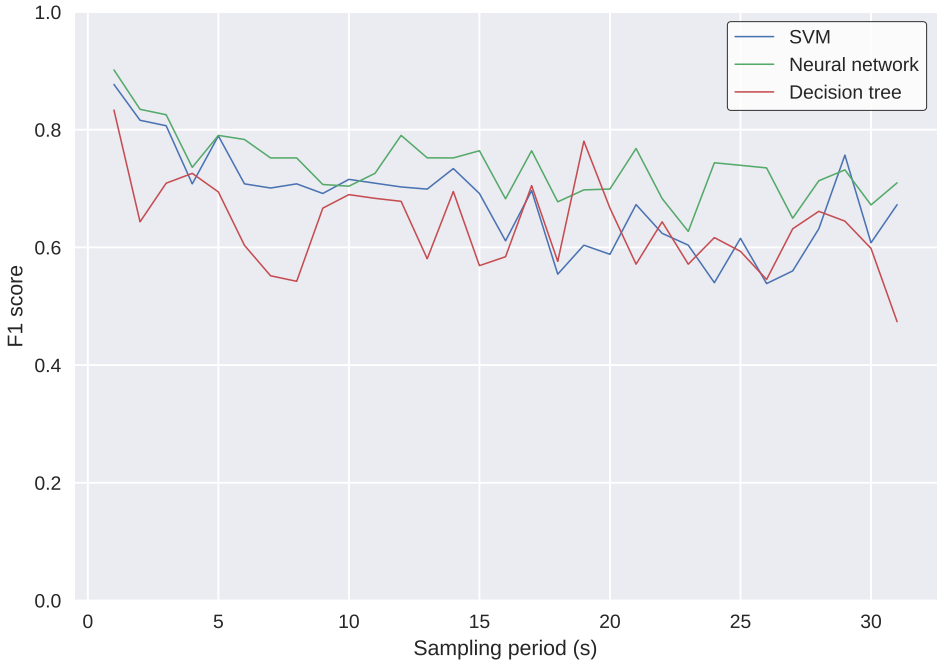

Figure 8.5: F_1 score for the classifiers evolution as the sampling frequency decreases

This may be counterintuitive, but the decision of transforming the input space from a time-based one to one of summary statistics rendered the classifiers robust

to this process of downsampling. The reason for this robustness is easily explained: when the distribution of values is taken into account, the time component is no longer relevant and neither is the total number of samples used. If sampling the signal results in a downsampled signal with approximately the same distribution of values as the original one, the overall distribution that is being considered when extracting the summary statistics does not change significantly, and nor do the summary statistics.

The assumption that the distributions of variables do not significantly change when downsampling should be tested. In order to do this, the original distribution of values has been compared with the distribution of values for the downsampled signals. This comparison has been carried out using the Jensen-Shannon divergence, a symmetric statistical measure based on the Kullback-Leibler divergence. The Jensen-Shanno divergence, defined for two discrete distributions of probabilities p and q by Equation 8.1, is 0 for identical distributions and saturates to $\ln 2$ for completely different ones.

$$JS_{div}(p,q) = \frac{1}{2}\sum_i \left[p_i \ln\left(\frac{2\,p_i}{p_i+q_i}\right) + q_i \ln\left(\frac{2\,q_i}{p_i+q_i}\right)\right] \tag{8.1}$$

For each of the 14 selected variables, Figure 8.6a shows how the Jensen-Shannon divergence evolves as the sampling period increases. Given the boundaries of this coefficient, the distributions do not diverge significantly from the original one. This comparison can be extended all the way to significantly larger sampling periods (e.g. 1000 seconds, with the resulting signals being comprised of three or so samples). Figure 8.6b shows precisely this (the curve has been smoothed using a LOWESS – locally weighted scatterplot smoothing – regression [17], in order to reduce the entity of the oscillations). In this case, as expected, the degradation is much more noticeable. This graph allows, after defining the maximum allowed degradation of the distributions, to decide a suitable sampling frequency.

8.5 Exclusion of strong predictors

So far, all variables available have been used as inputs for the classifiers. This, as shown in some experiments (see Subsection 9.1) introduces variables that are strong predictors, i.e. variables that easily separate the classes. While this is an excellent way of building reliable classifiers, the three problems listed below arise.

The first one is that, since one of the goals of this project is that of understanding the reasoning behind the classifications made (i.e. figuring out which are the variables that are mostly connected to the problem), having a strong predictor may conceal other weaker – yet important variables.

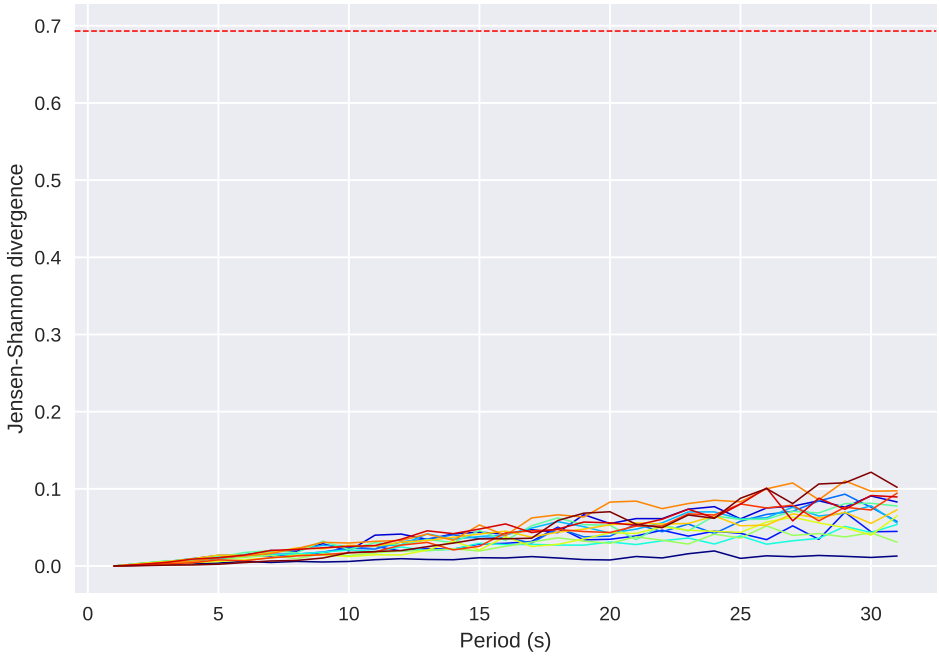

(a) Sampling period range: $1 \div 31$ seconds

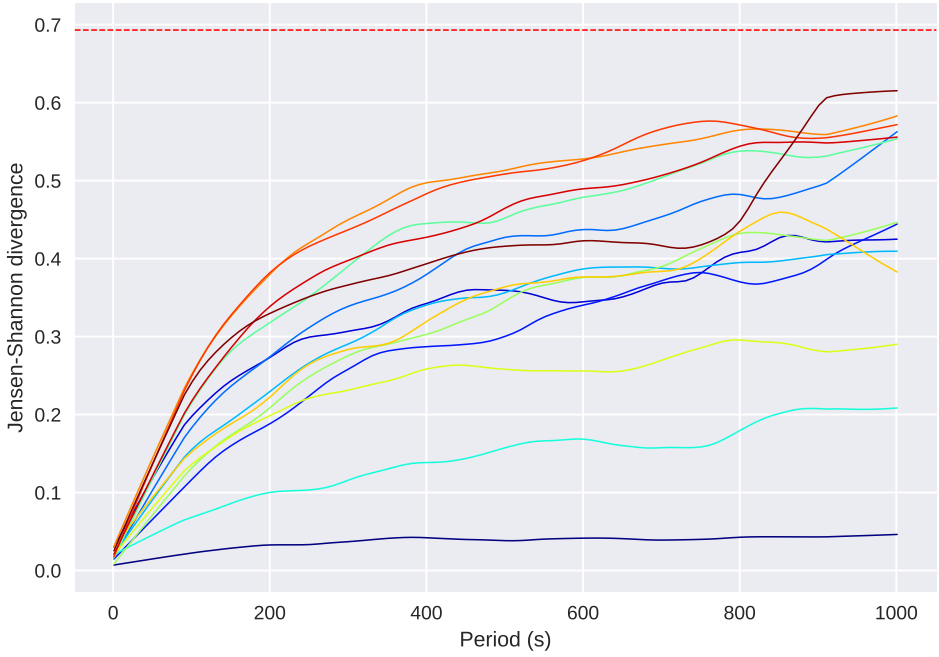

(b) Sampling period range: $1 \div 1001$ seconds

Figure 8.6: Jensen-Shannon divergence between the original and the downsampled distributions

The second problem is that building a classifier that bases its decisions upon a low number of variables (as shown, even just one) may be problematic if the given variable is not available for some reason (also known as the "single point of failure" problem).

The third problem, which concerns the introduction of the derivatives as part of the inputs to the classifier is that, when deployed on a larger scale on actual vehicles, the sampling frequency will be significantly lower (problem described in Subsection 8.4) and, as such, the computation of the discrete derivatives cannot be done[1] with the data available. Since programming ECUs to perform custom tasks (such as the computation of the derivative of the signal locally) is not a guaranteed option, the assumption that derivatives will be available may not hold in the future.

Because of the above, the original three-classes experiment has been carried out excluding first all the derivatives, and then the oxygen variable from the features used as input. These operations are expected to degrade the classifiers in terms of performance; the entity of these degradations will be presented next.

8.5.1 Derivatives

The exclusion of the derivatives from the pool of features available halves the total number of features used to train the classifier. This, on the one hand, reduces the entity of the original "large number of variables" problem but, as shown, derivatives heavily help during the classification process. The latter factor is significantly more influent on the overall results, as is shown by the degradation in performance of the classifiers trained without the derivatives in Table 8.5.

While lower than the original scores, the performance of the classifiers can still be considered acceptable overall, meaning that even the case where the derivatives cannot be computed could be handled satisfactorily.

8.5.2 Oxygen variable

The scenario where the oxygen variable is removed from the inputs is possibly the worst one, since the strongest of predictors is being taken away and the input dimensionality does not decrease significantly (from 208 down to 206 – since the oxygen and its derivative are no longer available). The results are those of Table 8.6 and, as expected, the values are significantly lower than the previously proposed cases. This is representative of the lack of existence of other strong predictors: weaker ones may still exist (given the better-than-random performance achieved),

[1] While it could, the results would yield no significance given the high frequency of most all signals

	Green	Yellow	Red
Precision	0.8537	0.7562	0.6563
Recall	0.8537	0.7423	0.6885
F_1 score	0.8537	0.7492	0.672
Accuracy		0.7809	

(a) Decision tree results

	Green	Yellow	Red
Precision	0.8647	0.8239	0.8305
Recall	0.8963	0.8037	0.8033
F_1 score	0.8802	0.8137	0.8167
Accuracy		0.8428	

(b) Neural network results

	Green	Yellow	Red
Precision	0.8302	0.648	0.697
Recall	0.8049	0.7791	0.377
F_1 score	0.8173	0.7075	0.4894
Accuracy		0.7268	

(c) SVM results

Table 8.5: Results for the classifier trained without the derivatives as inputs

but a combination of them needs to be considered. The decision tree generated, shown in Figure 8.7, shows the predictors identified other than the oxygen level.

	Green	Yellow	Red
Precision	0.7949	0.6089	0.4906
Recall	0.7561	0.6687	0.4262
F_1 score	0.775	0.6374	0.4561
Accuracy		0.6675	

(a) Decision tree results

	Green	Yellow	Red
Precision	0.8485	0.7673	0.6563
Recall	0.8537	0.7485	0.6885
F_1 score	0.8511	0.7578	0.672
Accuracy		0.7835	

(b) Neural network results

	Green	Yellow	Red
Precision	0.898	0.6699	0.6875
Recall	0.8049	0.8589	0.3607
F_1 score	0.8489	0.7527	0.4731
Accuracy		0.7577	

(c) SVM results

Table 8.6: Results for the classifier trained without the oxygen variable as input

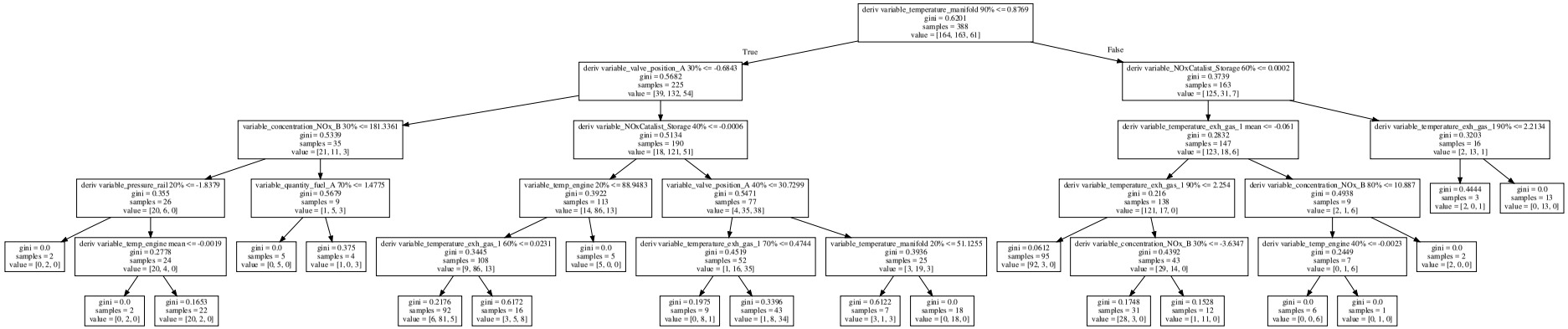

Figure 8.7: F_1 score for the classifiers evolution as the sampling frequency decreases

8.6 Processing the Model2 dataset

The entirety of the experiments and considerations made so far have been using the Model1 dataset because of the reasons explained in Subsection 3.1.4. The Model2 dataset is intrinsically similar to the Model1 one and, as such, it poses as the perfect candidate for the validation of the entire process.

Despite the similarities between the two datasets, the Model2 one has a lower number of records and, when keeping the same thresholds defined for Model1, the number of red cycles is only of 15. Changing the thresholds allows having a slightly larger cardinality for the red class: thresholds at 1.1 and 1.35 seconds have been set. This has significantly changed the proportions of the classes: Table 8.7 contains the number of cycles available for each of the three classes, as defined by the new thresholds.

Class	**Cardinality**
Green	31
Yellow	79
Red	74

Table 8.7: Cardinalities for the three identified classes

Given the large number of red cycles available (compared to the green and yellow ones) the performance of the classifier are expected to be acceptable, despite the lower number of overall cycles. The intermediate results (such as those presented while describing the process in the previous chapters) will not be reported for the Model2 dataset in order to avoid redundancy. Instead, only the results achieved are presented in Table 8.8.

As already mentioned for the previous experiments, the hyperparameters used are those already defined for the original classifiers: as such, the reported metrics could be slightly improved: despite that, given the low fcardinalities at play, the results are already satisfactory.

There are two important takeaways from this experiment: the first is that the defined process can be replicated on new data without any major change (with further considerations on the replicability and its limitations pointed out in Subsection 12.2.2). The second key point is that, as already stated multiple times, the definition of the classes is crucial: when keeping the original thresholds set for Model1, the cardinality of the red class was so low that it did not allow the classifiers to learn anything useful about the clogging problem, with the low performance that came with it.

	Green	Yellow	Red
Precision	0.7353	0.7711	0.8060
Recall	0.8065	0.8101	0.7297
F_1 score	0.7692	0.7901	0.7660
Accuracy		0.7772	

(a) Decision tree results

	Green	Yellow	Red
Precision	0.7647	0.7952	0.8507
Recall	0.8387	0.8354	0.7703
F_1 score	0.8000	0.8148	0.8085
Accuracy		0.8098	

(b) Neural network results

	Green	Yellow	Red
Precision	0.8929	0.7556	0.8333
Recall	0.8065	0.8608	0.7432
F_1 score	0.8475	0.8047	0.7857
Accuracy		0.8043	

(c) SVM results

Table 8.8: Performance results for the classifiers trained on the Model2 dataset

8.7 Precision-based tuning of the parameters

So far, the metric that has been used to evaluate classifiers has been the F_1 score for the red class. This measure is often proposed as a valid metric upon which to base considerations, as it represents the harmonic mean between precision and recall. Despite this theoretical predilection, real-life scenarios may have specific requirements that collide with the standard approaches.

This is the case with the clogging problem: the exchanges with the domain experts brought up the fact that, for the company, it would be preferable to avoid recalling vehicles that do not actually present any problem, as that would be an unnecessary burden for both the customer and the producer. Since this requires increasing the confidence of each "red" prediction, it naturally follows that some "red" cases (the ones where the classifier is not "entirely sure") may not be correctly identified: this, though, can be considered as acceptable, as it would most likely only introduce a delay in the detection of the problem (as the clogging gets worse, the classifier is expected to increase in confidence of the prediction).

The description of this requirement can be translated, in technical terms, to the fact that the classifier should focus on increasing the precision metric, accepting a lower recall score as a result. This requires re-tuning the hyperparameters of the classifiers using, as evaluation function, the precision.

This kind of optimization could result in classifiers that achieve a significantly

high precision but unacceptably low recall scores (e.g. by only predicting as "red" an incredibly small fraction of the actual red cycles, for which the classifier is certain about the outcome): as a consequence, the recall should be treated with an eye of regard despite the initial statement about the lower importance of this metric.

After re-tuning the hyperparameters, the results of the cross-validation are those shown in Table 8.9. The precision is, as expected, higher when compared to the original values. This comes, for the decision tree, with a significant decrease in recall score: this should be kept into account when deciding whether this is the option to with. For the other classifiers the recall has not decreased drastically.

	Green	Yellow	Red
Precision	0.843	0.7572	0.8605
Recall	0.8841	0.8037	0.6066
F_1 score	0.8631	0.7798	0.7115
Accuracy		0.8067	

(a) Decision tree results

	Green	Yellow	Red
Precision	0.903	0.8659	0.9153
Recall	0.9085	0.8712	0.8852
F_1 score	0.9058	0.8685	0.9
Accuracy		0.8892	

(b) Neural network results

	Green	Yellow	Red
Precision	0.8704	0.8059	0.875
Recall	0.8598	0.8405	0.8033
F_1 score	0.865	0.8228	0.8376
Accuracy		0.8428	

(c) SVM results

Table 8.9: Performance results for the classifier optimized using precision as the evaluation metric

Chapter 9

Labelling explorations

The thresholds for the green/yellow/red classes have been defined in Subsection 5.2.2 mostly based on the distribution of response time values, without accounting for any domain knowledge. This implies that the decisions made may not be the best for this problem: changing thresholds and labels would generate different classifiers, which in turn perform differently. An exhaustive exploration of the entire space of possible classes is not feasible, since the response time domain is continuous. Instead, experiments where the already defined classes have been manipulated have been carried out. These experiments show how important the definition of the classes is and how setting different goals result in different classifiers. Re-tuning the hyperparameters for all classifiers is an excessively time-consuming operation, as such the configurations already found for the original classifiers of Chapter 7 will be used instead.

9.1 Red and green binary classifier

A first, "radical" experiment is that of discarding the cycles belonging to the yellow class. This means discarding 163 cycles and training the classifiers using the remaining 225 ones. This substantially impacts the dataset size, but since yellow cycles are the ones that render the problem ill-defined, this experiment has been carried out anyway. The red and green classes are expected to be well separated, since they represent completely clogged cycles and completely unclogged ones, whereas yellow cycles are an intermediate stage that may be difficult for the classifier to label.

Given this uncertainty for the yellow subset, the performance for this experiment are expected to be higher than the ones already achieved in the original one. Indeed, Table 9.1 shows how the three classifiers achieve almost perfect scores.

Understanding why the results are this good is straightforward, since one of the models adopted (namely, the decision tree) is highly interpretable. Figure 9.1

	Green	Red
Precision	0.9939	1.0000
Recall	1.0000	0.9836
F_1 score	0.9970	0.9917
Accuracy	0.9956	

(a) Decision tree results

	Green	Red
Precision	0.9939	1.0000
Recall	1.0000	0.9836
F_1 score	0.9970	0.9917
Accuracy	0.9956	

(b) Neural network results

	Green	Red
Precision	0.9879	0.9833
Recall	0.9939	0.9672
F_1 score	0.9909	0.9752
Accuracy	0.9867	

(c) SVM results

Table 9.1: Results for the binary classification problem

shows the tree built for this simplified problem. The first split, based on the 90^{th} percentile of the derivative of variable_percent_oxygen_A, already partitions the dataset excellently, thus implying that the other models, being capable of even more complex separations, can handle the problem equally well. Figure 9.2 shows the values for the 90^{th} percentile of the derivative of the oxygen for the cycles in each class, with the threshold value identified marked by the vertical line. The red and green classes are indeed well separated by this threshold, as detected by the decision tree.

The already introduced prediction bars showing the position in time of the mispredicted cycles are proposed for this experiment in Figure 9.3.

The meaningfulness of the results of this and of the rest of the experiments will be further discussed in Section 12.3, where overall conclusions will be drawn considering the problem at hand, the results achieved and the methodology that has been laid out.

9.2 Yellow cycles classification by binary classifier

Given the binary classifiers of Subsection 9.1, the yellow, never-before-seen cycles can be classified to the already trained models. Based on Figure 9.2, the intuition is

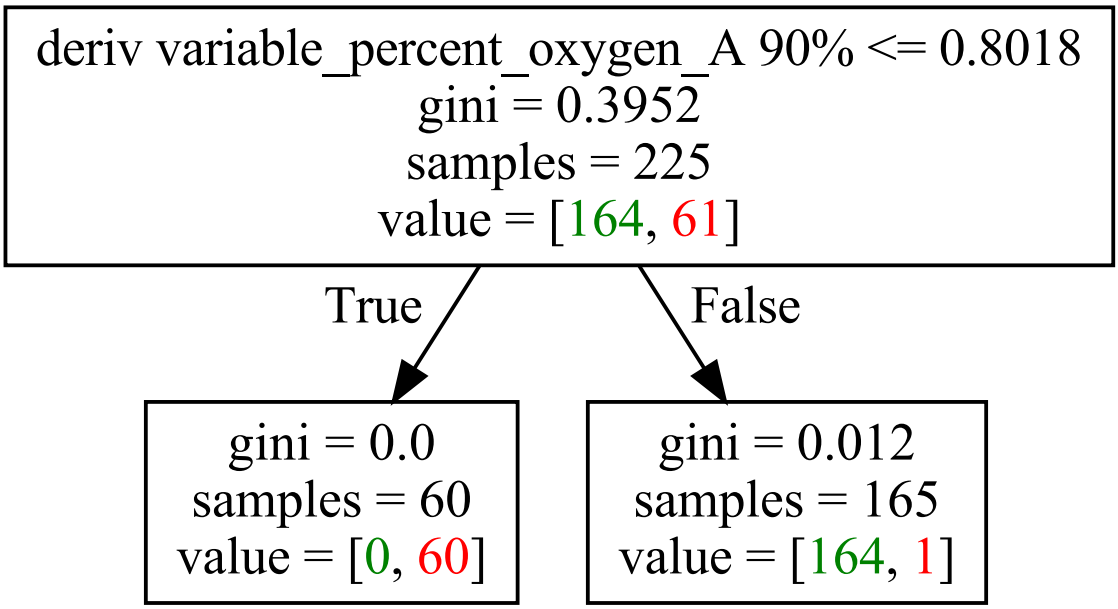

Figure 9.1: Decision tree built for the binary classifier

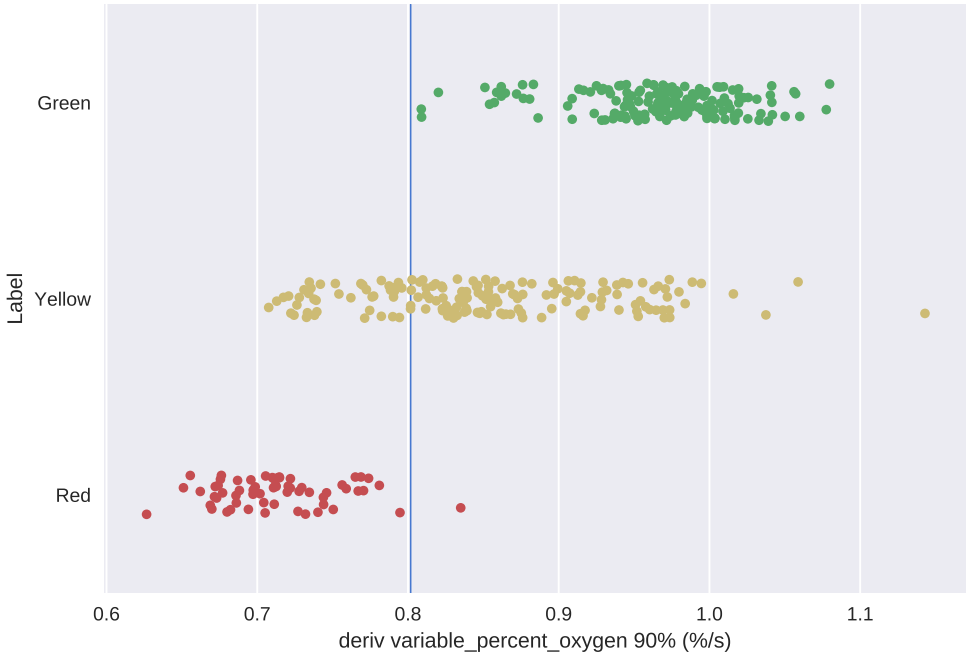

Figure 9.2: 90^{th} percentile of the derivative of the oxygen, by label. The vertical line indicates the split chosen by the decision tree. The vertical jitter has been introduced for visualization purposes

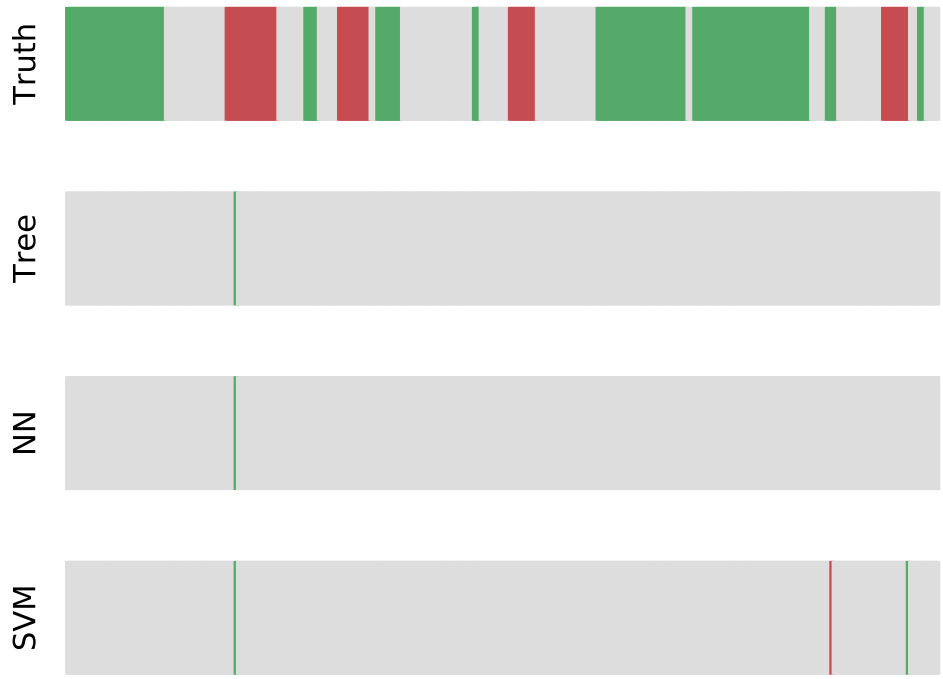

Figure 9.3: Precision bars for the binary classifier

that yellow cycles are classified based on their position with respect to the already identified threshold. In fact, this is precisely what happens for the decision tree, while the other models use more complex functions. Figure 9.4 illustrates the prediction bars for the re-labelled yellow cycles: since the "true" (yellow) label is not known (more precisely, it cannot be known to the classifiers, since they have been trained only using two classes), no mispredictions are shown (and do not exist). Despite that, the prediction bars show how neural networks and SVM roughly make the same predictions as the decision tree, meaning that these more sophisticated models are likely to be basing their decisions on a similar split as that identified by the tree.

9.3 Re-labelling of yellow cycles

The fact that no "true" labels exist for the yellow cycles for the previous experiment can be resolved by introducing a label that is either red or green for each cycle. This new label assignment could be made with the aid of the classifiers of Subsection 9.1 and in particular based on Figure 9.2, but the resulting classifiers would be, by construction, perfect predictors. Instead, the same label could be assigned to all the yellow cycles, with the performance of the trained classifiers as a measure

Figure 9.4: Prediction bars for yellow cycles, as classified by the binary predictor

of how good the change in label was. Since these cycles could be assigned either a red or a green label, both approaches have been tested.

9.3.1 Yellow cycles as green

Labelling all yellow cycles as green implies lowering the fraction of red cycles even further, rendering the problem a binary classification one with the red class significantly smaller that the dominant, green one. This makes it easier for the classifier to improve the green-related performance, while building a narrower, possibly better defined description of the red cycles. The red-related performance metrics (as reported by Table 9.2) are particularly promising and so are the green-related ones.

The prediction bars are illustrated in Figure 9.5. The number of mispredicted cycles is low (as expected, given the high values of accuracy reported) and, as it often occurs, the points of highest uncertainty are those transitioning from green to red and vice versa. This highlights, once again, how crucial the definition of the thresholds is.

	Green	Red
Precision	0.9602	0.7869
Recall	0.9602	0.7869
F_1 score	0.9602	0.7869
Accuracy	0.9330	

(a) Decision tree results

	Green	Red
Precision	0.9785	0.8571
Recall	0.9725	0.8852
F_1 score	0.9755	0.8710
Accuracy	0.9588	

(b) Neural network results

	Green	Red
Precision	0.9844	0.8358
Recall	0.9664	0.9180
F_1 score	0.9753	0.8750
Accuracy	0.9588	

(c) SVM results

Table 9.2: Results for the "yellow as green" binary classification problem

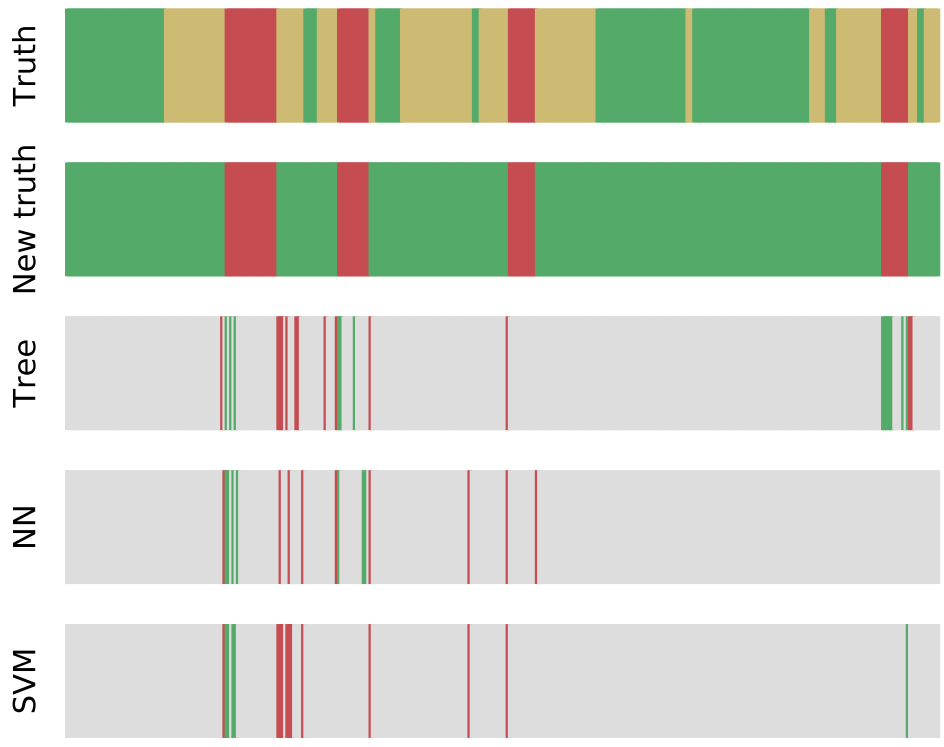

Figure 9.5: Prediction bars for the "yellow as green" binary classification problem

9.3.2 Yellow cycles as red

Labelling all yellow cycles as red changes the balance of the two remaining classes, with the red one now becoming the majority one. The conclusions that can be drawn from this are the same as those of Subsection 9.3.1, with the labels inverted (although the entity of the effect is lessened by the similar cardinalities of the green and red classes – 164 and 224 cycles respectively): the majority class is more easily identified and, indeed, the results in Table 9.3 support this assumption: the classifiers can now predict a larger number of red cycles accurately (as shown by the red-related performance) but the overall accuracy is lower when compared to the "yellow as green" scenario. This might be an indication of the fact that the yellow cycles are more similar in nature to the green, rather than the red ones (Figure 9.2 shows indeed, based on the derivative of the oxygen, why this is the case).

	Green	Red
Precision	0.8457	0.8805
Recall	0.8354	0.8884
F_1 score	0.8405	0.8844
Accuracy	0.8660	

(a) Decision tree results

	Green	Red
Precision	0.8706	0.9266
Recall	0.9024	0.9018
F_1 score	0.8862	0.9140
Accuracy	0.9021	

(b) Neural network results

	Green	Red
Precision	0.9211	0.8983
Recall	0.8537	0.9464
F_1 score	0.8861	0.9217
Accuracy	0.9072	

(c) SVM results

Table 9.3: Results for the "yellow as red" binary classification problem

The prediction bars are shown in Figure 9.6. As expected, the number of mispredictions is larger than that of the other binary classifiers, but the situation is still better than that of the original problem. Once again, the mispredicted cycles are roughly the same for all classifiers, with the decision tree performing worse still, and the neural network and SVM making similar mistakes.

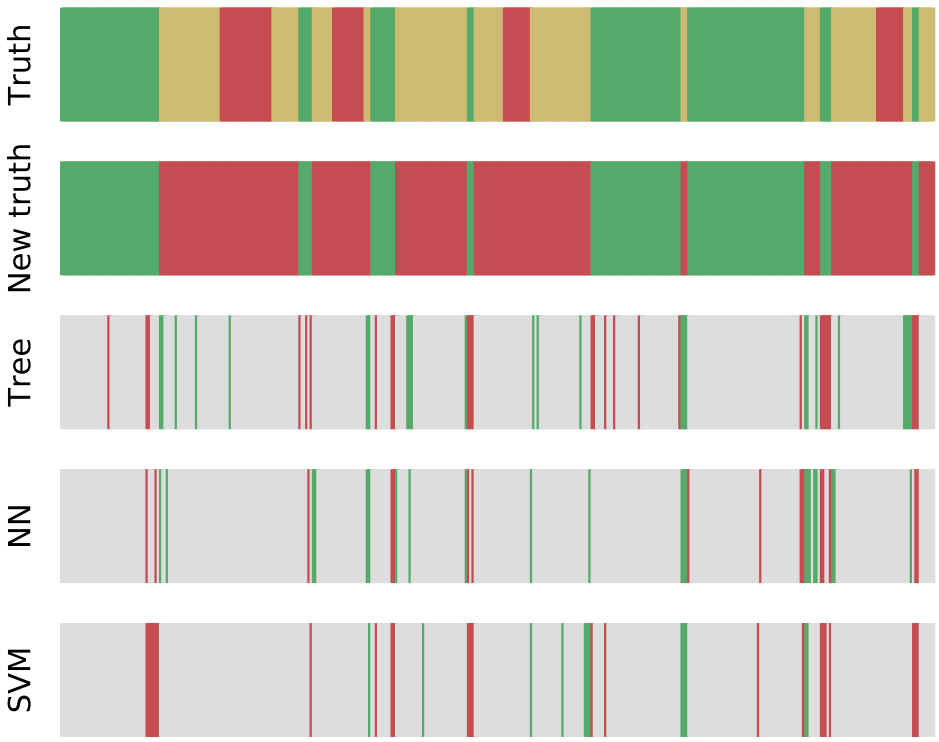

Figure 9.6: Prediction bars for the “yellow as red” binary classification problem

Chapter 10

Clusters analysis

The data exploration required by this project (and some additional ones) have been presented as part of the previous chapters. This chapter will cover some final analyses that have been carried out following the discovery of peculiar behaviors in the available cycles. The results and the conclusions that can be drawn from this section are not relevant to the project *per se*, but are of interest nonetheless and, as such, will be included as part of this thesis.

10.1 Anomalous variables grouping

As already mentioned, only those explorations that have yielded meaningful results have been reported as part of this thesis, with many others (those leading to dead ends or that have been carried out to answer side questions) have been omitted. One such analysis, initially intended to shed light on a problem concerning some faulty readings of a specific sensor, brought up the existence of well-defined clusters within the available Model1 dataset.

This analysis consisted in plotting, for all the available signals (as selected by the correlation-based feature selection algorithm defined in Subsection 6.1.1), mean and standard deviation on a 2D plane. The result is that clusters of similar signals (as represented by the signal's summary statistics used) can be visually identified. Figure 10.1 represents one of these plots for the variable_temperature_exh_gas_1 variable. While some weak clustering might have been expected based on different conditions, the clusters that show up are actually highly cohese, indicating that some cycles are strongly similar to some others, but further away from the rest.

This same behavior shows up for other variables as well, as shown by the plots in Figure 10.2. Different hypotheses can be made regarding the origin of these clusters but, without the required domain expertise and, most importantly, without any direct interaction with the engineers that carried out the experiments, these hypotheses cannot be easily tested. Despite that, Section 10.4 will attempt

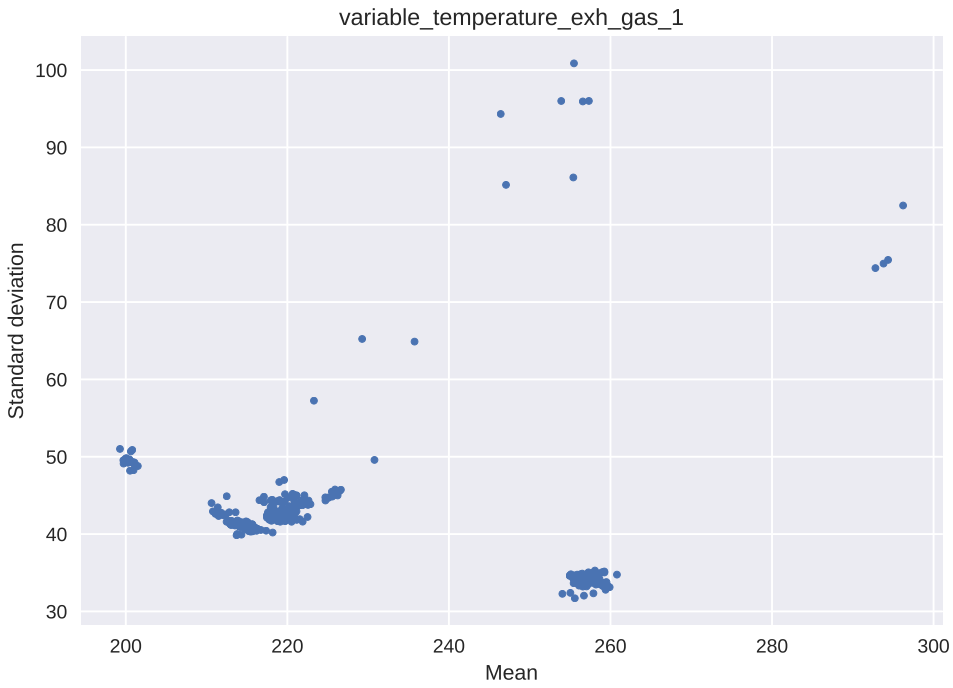

Figure 10.1: Scatter plot of mean and standard deviation of the cycles for the variable variable_temperature_exh_gas_1

to find a plausible explanation.

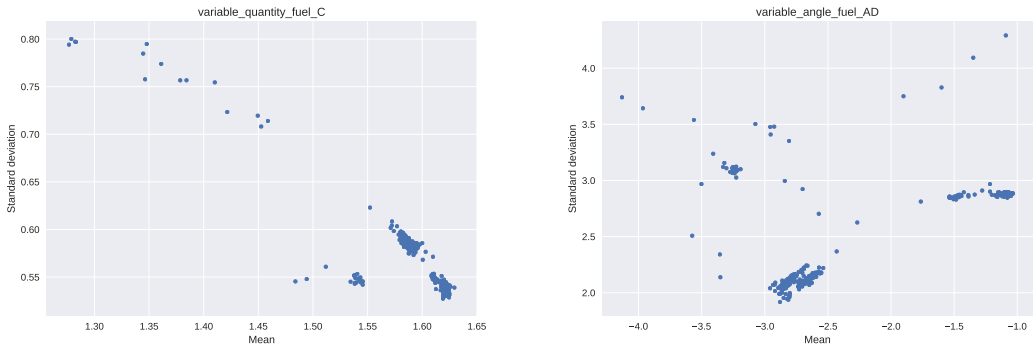

(a) (b)

Figure 10.2: Scatter plot of mean and standard deviation for 2 variables

10.2 Consistency throughout the features

As shown in Figure 10.2, some clusters show up for different variables and, by trying the same approach on different summary statistics available (e.g. plotting the same 2D plot but using percentiles), clusters keep showing up. Before trying to

find possible explanations for their existence, it is first useful to figure out whether the clusters that keep showing up are comprised of the same cycles as the variables change: this section will precisely test this.

10.2.1 Definition of the clusters

A possible approach to deciding whether the clusters are consistent is that of running a clustering algorithm on the available dataset, and draw conclusions based on how cohese the resulting clusters are. This approach, though, presents some problems and does not directly answer the question of whether the initial 2D clusters are consistently the same (the clusters identified would then have to be compared to the initial ones, not really solving the initial problem).

A different solution is that of hand-assigning a label to each of the cycles based on the cluster they visually belong to for a given variable and, after that, visualizing how these cycles are spread for other variables. Since the variable shown in Figure 10.1 already presents well separated clusters, this very plot will be used to define the clusters. Figure 10.3 shows the lines that have been used for their definition. The clusters have been color-coded to make them easier to identify. The top-most, blue "cluster" contains those cycles that might be defined as outliers, as they do not belong to any of the identified clusters.

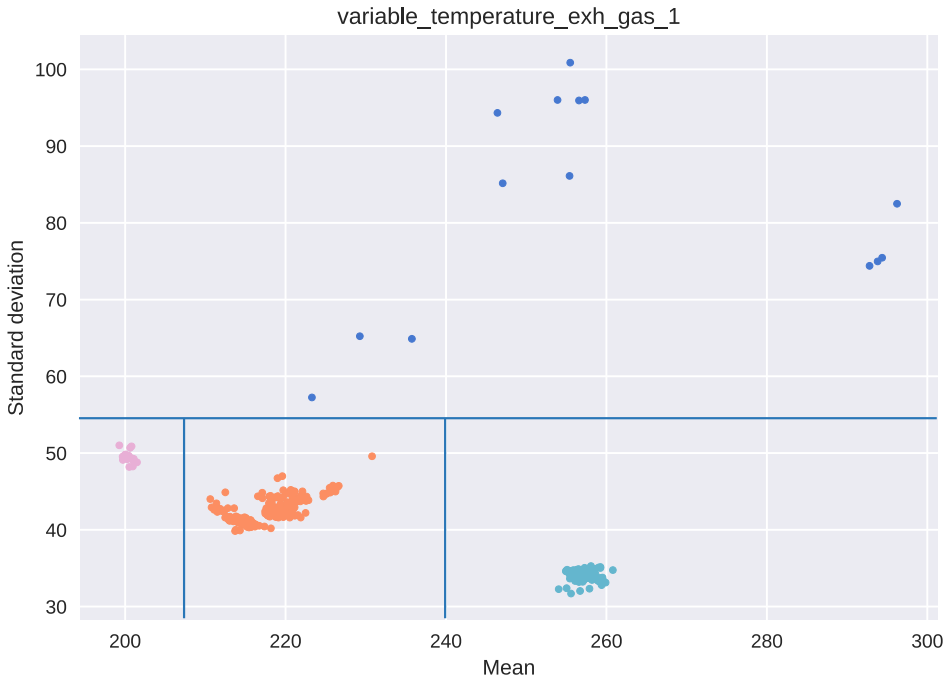

Figure 10.3: Assignment of the clusters based on the mean and standard deviation for the variable_temperature_exh_gas_1 variable

10.2.2 Inter-feature analysis

Figure 10.4 shows the scattering of the cycles for some of the variables. It overall appears that the clusters do show up throughout the different variables consistently. The least clustered variable is variable_temp_engine, shown in Figure 10.4b. The rest of the variables all visually appear to be consistent, with some single points (or cycles) behaving as exceptions: this might be due to the rudimentary label assignment process.

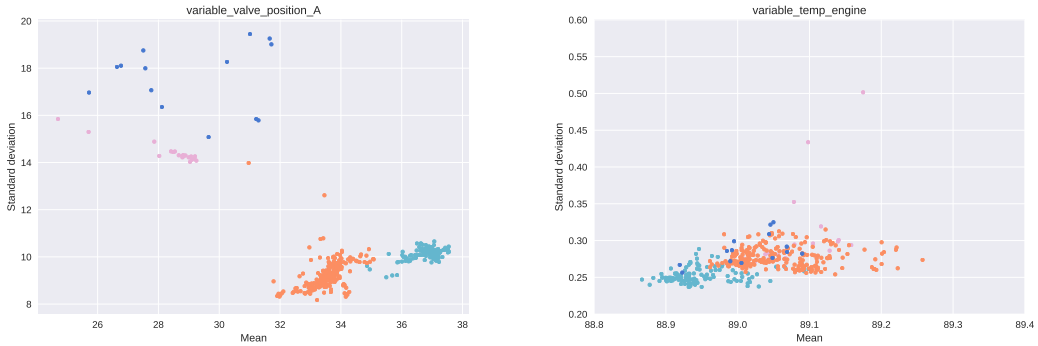

(a) (b)

Figure 10.4: Scatter plot of mean and standard deviation for 2 variables, colored based on the clusters of Figure 10.3

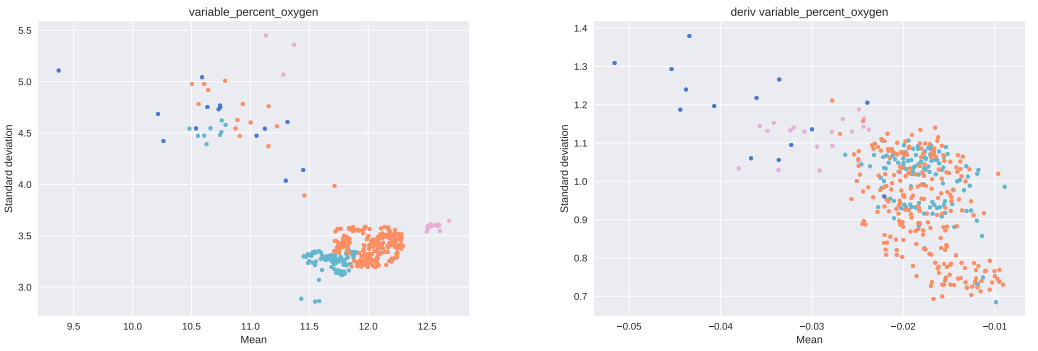

(a) (b)

Figure 10.5: Scatter plot of mean and standard deviation for the oxygen variable and its derivative, colored based on the clusters of Figure 10.3

This is significant of the fact that, regardless of the reason behind this behavior, the overall system is influenced. Figure 10.5 show the scatter of the oxygen level and its derivative, with the color representing the predefined clusters. The oxygen variable appears to be well clustered. As for the derivative, other than the outliers (and, partially, the fuchsia cycles), the rest of the clusters present limited clustering and actually significantly overlap (even more so when only considering the mean).

This serves to show that the derivatives of the signals are not as affected by the clusters as the signal themselves: a possible explanation for this reason is given as part of the discussion of the results, in Section 12.4.

Other than this, the existence of these clusters and the consistency throughout the variables allows for the definition of a unique label for each cycle, allowing for further considerations to be drawn. One such consideration, covered in the following section, is about the distribution of the labels through time.

10.2.3 Clusters definition through time

Each cycle, as explained, can be assigned a unique label depending on the cluster it belongs to. Cycles, additionally, can be sorted based on the moment in time they were recorded (remember that each cycle lasts an hour and that all cycles were recorded in a 2-months period). The already introduced "prediction bars" can be repurposed in this context to display the distribution in time for the clusters. Figure 10.6 shows precisely this. The distribution of the original (red/yellow/green) labels has also been included in order to allow for additional considerations.

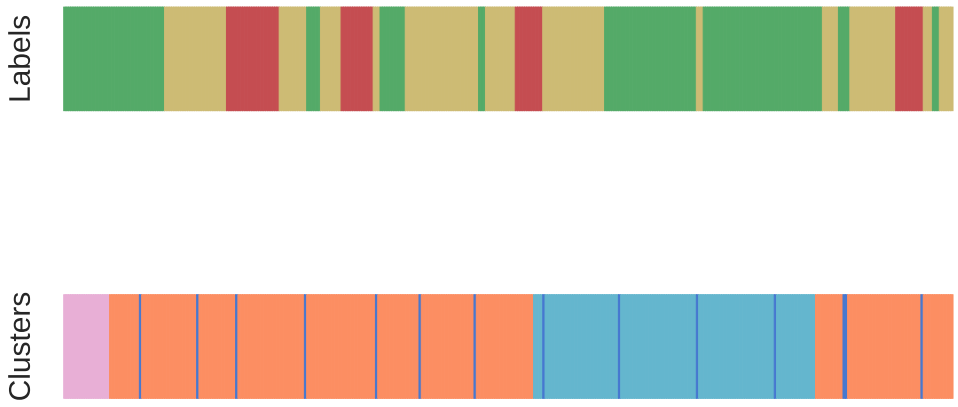

Figure 10.6: Distribution of the labels (top bar) and clusters (bottom bar) throughout the cycles

This figure is of particular interest, highlighting the importance of the time component in the characterization of the type of cycle (as represented by the cluster assigned). Cycles belonging to the same cluster were recorded during similar time

periods, with the exception of the "outliers" (blue) cluster, whose cycles mostly occur at regular intervals.

When compared to the distribution of the original, clogging-related labels, no particular correlations can be inferred. This helps excluding clogging as the cause of this clustering phenomenon. Since no plausible explanation for this behavior has been found by the domain experts based on the already presented work, the following section will focus on providing a better description of the profile of the clusters and the characterizing aspects of the cycles comprising them.

10.3 Description of the clusters

A possible approach to describing the various groups is that of identifying the list of most recurrent characteristics for the cycles belonging to each cluster. The typical way of doing this is by finding the so-called frequent itemsets of a dataset. This allows for the extraction of the sets of values that co-occur the most often. The values available for each cycle can be, for example, the features extracted (i.e. the summary statistics – using only the signals and not their derivatives: the behavior has already be shown to be perfectly described by the signals themselves, with no need to introduce the derivatives, which are not as well clustered as the original signals, and would double the number of variables to be analyzed).

The problem with the features extracted is that they are continuous in nature, while the frequent itemsets extraction algorithms work on discrete sets (since the items are expected to be present multiple times within the dataset, which is hardly the case with continuous values).

The values available can be discretized by bucketing them: the continuous domain is divided into ranges and, based on the range a value belongs to, a discrete bucket is assigned. This introduces some problems, which will be addressed in the following subsection. After having described each cycle with discrete values, the frequent itemset extraction algorithm (called FP growth) is applied, and the results will be proposed as part of Subsection 10.3.2.

10.3.1 Generation of buckets of values

While the discretization of a continuous range of values may, at a first glance, appear to be a trivial task, the decision of how the ranges should be defined requires some careful considerations. Dividing the range into n sub-ranges of equal width, or so as to have same-cardinality buckets is problematic in that the divisions do not account for possible clusters existing within the range, thus possibly separating cycles that were meant to be clustered together. A possible alternative is that of

using a clustering algorithm on each of the features, so as to correctly group points that are supposed to be clustered together.

Of the many clustering algorithms available, k-means [18] has been chosen because of its simplicity and suitability for this problem: this algorithm clusters the dataset into k clusters by initially randomly assigning k centroids, and then having the centroids move until they reach the center of a cluster. Other algorithms may better suit this 1D clustering problem [19], but since k-means has proven to yield satisfactory results, it has been kept as the method of choice. K-means requires the *a priori* definition of the number k of clusters to be identified, and this is not immediate: although the overall number of clusters identified has been of 4 (3 plus the outliers), not all variables are well grouped using this number of clusters. Since the number of buckets each variable is divided into is not required to be the same, a different number of buckets has been introduced for each variable, depending on the suitable number identified.

This suitable number of clusters is decided based upon the silhouette coefficient [20], a score that ranges between -1 and +1 that indicates, for each sample, how similar it is to the ones in its own cluster, and how far from the others. The silhouette can be computed for each sample but, as an overall coefficient, the average silhouette for all samples can be computed, in order to assess how good an overall configuration is. With this method of evaluating how good a clustering configuration is, each variable is clustered using k-means with a value for k ranging from 2 to 5. For each result the silhouette score is then evaluated.

The most intuitive approach to selecting the best number of clusters is that of selecting the number k that produced the largest silhouette score. This, though, has been observed to favour a small number of buckets, even when the result is visually not the desired one (one of the advantages of clustering on a low number of dimensions is that the results can be visually inspected). Because of this, a heuristic that favors a larger number of buckets has been introduced: instead of selecting the clustering k with the largest silhouette, the highest value for k for which the clustering exceeds the 0.8 silhouette score[1] is selected instead. If the 0.8 threshold value is not exceeded by any k, the largest silhouette achieved is chosen. Figure 10.7 shows the clustering of some of the features, based on the algorithms and heuristics described in this subsection.

[1]The value has been selected considering the available clustering outcomes. A silhouette mean value of 0.8 is, in most cases, exceedingly high but it is often achieved in this scenario because of the low dimensionality of the problem

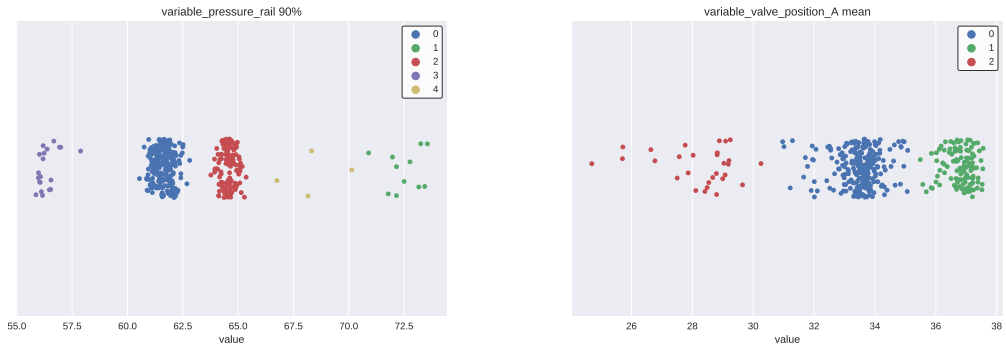

(a) (b)

Figure 10.7: Bucketing of two of the variables using 1D k-means

10.3.2 FP growth and frequent itemsets

With the bucketization, each cycle can be described in terms of a small number of discrete items (one for each feature). For each cluster of cycles available, the list of frequent itemsets (i.e. the sets of items that occur frequently, where frequently is defined by a minimum number of occurrences) can be extracted using the FP growth algorithm [21]. The algorithm builds the so-called FP tree and, from this, it extracts all itemsets that show up with a frequency above a threshold one.

The itemsets identified by the FP growth algorithm are all those that occur in a given fraction of the entries available (this fraction is referred to as minimum support, or minsup for short). This means that, if a given itemset of length N is found, all $2^N - 1$ combinations of the items of the original itemset will be extracted as well. This is not ideal: smaller itemsets do not bring any additional information that is not contained in the larger one and, since the number of itemsets found grows exponentially with the length of the largest itemset found, the problem grows quickly. Because of these reasons, only the maximal frequent itemsets are kept. The maximal frequent itemsets are all those itemsets that are identified as frequent and that are not a subset of another frequent itemset.

The only parameter that needs to be defined is the minsup. This can be defined based on different considerations. The domain may at times offer a good definition of what "frequent" means. Alas, this is not the case. Another approach is that of deciding what a meaningful number of itemsets is, and adjust the minsup accordingly.

Figure 10.8 shows how the number of maximal frequent itemsets identified changes as the minsup varies between the values of 0.7 and 1.0. While intuition dictates that the number of itemsets found should decrease as minsup increases, this is not the case: in fact, even though a given itemset might not be considered frequent above a certain minsup, some subsets of it might still be, thus "generat-

ing" multiple frequent itemsets from a single one.

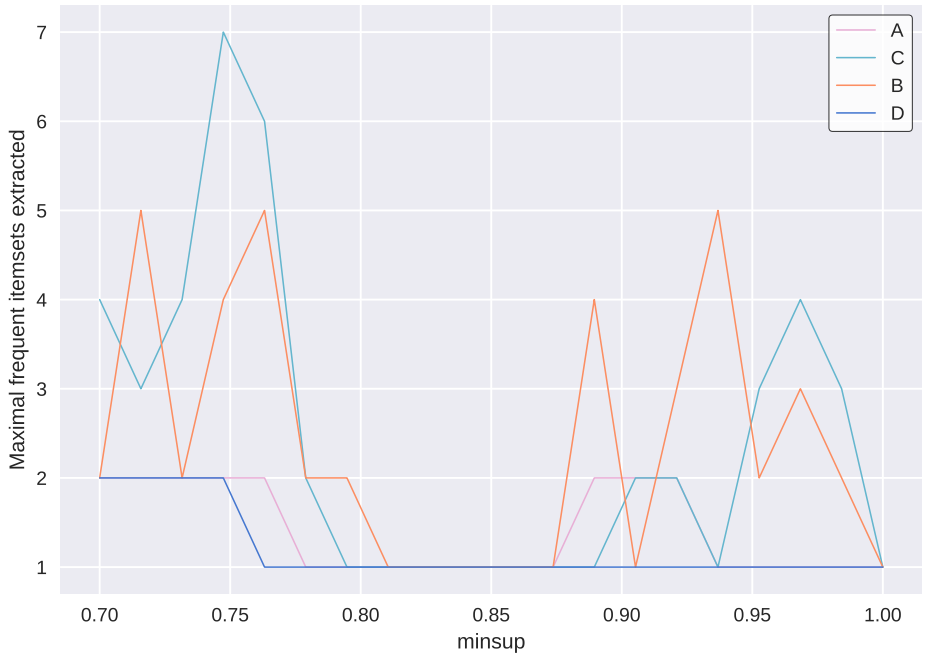

Figure 10.8: Number of maximal frequent itemsets found for each cluster depending on the minsup threshold

In order to provide less confusing results, each cluster should be described by a single itemset: this occurs around the value 0.85: consequently, this will be selected as minimum support. With this value defined, the single most frequent itemset can be extracted for each of the clusters: Tables 10.1, 10.2, 10.3 and 10.4 represent the maximal frequent itemsets for the fuchsia, orange, azure and blue clusters.

The three main clusters (fuchsia, orange, azure) are all represented by long (approximately 20 items) itemsets, meaning that, despite the large minsup, the discretized values often occur simultaneously. The outliers have a significantly smaller shared description: this is because, due to their heterogeneity, there are not many characteristics in common. In *italic* are the entries that are shared among clusters (with the exception of the outliers): these can be considered as values that are not as relevant when searching for unique characteristics in the clusters.

The contents of the itemsets are not of particular interest when maintaining the domain-unaware approach kept so far. On the other hand, the length of the itemsets themselves is significant once again of the strong similarities between clusters, and the low number of items shared across clusters indicates that these are well separated from one another. While these conclusions could already be

Feature	Range (bucket)
variable_temp_engine std	*[0.24; 0.5]*
variable_quantity_fuel_B mean	[1.09; 1.31]
variable_quantity_fuel_B std	[1.72; 1.84]
variable_quantity_fuel_A mean	[1.29; 1.3]
variable_quantity_fuel_A std	[0.26; 0.29]
variable_angle_fuel_AD mean	[-4.13; -3.07]
variable_angle_fuel_AD std	[3; 3.24]
variable_valve_position_A mean	[24.7; 30.26]
variable_valve_position_A std	[12.61; 19.44]
variable_temperature_exh_gas_1 mean	[199.28; 201.49]
variable_temperature_exh_gas_1 std	*[31.7; 57.25]*
variable_temperature_exh_gas_3 mean	[175.11; 218.1]
variable_temperature_exh_gas_3 std	[36.23; 61.19]
variable_temperature_manifold mean	[47.42; 52.08]
variable_temperature_manifold std	[5.08; 5.86]
variable_pressure_rail mean	[35.9; 36.66]
variable_pressure_rail std	[13.29; 13.78]
variable_concentration_NOx_B mean	[231.86; 239.9]
variable_concentration_NOx_B std	[102.59; 107.97]
variable_percent_oxygen_A mean	*[11.37; 12.69]*
variable_percent_oxygen_A std	*[2.86; 3.99]*
variable_quantity_reductant mean	[2.22; 5.46]

Table 10.1: Description for cluster A

Feature	Range (bucket)
variable_temp_engine std	*[0.24; 0.5]*
variable_quantity_fuel_B mean	[1.36; 1.6]
variable_quantity_fuel_B std	[1.72; 1.84]
variable_quantity_fuel_A mean	[1.31; 1.32]
variable_quantity_fuel_A std	[0.26; 0.29]
variable_angle_fuel_AD mean	[-2.96; -2.27]
variable_angle_fuel_AD std	[1.92; 2.37]
variable_valve_position_A mean	[30.97; 35.08]
variable_valve_position_A std	[8.17; 10.79]
variable_temperature_exh_gas_1 mean	[210.61; 235.75]
variable_temperature_exh_gas_1 std	*[31.7; 57.25]*
variable_temperature_exh_gas_3 mean	[175.11; 218.1]
variable_temperature_exh_gas_3 std	[27.22; 32.03]
variable_temperature_manifold std	[3.3; 3.99]
variable_pressure_rail mean	[36.81; 37.9]
variable_pressure_rail std	[15.24; 15.87]
variable_percent_oxygen_A mean	*[11.37; 12.69]*
variable_percent_oxygen_A std	*[2.86; 3.99]*
variable_quantity_reductant mean	[2.22; 5.46]
variable_quantity_reductant std	[6.13; 7.04]
variable_NOxCatalist_Storage mean	[1.88; 2.02]
variable_NOxCatalist_Storage std	[0.23; 0.28]

Table 10.2: Description for cluster B

Feature	Range (bucket)
variable_temp_engine std	*[0.24; 0.5]*
variable_quantity_fuel_B std	[1.59; 1.71]
variable_quantity_fuel_A mean	[1.32; 1.34]
variable_quantity_fuel_A std	[0.24; 0.26]
variable_angle_fuel_AD std	[2.51; 2.97]
variable_valve_position_A mean	[35.49; 37.56]
variable_valve_position_A std	[8.17; 10.79]
variable_temperature_exh_gas_1 mean	[246.41; 260.8]
variable_temperature_exh_gas_1 std	*[31.7; 57.25]*
variable_temperature_exh_gas_3 mean	[227.55; 261.17]
variable_temperature_exh_gas_3 std	[20.56; 22.56]
variable_temperature_manifold mean	[56.52; 60.02]
variable_temperature_manifold std	[4.17; 5.01]
variable_pressure_rail std	[15.97; 16.83]
variable_percent_oxygen_A mean	*[11.37; 12.69]*
variable_percent_oxygen_A std	*[2.86; 3.99]*
variable_quantity_reductant mean	[5.58; 9.29]
variable_quantity_reductant std	[5.08; 6.09]
variable_NOxCatalist_Storage mean	[2.18; 2.23]
variable_NOxCatalist_Storage std	[0.06; 0.16]

Table 10.3: Description for cluster C

Feature	Range (bucket)
variable_temp_engine std	[0.24; 0.5]
variable_valve_position_A std	[12.61; 19.44]
variable_temperature_exh_gas_1 std	[64.89; 100.86]
variable_pressure_rail std	[17.09; 18.25]
variable_percent_oxygen_A mean	[9.37; 11.31]
variable_percent_oxygen_A std	[4.04; 5.45]
variable_NOxCatalist_Storage std	[0.65; 0.84]

Table 10.4: Description for cluster D (outliers)

drawn for the single variable, the extraction of the itemsets allowed to infer a more general correlation between variables, while providing a succinct description of the clusters. Building on the information gathered so far, the next section will attempt to find an explanation for the existence of these clusters.

10.4 Possible causes

All the analyses carried out so far seem to indicate that the cycles belonging to the same cluster have all been affected in a similar way. The driver of this influence, though, has yet to be discovered. It should be noted that, when performing the same kind of analysis on different datasets (e.g. the Model2 one), these clusters were not present.

A possible approach to discovering this driver is that of starting from the independent variables (i.e. those variables that are controlled by the engineers recording and piloting the cycle) and figuring out whether these already present the observed behavior. If so, the reason for this clustering is that whoever ran the experiments (note that these people did not, at any time, work on this project, so asking them was not an option) deliberately decided to run them in different ways, although such a behavior has been deemed unlikely by those experts that did work on this project. Otherwise, those variables that are directly influenced by the independent variables should be analyzed next, thus exploring the graph of dependencies until all variables are extracted: when the first clustered variable appears, the cause behind the clusters can be pinpointed to it.

This would theoretically work, but without the required domain expertise, building the graph of dependencies is not feasible. As a consequence, only the variable that is already known to be independent will be analyzed. This independent variable is the status of the accelerator pedal: a predefined track (shown in Figure 3.1) is used to pilot each cycle and, since this variable is fed as input, it can be considered as being the driver of the entire cycle.

The assumption that has been made *a priori* is that all tracks used in the available cycles are identical. Because of this, if the mean and the standard deviation of the accelerator pedal signal are extracted for each cycle, the expectation is that no particular difference should be found among them. The mean and the standard deviation have been chosen because they well represent the behavior of the signal: the mean indicates the "offset" the signal has, while the standard deviation provides an indication of the amplitude of the peaks of the signal throughout the cycle (a larger standard deviation indicates that the pedal has diverged more significantly from the mean). Figure 10.9 shows the results for the two statistics measured for all the cycles. It is clear that some anomaly is already present in the

accelerator signal and, when overlapping this result with the identified clusters (as shown by the background colors), the match is perfect.

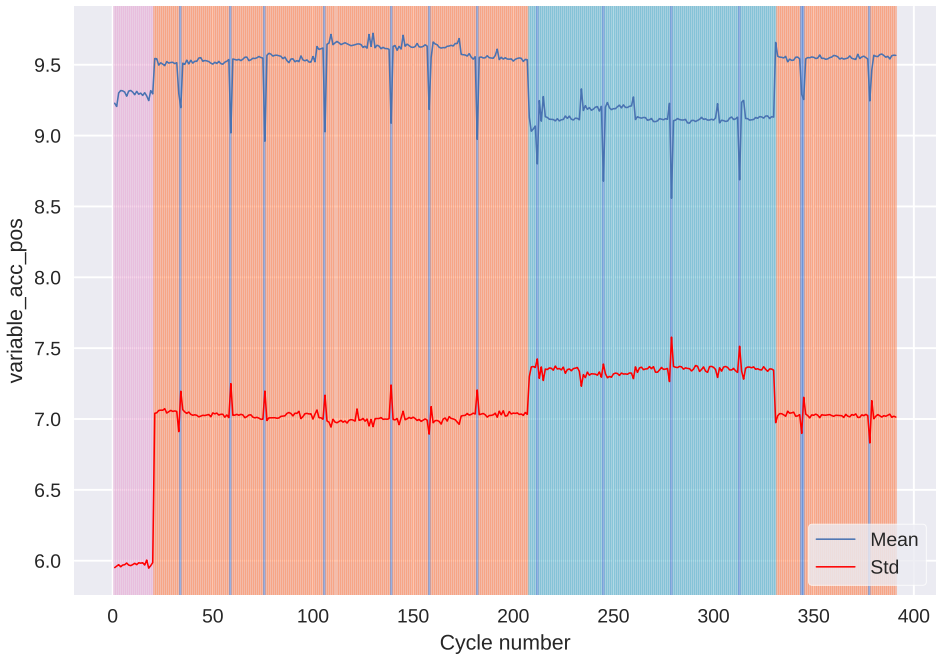

Figure 10.9: Mean and standard deviation trend of the gas pedal signal throughout the cycles

In conclusion, the cause of this clustering can be found in the driver of the cycles. The implications that this finding has on the already presented results will be discussed as part of the findings in Section 12.4, along with some additional conclusions that can be drawn from this side exploration that has been carried out to get to the bottom of this situation.

Chapter 11

Implementation details

Given the information available on the dataset, the objectives of the study and the constraints in place, the hardware and software required for the study can be defined.

11.1 Hardware

A machine is required in order to process the dataset. Given the constraints introduced by the automobile manufacturer, the data needed to be stored on a dedicated server: as a consequence, a machine provided by the DBDMG (DataBase and Data Mining Group) has been used for the purpose. The specifications for the machine are listed in Table 11.1. While the specifications would allow for the entire dataset to be loaded onto the main memory (based on the considerations of Subsection 3.1.4), this operation has been avoided throughout the work, in order to allow for the solution to scale to larger datasets (though the leap to big data techniques will still be necessary at some point).

Main memory	32 GB
Storage	5×3 TB
Number of cores	12
Clock frequency	2.67 GHz
Operating System	Ubuntu 16.04

Table 11.1: Server specifications

11.2 Software

The programming language selected for this project was Python. This language is interpreted, thus allowing for rapid prototyping, which is essential given the exploratory nature of the study. Python offers an incredibly rich ecosystem of

libraries and modules available, particularly in the data science field. The following is a list of the libraries and packages used most extensively (all of them are widely used in the scientific community):

- **Matplotlib** [22]: a 2D plotting library which produces publication quality figures in a variety of hardcopy formats and interactive environments
- **seaborn** [23]: a visualization library based on matplotlib, which provides a high-level interface for drawing statistical graphics
- **NumPy** [24]: the fundamental package for scientific computing
- **pandas** [25]: a library providing high-performance, easy-to-use data structures and data analysis tools
- **scikit-learn** [26]: a simple and efficient tool for data mining and data analysis

Chapter 12

Findings

This chapter will focus on the discussion of the outcomes of the experiments, highlighting the most interesting aspects of the study and the most important takeaways. These considerations regard both the original and the additional experiments carried out (Chapters 7, 8 and 9), plus some comments regarding the clusters identified in Chapter 10.

12.1 Classification results

The original process, as defined in Chapters 5, 6 and 7, achieved satisfactory results in terms of precision, recall and accuracy. The numeric values can be found in Table 7.1. Other than this general observation, other considerations can be made when comparing the different classifiers and metrics.

As expected, the decision tree performs generally worse than neural networks and SVM: this was expected, given the limitations that come with the simplicity and interpretability of the model. Despite that, the difference is not abyssal, with many of the metrics being less than 10% lower than those of the other classifiers. The precision, recall and F_1 score for the three classes are comparable for the three models meaning that, although the hyperparameters were tuned so as to maximize the red-related performance, the other classes did not suffer particularly. The accuracy metric shows how the three classifiers correctly assign the labels for 80 to 90% of the cycles available.

12.1.1 Misclassifications

The way these labels are assigned is shown in Figure 7.4. This kind of visualization has been introduced to provide better insights on how the classifiers behave and where the classifiers are most often mistaken. Most notably, the three classifiers all get wrong a group of 5-6 cycles on the left-hand side of the bars (around cycle

340, based on Figure 5.8c and 5.6), with all the classifiers making the same mistake (predicting green cycles instead of yellow). This can either be because all three classifiers learned the wrong patterns or, possibly, because the labelling used is incorrect and those cycles should actually be green. The labelling procedure used introduces uncertainty: first because it is based on the measurement of a signal (with the problems that come with it, as already discussed in Sections 5.1 and 8.2 and, second, because the classes introduced to label the cycles are not perfect and could be improved (as attempted in the labelling experiments of Chapter 9). This uncertainty means that not all the mistakes made by the classifiers should actually be considered as mistakes, but instead they could provide insights on how to tune the classes: this, though, would result in a classifier biased by the dataset: without any separate test set to verify the classifiers' true performance, this operation could lead to overfitting. Since the number of cycles available is low, this kind of experiment has not been carried out.

Another interesting group of 2 cycles mispredicted by the three classifiers is the one around 270, where two yellow cycles exist in the middle of a long sequence of green cycles. These two cycles are predicted as green by all the classifiers: upon inspection of Figure 5.6, the reason can be found: the response time of a single value spiked and, when introducing the smoothing, the neighboring cycles got affected as well, becoming yellow. This is one of the negative aspects that led to the decision of running an experiment without applying the smoothing process. The results will be discussed in Section 12.2.1.

A final note of interest concerning the mistakes made by the classifiers regards the types of mistakes made: in almost no circumstance (except for one case, for the SVM) have the classifiers predicted a green cycle as a red one, or vice versa. This can be deduced from the bars and it is clearer still when checking the confusion matrices of Figure 7.3. This means that the classifiers actually managed to infer an order among classes, with the green being the furthest away from the red one, and the yellow one in between: if this was not the case, and the classifiers were assigning labels "randomly" (or using other unrelated criteria), cycles would be misclassified in each of the other classes with similar frequencies.

12.1.2 Classifiers' rationale

The decision tree offers insights on the rationale behind the labels assigned. It has been mentioned that the decision tree is a simple classification model but, as already shown, it fares so well that its results are comparable with those of more complex models. Because of this, the variables considered as relevant by the tree can be expected to be approximately the same used by the black box models.

The most relevant variables are typically the ones used near the root of the tree: these represent the variables that best split the initial dataset. As the path gets deeper, the splits made by the tree concern a smaller number of cycles, thus not being quite as insightful (and possibly leading to overfitting – hence the early pruning often introduced). The most interesting variable that is being used by the root and some of the highest nodes in the decision tree of Figure 7.2 is the derivative of variable_percent_oxygen_A (with various percentiles being taken into account).

Since the proposed decision tree grows rather large. A simpler – yet leading to the same conclusions – case is that of the binary decision tree classifier represented in Figure 9.1. In this case, the decision tree only uses a single test. This test once again uses the derivative of the oxygen variable (more precisely, the 90^{th} percentile): if this quantity is below the identified value of 0.8018 the cycle is labelled as red, otherwise green. The meaning of this simple test is the following: if the majority of the values of the derivative of the oxygen is "low" (with low defined by that threshold), the cycle is red. This means that those cycles where the oxygen level changes slowly are identified as red: as shown in Figure 9.2, the variable identified by the binary model splits red and green cycles well, with the yellow ones being in between. The fact that this variable (or set of variables, when considering the other statistics of that derivative) is a strong predictor might appear trivial, but it is actually significant.

The clogging problem, as already mentioned, slows the oxygen level read by the sensor: in order to understand how clogged each cycle is, a cut-off that occurred in approximately the same conditions for all cycles has been used to measure the response time. The longer the response time, the slower the reading of the oxygen sensor and the stronger the clogging problem. Therefore, it might seem trivial that the classifier identifies the clogged cycles as the ones having a generally slower signal. The reason why this is not trivial at all and, actually, it provides interesting information is that the response time has been measured using a sampling rate of 320 Hz, while the inputs provided were sampled at the much lower frequency of 1 Hz. This lower sampling frequency did not allow for a significant measurement of the response time, but the classifiers still managed to infer useful information from it. This decouples the identification of clogged cycles from the particular cut-off maneuver and from the high sampling frequency.

This decoupling is particularly relevant when considering that this project serves as a feasibility study for a larger version where data is collected from millions of vehicles and processed in real time: high sampling frequencies are unfeasible (even 1 Hz is too high, hence the downsampling study) and the drivers will not be required to perform any particular maneuver. By collecting enough data

from a fleet of vehicles, new distributions can be computed for the derivative of the oxygen variable in normal conditions (perhaps only collecting data in particular conditions, so as to reduce the variability of the signals). Once this data is collected, along with the actual conditions of the lambda sensor, new models can be built to better adapt to real driving conditions (as opposed to the conditions used for the cycles).

Additional considerations regarding the scalability of this project will be made, as part of the conclusions, in Section 13.2.

12.2 Process manipulation outcomes

The original process presented different opportunities for alternative choices. These choices have been taken while devising the process based on considerations that resulted in some decisions being taken rather than others. On top of that, the feasibility analysis of the scaling-up project imposed additional constraints (namely on the sampling frequency used for the signals): this required additional experiments in order to assess the degradation of the results. This section will cover the main results regarding some of these matters. In some cases, the conclusions to be drawn have already been presented as part of the presentation of the work: when that is the case, no additional considerations will be added here.

12.2.1 Removal of the smoothing process

The smoothing process has been assumed to be introducing some mislabellings (see Subsection 12.1.1). It is only natural, therefore, to wonder whether the decision of using this labels manipulation led to any improvement at all. In order to answer this question, the entire process has been run with no smoothing (note that, because of the nature of the parameter k, this is equivalent to running the experiment setting $k = 0$). The results are presented in Table 8.4.

The results in terms of accuracy are comparable, if not better, to those of the original experiment. The same goes for the green-related performance, while the red-related ones actually degrade noticeably. While a brief comment regarding this behavior has already been included when presenting the experiment, further coverage may be needed in order to explain this behavior.

Figure 5.8 shows how the response times change as the size of the sliding window of the smoothing process gets larger. Of particular interest are the red "bands": these bands are shrinking, thus effectively reducing the number of red cycles as k gets larger. It might seem counterintuitive that the performance metrics for the minority class improve as the cardinality of the class gets smaller. But, as the

class gets smaller, only the "most clogged" cycles (i.e. those cycles that still have a slow response time despite the smoothing) get assigned to the red class: this increases the purity of the red class, excluding those cycles that can be considered as borderline yellow. This helps providing a better definition of "red", with the improvement in performance that comes with it.

When comparing the prediction bars of Figure 8.4 with those of the original experiment (Figure 7.4), some interesting considerations can be made. Two of the situations that were highlighted in Subsection 12.1.1 are those around cycles 270 and 340. The yellow cycles in the middle of the green cluster are still mispredicted by this new classifier. This means that the smoothing process only marginally influenced the labels here: those cycles are actually considered by the classifiers as being green and the problem here might be with the way the labels were assigned in the first place.

The situation around cycle 340, instead, improved for the neural network and the SVM, while still being partially problematic for the decision tree. This might be part of the reason why the green-related performance improved.

12.2.2 Effects of downsampling

The deployment of this project on a larger scale imposes some constraints due to the limited network capabilities. The data exchanged between the vehicles' ECU and the central server should be reduced to a minimum: on the one hand, the feature selection applied managed to narrow the number of variables used (and that therefore should be sent over to the server) down to 14; on the other, the sampling frequency should be reduced even further. This renders the 320 Hz sampling frequency used for ProgramB completely useless, and even the 1 Hz rate of ProgramA is still much to high. The experts reckon that a more feasible rate would be in the order of the minutes, thus reducing the sampling rate by a couple of orders of magnitude.

Section 8.4 analyzed how much the downsampling influences both the classifiers' performance (in terms of F_1 score) and in terms of degradation of the inputs. The main result was that the classifiers were not significantly affected by a modest downsampling: the reason for this can be found in the degradation of the distributions of values. These distributions of values remain approximately the same (as indicated by the Janson-Shannon divergence) for modest reductions in the sampling frequency. Since the classifiers receive as input a series of summary statistics that can be extracted from the distribution of values of each signal, the low degradation implies a low alteration of the inputs, with the resulting stability that comes in terms of classifiers' performance.

Thus, the decision of using summary statistics instead of the single values as inputs helped both in terms of reduction on the number of inputs (necessary given the low number of cycles available) and in terms of robustness to downsampling. Additionally, building a classifier that uses the original signal samples as inputs could have resulted in models that cannot be deployed in the real world, where the vehicles are not subject to a pre-established gas pedal track.

Additionally, Figures 8.6a and 8.6b provide a way of deciding different sampling rates for the different signals, based on the maximum degradation acceptable. This could help with an even further reduction of the data exchanged between vehicle and server: signals that do not degrade significantly when downsampled can be recorded using lower frequencies. Since the inputs of the classifiers are based on the distribution of values, the process allows for signals to be sampled at different rates.

A final consideration is that downsampling might not even be needed under certain assumptions. If the ECU can be programmed as desired, the signals could be sampled locally and then stored for a given amount of time. Then, the ECU could compute the summary statistics required on the densely sampled signals, thus sending the server only a low number of already-computed features. This assumption on the ECU availability for programming, though, has not been verified: making sure that the system can handle downsampled signals is still extremely useful.

12.2.3 Exclusion of strong predictors

The comments regarding the classifiers trained without using those variables that can be considered as strong predictors are heavily related to the observations made in Subsection 12.1.2. In other words, the classifiers all heavily rely on the derivative of the oxygen level signal: removing this significantly affects the classifiers. Removing the derivatives affects the results the least, since the classifier still has access to the oxygen variable, managing to extract useful information from it. Instead, when the oxygen variable is removed, its derivative is not available either, thus significantly lowering the classifiers' performance.

The conclusion that can be drawn from this experiment is that no other significant variables other than the oxygen level have been found to be correlated to the clogging problem. While these variables might be there, the classifiers used were not able to identify and exploit them to improve in performance. Those variables that actually where used might be weakly correlated to the clogginess of the sensor but, given the poor performance of the classifiers, they should not be relied upon (other than when presenting the results to the domain experts, thus offering some

of the data-driven, domain-unaware insights).

The (discrete) derivatives used have been computed starting from the signals sampled at a 1 Hz rate. A possible concern, when scaling up to real-world cases, is that lowering the sampling frequency (so as to meet the constraints imposed by the communication with a remote server) might lead to meaningless derivatives, as they are computed as the difference quotient between subsequent values and lowering the sampling rate implies increasing the denominator of the quotient. This, though, might not be the case: the ECUs already require reprogramming in order to transmit the necessary data; the update could introduce the "sampling" of the derivative of the signals (e.g. by sampling the signal twice in a short period of time and computing the difference quotient on it). The measurement of a meaningful derivative should not be a problem, thus the degradations imposed by the lack of this kind input should not be of any significant concern.

12.2.4 Application of the process to the Model2 dataset

The application of the process to the Model2 dataset does not present any particularly significant surprise and, as such, it will not be commented in depth. Despite that, there are two important takeaways that come with it.

The first one is that the devised process can be applied to new datasets easily and without significant adjustments. This was one of the aims of the project and it can be considered as achieved. The second one is that the low number of cycles affects the results of the models: the more inputs are available, the better the classifier can learn.

12.3 Labelling experiments discussion

The labelling process presented is comprised of three parts: the measurement of the response times, their smoothing and the assignment of a label based on predefined classes. The first two steps have already been analyzed and commented, with some alternatives presented to show if and how different approaches could yield better results. The response time measurement is expected to introduce some uncertainty in the labelling process, since a wrong reading of the time influences the label assigned. When smoothing is introduced, this uncertainty propagates to the neighboring cycles.

The third and final step, that of the definition of classes and the assignment of the labels, introduces even further uncertainty: no quantitative definition of the clogginess of a cycle was available in terms of response time ranges, so an educated guess was needed in order to continue with the process. The definition of these

ranges has been accepted as plausible by the domain experts that worked on this project but with the catch that, since this sensor was not their particular field of expertise, the classes could require some refinements and were not guaranteed to be accurate. Because of this, the entire process – and its implementation – have been designed so as to accommodate for future changes in classes' ranges (and all of the parameters discussed in this thesis).

The lower and upper bounds for the response time are respectively 0 and $+\infty$, thus effectively requiring two parameters in order to define three ranges (namely the thresholds between green and yellow, and the one between yellow and red). Exploring the resulting bidimensional space (so as to find the optimal range values) has been deemed to be unfeasible (when exploring the range $0 \div 2$ seconds with increments of 0.01 seconds would result in approximately $\frac{1}{2} \cdot (\frac{2s-0s}{0.01s})^2 = 20,000$ possible values (the number of options has been halved since the second threshold is required to be lower than the first one). Exploring this many possibilities is not currently feasible and, as such, this option has been discarded.

Despite that, some alternative experiments have been devised: for these experiments, the labels assigned to the cycles have been changed based on some considerations. These experiments have been presented as part of Chapter 9. This section will comment some of the most interesting results.

12.3.1 Binary classifier

The introduction of the binary classifiers (i.e. classifiers that does not consider the yellow cycles) comes from the decision of trying to simplify the problem and observe how the models behave for this different, easier problem.

The binary classifiers are the best performing models produced as part of this study. The reason behind this excellent performance has already been covered in detail and can be summarized by saying that red and green cycles are significantly different when it comes to the distribution of the derivative of the oxygen signal. All three classification algorithms can separate these two categories of cycles well, thus explaining the performance measured.

Introducing the yellow cycles complicates the situation (as shown in Figure 9.2), making it harder to separate green from red cycles. Since any real-world application naturally presents yellow conditions, this binary classifier might seem like a simplification that does not lead to any meaningful results. Despite that, this experiment (along with the decision of using an interpretable model) helped identifying the best predictor available. In order to understand how the yellow condition would be handled, all the yellow cycles available (that had been taken away when building the classifiers) have been fed to the models, in order to be

assigned a binary label.

12.3.2 Labelling of yellow cycles with the binary classifiers

This experiment introduces a third class in a binary classifier: since this classifier does not know about the existence of this third class, it will attempt to assign each of these never-before-seen cycles to either of the two known classes. Since the yellow cycles are neither red nor green, it does not make sense to talk about performance of the classifiers. What makes sense, instead, is showing how each cycle is labelled. This is shown in the prediction bars of Figure 9.4.

Interestingly, the three classifiers mostly agree on the decisions taken and, since the rationale of the decision tree is known, it is reasonable to assume that the other two classifiers heavily rely on the same information. Based on the decision tree, the information used is shown in Figure 9.2: those cycles on the left-hand side of the threshold are labelled as red, the others green.

Since the majority of the yellow cycles are on the right-hand side of the threshold, most of them are labelled as green. The yellow cycles that are labelled as red are mostly those that, in the prediction bars, are surrounding the cycles that are known to be red. This, when paired with the knowledge that the soot cumulates (thus resulting in continuous cycles having similar clogginess), is reassuring of the fact that the rationale used by these classifiers (and, by extension, by the others) is consistent: if it was not, red and green cycles would be scattered randomly, with no relation to the position of the established green and red ones.

12.3.3 Yellow cycles as green/red

Relabelling the yellow cycles as either red or green transforms the original problem in a new binary one, where all the cycles are considered during the training. The results of the two experiments have already been presented in Tables 9.2 and 9.3 and Figures 9.5 and 9.6. Comments regarding the results have already been made when presenting them.

This particular one can be seen as a different way of approaching the "playing it safe" approach that has been deemed to be the best one when making a prediction about the sensor's conditions: in other words, the experts asserted that, in their opinion, it would be best to only alert the car owner about the problem when it is sure that the problem exists or, using yet a different phrasing, the model should try to minimize the false positives. This is because offering this prognostics service is an extra, non-vital (yet) feature: if not alerted, the owner will be none the wiser and will keep using the vehicle as they would have, had this system not been in place; but, if the owner is asked to bring the car in for a problem that

does not really exist, this could be seen as a waste of time and resources. The already presented solution proposed to solve this problem is that of optimizing the classifiers using the precision as the performance evaluation metric, instead of the F_1 score. This approach led to more precise models, but with a lower recall.

Another approach to this problem is given by these two proposed experiments. When the yellow cycles are labelled as green, what is really happening is that those "borderline" cases are demoted to "alright" while, when considering them as red, they are promoted to "clogged"[1]. This represents the two possible approaches to the alerting of the customer: the first case is the one where the owner is only alerted when the system is particularly sure about the existence of the problem; the second case is the one where the owner is immediately alerted about anything that remotely resembles a clogged sensor.

Based on the "playing it safe" policy, the "yellow as green" scenario is the one that best suits the requirements. The advantages and disadvantages of this experiment over the "yellow as red" one have already been presented as part of Subsections 9.3.1 and 9.3.2: in short, the "yellow as green" experiment achieves better accuracy and green-related performance (being the green class the majority one), while the "yellow as red" experiment produced better red-related scores (being this the new majority class).

12.4 Dataset clustering comments

The discovery of three well-defined clusters in the dataset required revising all of the considerations made thus far, in order to account for the existence of these clusters. The main conclusion is that these clusters have not significantly affected the results of the classification: there is no clear correlation between the green/yellow/red labels and the identified clusters and, given the good results achieved by the classifiers, the logical conclusion is that they managed to discard the information that differentiates the clusters and, instead, focused on the one that helped figuring out the existence of a clogging situation.

This conclusion can be corroborated by two pieces of evidence. The first is given by Figure 9.2, which clearly shown how the 90^{th} percentile of the oxygen derivative is well distributed between the three classes: if this was not the case, and the clusters actually influenced the oxygen derivative, the three clogging classes would not be as well distributed. The second piece of evidence is that, as shown by Figure 10.5, the derivatives seem to be less affected by the clusters than are the original variables. This holds true, as shown, for the oxygen. In particular,

[1]The terms "demoting" and "promoting" are of course used loosely in this situation

the "mean" derivative values seem to be affected the least as far as the azure and orange cycles go, and these include the vast majority of the dataset.

This lower influence of the clusters on the derivatives can be explained basing the considerations on Figure 10.9. Here, mean and standard deviation of the gas pedal are shown to change consistently with the clusters and, since the rest of the variables are affected by the gas pedal, similar graphs can be expected for these as well. In particular, the mean has been explained to be somewhat representative of the (constant) offset each variable has: since adding a constant to a function does not alter its derivative, this offset does not influence it significantly. The same considerations cannot be made for the standard deviation, but the overall conclusion is that derivatives are not heavily affected by the clusters.

This is fortunate, because the classifiers significantly rely on the derivatives. Fortune, though, should not have any role in a research project. Having a dataset with such a bias could have affected the entire work and, had the existence of these clusters not been discovered, the results would have been completely inaccurate and nobody could have figured it out. Since the domain experts that worked on this project were not aware of the existence of this problem and did not work on the collection of the data, two important lessons can be learned. The first one is that the data provided should not be assumed to be fine without thoroughly exploring it first (in this case, a classification problem proved to require clustering as well). The second one is that communication with the experts that actually gathered the data is fundamental: other reasons that back this assertion have already been provided but, even in this case, an explanation might have been available for the existence of these clusters. These are two (of the many) valuable lessons learned from this pilot project and that will prove useful for the projects to come.

Additional comments can be made about the identified clusters. The first one is that, for some variables, smaller "sub-clusters" could be identified. These smaller clusters, though, could not be easily spotted for all the variables and, because of that, only the three (plus outliers) main clusters have been reported. Figure 10.9, though, shows how these subclusters can be once again explained in terms of different gas pedal tracks used: the mean of the cycles 100 through 170 and 230 through 260 are slightly higher than the surrounding ones, although the standard deviation is not. This explains why these smaller clusters were not as well defined as the others.

A final comment regarding the reason for the existence of the clusters can and should be made. Chapter 10 identified the different gas pedal tracks used as the cause for the existence of the clusters, as shown in Figure 10.9. It is not known, though, whether this behavior was intentional or not, since different considerations seem to point in different directions. The Model2 dataset did not present any of

these clusters, making it hard to believe that the people who collected the data decided to fiddle with one engine and not the other, but the similarity of the cycles belonging to each cluster make it hard to believe that the result was due to chance. Unfortunately, no definite answer can be provided in this thesis.

Chapter 13

Conclusions

This work of thesis started with the goal of finding a data-driven approach to the predictive maintenance of the oxygen sensor. An already recorded test bench dataset has been made available by the collaborating company along with the availability of different domain experts, who provided the necessary feedback and support throughout the work. Starting from the high-level data mining process, an ad-hoc procedure has been devised so as to account for the peculiarities that came with the dataset available. This process has been implemented and tested, achieving satisfactory results. Many of the choices made during the definition of the process were supported by *a priori* considerations and assumptions. A part of the presented work consisted in verifying whether these assumptions held *a posteriori*, i.e. when the classifiers' results were available. This kind of validation provided better insights on the dataset and on the rationale used by the classifiers in order to make decisions.

The most interesting result regards the usage by the classifiers of the derivative of the oxygen level signal. This signal was not, at the beginning, thought to be accurate enough (in terms of samples available) in order to draw meaningful conclusions on the clogginess state of the sensor (so much so that a separate dataset, sampled at 320 times the original frequency was used to assign the labels).

Other interesting experiments provided information that can be used when scaling up this project to a larger scale, where the conditions are not as pristine as the ones currently available.

Finally, an extensive exploration of the dataset showed the existence of anomalous clusters of cycles that were not expected to be found: the final part of this work consisted in analyzing this phenomenon, trying to characterize the clusters and aiming to find an explanation that could justify such a behavior. These analyses traced the origin of the problem back to gas pedal track used to drive the test bench: whether the decision of changing the cycles' track was made by the experts who ran the experiments or if some external factor influenced the track, it cannot

be known.

This chapter wraps up the work by covering the novelty aspects of this study first, then focusing on the limitations that this work has encountered and, finally, an overview of the work that lies ahead of this pilot project will be presented.

13.1 Novelty of the study

When compared to the relevant literature found, this work of thesis presented different aspects covered seldom, if at all. The first important difference is that this study is based on real data collected from real test bench engines: most studies available either provide overviews on possible techniques that can be adopted, or are based on synthetic data generated from simulations or the likes of it. The availability of real data allowed to better assess the feasibility of the project and of its future developments, while providing an early validation of the models that is not available for "synthetic data"-based models until deployed in real scenarios (if that is even an option).

The effort of keeping the process as interpretable as possible led to meaningful contributions. For starters, the correlation-based feature selection algorithm proposed helps with the reduction of the number of input variables using intuitive criteria and without transforming the original features (operation that most always renders the features meaningless at the eyes of the experts).

Other than this feature selection algorithm, even the rest of the devised process shows elements of novelty. This is necessary, given the characteristics of the data used: having to work with two different datasets, one for the labelling and one for the training is not a typical scenario. This duality requires splitting the typical data mining process in two. Another element of interest is the duality of the time component. This component is, in fact, present on two different levels: the time within a cycle and, on a larger scale, the ordered sequence of cycles, which were recorded continuously (except for those pauses shown in Figure 5.4a). This required making considerations on two levels of time.

On top of the novelties introduced by the process, even the problem approached is new: in literature, no other oxygen sensor-related predictive maintenance case study (neither data-driven, nor model-based) has been found. In fact, the literature has been shown to be particularly wanting of articles other than electric vehicles/battery-related case studies.

Finally, in addition to the already mentioned novel aspects, this project was a pilot one and will be followed by other collaborations aimed at strengthening the data-driven approach to the automotive industry in the company. This means that all the lessons learned will be used for devising new experiments, changing

the relationship between domain and data experts and more. As for this particular project, in the near future, it will be scaled and tested on a larger fleet of vehicles. In conclusion, this work of thesis paved the way for a number of different projects potentially capable of pushing the boundaries of prognostics further and further still.

13.2 Limitations

Despite the satisfactory results achieved by this work, it has not been without difficulties that hindered the potential achievements. The major problem found was with the dataset available: the size of it was small, limiting the potential of the algorithms used and preventing the usage of others[1]. The other problem with the dataset was the presence of anomalous clusters: this might have yielded unreliable results. Another problem encountered was the difficulty in defining the classes for the clogginess of the sensor: as shown, this decision is crucial and needs to be taken with care.

These problems are obviously nobody's fault and are to be expected when taking up a pilot project: the fact that some meaningful results were achieved should by itself be a success. These limitations due to the dataset should be overcome when new data is acquired for the upcoming projects. In these cases, the data is being collected for the specific data mining projects and none of the encountered problems should present anymore (and, if they do, they will most definitely be of lesser entity).

Other than these technical limitations, other more significant ones exist and might prove to be difficult to overcome. All of these limitations might be problematic when scaling up to vehicles driven in the real world. The main one is the assumption that, over large amounts of data, the distribution of values for any given variable for a single vehicle is consistent with the overall data available. This was the case for the cycles used thus far because each cycle approximately followed the same track (although not entirely, as explained in Chapter 10), but it might not be in other situations, where different drivers might have different styles and be in different settings (e.g. weather conditions, road type). If the distributions cannot be generalized over large amounts of data, the situation might be problematic and the process might require additional steps. These steps would be targeted at identifying the "context" the car is in and, based on that, build macro clusters. Then, for each of these clusters, different models are built and, when new data needs to be labelled, the system first selects the best-matching cluster and then

[1] A random forest, for example, might have been an excellent choice, were it not for the small number of samples available

applies the respective model.

Another significant limitation is the fact that the classifiers rely on the derivative of a signal: this requires being able to measure it (as a difference quotient) by the ECU on board of the vehicle. This is not a computationally expensive task to perform, but the constraint might be on the degrees of freedom allowed by the ECU. If it only supports limited additional functionalities, the derivative might not be computed and the classification results would degrade as shown in one of the experiments. This, though, is a less worrying problem since ECUs, as many other intelligent devices, can often be programmed easily.

Another (less significant) problem is the large number of parameters that needs to be configured in order to get the process to work: valid default values have already been provided, along with the rationale behind the decisions, so as to allow for future adjustments. Manipulating these parameters, though, requires some knowledge of the underlying process and the steps it is comprised of. Given the documentation and the modular implementation provided, along with the intense participation of the domain experts throughout the entire project, this should not be a significant problem.

A final problem involves the collection of data for the training of the classifiers. This can be done through an actual vehicle (and possibly a fleet of them), but the main concern regards the accurate identification of the clogging situation. For this project, sampling the signals using a high sampling rate was an option, but it might not be in the future. This, though, is a limitation that is not dependent on the proposed approach: on the contrary, the defined process is design so as to accept labels from a source other than the original dataset. Given the modularity of the process, changing the labelling blocks with the new ones (depending on the approach found to measure the clogginess) is enough. It is up to the domain experts to find a suitable alternative to label the new data to be used for the training.

13.3 Future work

The project covered in this thesis will continue beyond the presented work, with the goal of deploying a working version offered to those customers whose vehicles are Internet-enabled or will be in the years to come. The road to this final goal is long and has several milestones to be reached before the final one. A first one is that of collecting the data from a fleet of vehicles. Depending on the quantity of data collected, one or more servers should be deployed to store and process the data (depending on the volume and velocity, a big data approach might be in order). Then, the data is processed using the proposed process (or a variation of it,

based on the needs and constraints in place), thus producing a working classifier. This classifier is then evaluated based on the metrics of interest: if it is not deemed acceptable, the introduction of "contexts" (as proposed in Section 13.2) might be in order. Once the classifiers are working well enough, data from new vehicles can be processed and labelled, thus effectively providing the customers with a prognostics service.

This project was only the first one of a possibly longer series of data mining applications in this automotive context. Additional projects are being defined given the interest of the company in pursuing the topic of prognostics even further. These new projects will build on top of the work already presented, using similar methodologies, approaches and tools. In this sense, this work of thesis is only the beginning of an hopefully strong involvement of the company in what is becoming a more data-driven future of the automotive industry.

Bibliography

[1] Mark Schwabacher. "A survey of data-driven prognostics". In: *Proceedings of the AIAA Infotech at Aerospace Conference*. 2005, pp. 1–5.

[2] Annamalai Pandian and Ahad Ali. "A review of recent trends in machine diagnosis and prognosis algorithms". In: *Nature & Biologically Inspired Computing, 2009. NaBIC 2009. World Congress on*. IEEE. 2009, pp. 1731–1736.

[3] Andrea Cordoba-Arenas, Jiyu Zhang, and Giorgio Rizzoni. "Diagnostics and prognostics needs and requirements for electrified vehicles powertrains". In: *IFAC Proceedings Volumes* 46.21 (2013), pp. 524–529.

[4] Somnath Pradhan and Joydeb Roychaudhury. "A machine learning approach to predict future power demand in real-time for a battery operated car". In: *IMpact of E-Technology on US (IMPETUS), 2014 International Conference on the*. IEEE. 2014, pp. 49–56.

[5] S Jagannathan and GVS Raju. "Remaining useful life prediction of automotive engine oils using MEMS technologies". In: *American Control Conference, 2000. Proceedings of the 2000*. Vol. 5. IEEE. 2000, pp. 3511–3512.

[6] Mitchell Lebold et al. *Detecting injector deactivation failure modes in diesel engines using time and order domain approaches*. Tech. rep. PENNSYLVANIA STATE UNIV STATE COLLEGE, 2012.

[7] David Gucik-Derigny, Rachid Outbib, and Mustapha Ouladsine. "Estimation of damage behaviour for model-based prognostic". In: *IFAC Proceedings Volumes* 42.8 (2009), pp. 1444–1449.

[8] Rudolph Emil Kalman et al. "A new approach to linear filtering and prediction problems". In: *Journal of basic Engineering* 82.1 (1960), pp. 35–45.

[9] Junbo Son et al. "Remaining useful life prediction based on noisy condition monitoring signals using constrained Kalman filter". In: *Reliability Engineering & System Safety* 152 (2016), pp. 38–50.

[10] Gregory Piateski and William Frawley. *Knowledge discovery in databases*. MIT press, 1991.

[11] Harold Hotelling. “Analysis of a complex of statistical variables into principal components.” In: *Journal of educational psychology* 24.6 (1933), p. 417.

[12] Leo Breiman et al. “Classification and decision trees”. In: *Wadsworth, Belmont* 378 (1984).

[13] Corrado Gini. “Variabilità e mutabilità”. In: *Reprinted in Memorie di metodologica statistica (Ed. Pizetti E, Salvemini, T). Rome: Libreria Eredi Virgilio Veschi* (1912).

[14] Sankar K Pal and Sushmita Mitra. “Multilayer perceptron, fuzzy sets, and classification”. In: *IEEE Transactions on neural networks* 3.5 (1992), pp. 683–697.

[15] Corinna Cortes and Vladimir Vapnik. “Support vector machine”. In: *Machine learning* 20.3 (1995), pp. 273–297.

[16] William W Cohen. “Fast effective rule induction”. In: *Proceedings of the twelfth international conference on machine learning*. 1995, pp. 115–123.

[17] William S Cleveland. “LOWESS: A program for smoothing scatterplots by robust locally weighted regression”. In: *The American Statistician* 35.1 (1981), pp. 54–54.

[18] John A Hartigan and Manchek A Wong. “Algorithm AS 136: A k-means clustering algorithm”. In: *Journal of the Royal Statistical Society. Series C (Applied Statistics)* 28.1 (1979), pp. 100–108.

[19] Haizhou Wang and Mingzhou Song. “Ckmeans. 1d. dp: optimal k-means clustering in one dimension by dynamic programming”. In: *The R journal* 3.2 (2011), p. 29.

[20] Peter J Rousseeuw. “Silhouettes: a graphical aid to the interpretation and validation of cluster analysis”. In: *Journal of computational and applied mathematics* 20 (1987), pp. 53–65.

[21] Jiawei Han, Jian Pei, and Yiwen Yin. “Mining frequent patterns without candidate generation”. In: *ACM sigmod record*. Vol. 29. 2. ACM. 2000, pp. 1–12.

[22] J. D. Hunter. “Matplotlib: A 2D graphics environment”. In: *Computing In Science & Engineering* 9.3 (2007), pp. 90–95. DOI: 10.1109/MCSE.2007.55.

[23] Michael Waskom et al. *seaborn: v0.7.1 (June 2016)*. June 2016. DOI: 10.5281/zenodo.54844. URL: https://doi.org/10.5281/zenodo.54844.

[24] *NumPy*. Online. 2017. URL: http://www.numpy.org/.

[25] *pandas: Python Data Analysis Library*. Online. 2012. URL: http://pandas.pydata.org/.

[26] F. Pedregosa et al. “Scikit-learn: Machine Learning in Python”. In: *Journal of Machine Learning Research* 12 (2011), pp. 2825–2830.